

THERMODYNAMIC BEHAVIOUR  
OF SOME AROMATIC FLUOROCARBON SOLUTIONS

A thesis presented for the degree of

Doctor of Philosophy

in the

Faculty of Science

of the

University of Leicester

by

Jennifer M. Brindley

Department of Chemistry,

The University

Leicester,

LE1 7RH.

August, 1975.

UMI Number: U419105

All rights reserved

INFORMATION TO ALL USERS

The quality of this reproduction is dependent upon the quality of the copy submitted.

In the unlikely event that the author did not send a complete manuscript and there are missing pages, these will be noted. Also, if material had to be removed, a note will indicate the deletion.



UMI U419105

Published by ProQuest LLC 2015. Copyright in the Dissertation held by the Author.  
Microform Edition © ProQuest LLC.

All rights reserved. This work is protected against  
unauthorized copying under Title 17, United States Code.



ProQuest LLC  
789 East Eisenhower Parkway  
P.O. Box 1346  
Ann Arbor, MI 48106-1346





THESIS  
491861  
13. 11. 75

X753034351

STATEMENT

All of the work presented in this thesis has been carried out by the author in the laboratories of the Department of Chemistry, University of Leicester, between October 1972 and June 1975, unless otherwise accredited.

The work has not been presented, and is not concurrently being presented, for any other degree.

Signed

*J. M. Brindley*

J. M. Brindley

August 1975

### ACKNOWLEDGEMENTS

The author wishes to express gratitude to:-

Dr. K. W. Morcom for his supervision and continued interest throughout the research work and the preparation of this thesis.

Dr. D. A. Armitage and Mr. J. Sprey both from Leicester Polytechnic who have assisted with computing and glass blowing.

The Chemistry Department Staff for their help with many technical matters.

Colleagues, past and present, for their friendship and helpfulness.

Mrs. C. M. Weller for the typing involved.

And the Science Research Council for the award of a studentship.

Not forgetting her husband who has been most tolerant during the commuting between Birmingham and Leicester.

FOR MY HUSBAND

ROD.

### SUMMARY

An apparatus has been developed to measure the vapour pressures of mixtures by a static technique.

The apparatus has been tested by reproducing the vapour pressures and excess Gibbs functions for mixtures of hexafluorobenzene + cyclohexane.

Excess Gibbs functions have been determined for hexafluorobenzene + *N,N*-dimethylaniline, and isopropylcyclohexane. An equilibrium constant for complex formation  $K_x$ , has been calculated from these quantities and compares favourably with the spectroscopically determined  $K_x$ .

Excess Gibbs functions have also been determined for mixtures of pentafluorocyanobenzene + cyclohexane at two temperatures.

The solid-liquid phase diagram has been determined for hexafluorobenzene + *N,N*-dimethyl *p*-toluidine and shows the existence of a 1:1 complex in the solid.

The liquid-liquid phase diagram for pentafluorocyanobenzene + isopropylcyclohexane has also been determined, and the system shows an upper critical solution temperature.

Excess volumes of mixing have been obtained for hexafluorobenzene + *N,N*-dimethylaniline, *N,N*-dimethyl *p*-toluidine and isopropylcyclohexane and pentafluorocyanobenzene + *N,N*-dimethylaniline, *N,N*-dimethyl *p*-toluidine, benzene, toluene and *p*-xylene.

Excess enthalpies of mixing have been measured at two temperatures for pentafluorocyanobenzene + cyclohexane, benzene, toluene and p-xylene.

The experimental evidence suggests that strong complexing occurs in solution between aromatic fluorocarbons + aromatic hydrocarbons, and also aromatic amines.

In the former case the interaction appears to be mainly of an electrostatic nature, whereas in the latter case the major contribution to the interaction arises from charge transfer forces, the amine acting as an electron donor.

## CONTENTS

<u>CHAPTER ONE - INTRODUCTION</u>	1
1.1 Fluorocarbon solutions	2
1.2 Aromatic fluorocarbon + alicyclic hydrocarbon systems	3
1.3 Aromatic fluorocarbon + aromatic hydrocarbon systems	4
1.4 Aromatic fluorocarbon + aromatic amine systems	11
1.5 Aromatic fluorocarbon + substances other than previously mentioned.	13
1.6 The development of the present work	14
<u>CHAPTER TWO - MATERIALS</u>	16
2.1 Introduction	17
2.2 Mercury	18
2.3 Fluorocarbons	19
a) Hexafluorobenzene	19
b) Pentafluorocyanobenzene	19
2.4 Aromatic amines	20
a) N,N-dimethylaniline	20
b) N,N-dimethyl p-toluidine	20
2.5 Cyclo alkanes	21
a) Cyclohexane	21
b) Isopropylcyclohexane	21
2.6 Benzene and arenes	22
a) Benzene	22
b) Toluene	22
c) P-xylene	23
<u>CHAPTER THREE - THE DESIGN AND OPERATION OF AN APPARATUS TO MEASURE VAPOUR PRESSURE</u>	24
3.1 Introduction	25
3.2 General description of the present apparatus	26
3.3 The thermostat	28

3.4	Temperature measurement	29
3.5	The manometer	30
3.6	The main vacuum line	31
3.7	The nitrogen line	32
3.8	The ampoule breaking apparatus	32
3.9	The sample preparation line	33
3.10	The design and preparation of ampoules of volatile components	34
3.11	The design and preparation of cells for involatile components	37
3.12	Operation of the apparatus	38
3.12.1	Determination of the vapour volume	38
3.12.2	Introduction of a volatile sample and measurement of vapour pressure	38
3.12.3	Introduction of an involatile sample	41
3.13	Calculation of the vapour pressure	42
<u>CHAPTER FOUR - THE VAPOUR PRESSURE RESULTS AND THE CALCULATIONS OF THE EXCESS GIBBS FUNCTIONS</u>		45
4.1	The thermodynamics of liquid-vapour equilibrium	46
4.2	The Barker method (and its modification) for calculating excess Gibbs functions	48
4.3	Test measurements	49
4.4	The vapour pressure results for the pure components	52
4.4.1	Cyclohexane	52
4.4.2	Hexafluorobenzene	52
4.4.3	N,N-dimethylaniline	52
4.4.4	Isopropylcyclohexane	52
4.4.5	Pentafluorocyanobenzene	56



4.5	The vapour pressure results and the calculated $G^E$ values for the mixtures studied.	56
4.5.1	N,N-dimethylaniline + hexafluorobenzene	56
4.5.2	Isopropylcyclohexane + hexafluorobenzene	59
4.5.3	Pentafluorocyanobenzene + cyclohexane	61
4.6	Correlation of vapour pressures with molar excess enthalpies	64

## CHAPTER FIVE - EXCESS ENTHALPIES OF MIXING 65

5.1	Introduction	66
5.2	Calorimeter vessels	69
5.3	Heater circuit	70
5.4	Thermistor circuit	71
5.5	Calorimeter jacket	72
5.6	Stirring mechanism	72
5.7	The thermostat	72
5.8	Loading of the calorimeter	73
5.9	Endothermic measurements - operation of apparatus	75
5.10	Exothermic measurements - operation of apparatus	77
5.11	Calculation of the endothermic molar excess enthalpy change	78
5.12	Calculation of the exothermic molar excess enthalpy change.	81
5.13	Test measurements	83
5.14	Molar excess enthalpy of mixing results	85

## CHAPTER SIX - EXCESS VOLUMES OF MIXING 93

6.1	Introduction	94
6.2	The present method : apparatus	95
6.3	Experimental technique	95
6.4	Calibration of capillary tubes	97
6.5	The water thermostat	97

6.6	Results	99
<u>CHAPTER SEVEN - PHASE DIAGRAMS</u>		109
7.1	Introduction	110
7.2	Liquid - liquid equilibria technique	110
7.3	Liquid - liquid equilibria results	111
7.4	Solid - liquid equilibria apparatus	111
7.5	Calibration of thermocouple	115
7.6	Operation of apparatus	117
7.7	Test measurements	117
7.8	Results	119
<u>CHAPTER EIGHT - DISCUSSION</u>		121
8.1	Hexafluorobenzene systems	122
8.1.1	Introduction	122
8.1.2	Excess Gibbs functions	123
8.1.3	Solid - liquid phase diagrams	128
8.1.4	Excess volumes of mixing	128
8.1.5	Summary	129
8.2	Pentafluorocyanobenzene + hydrocarbon systems	130
8.2.1	Excess volumes of mixing	130
8.2.2	Excess enthalpies of mixing	132
8.2.3	Excess Gibbs functions	135
8.3	Pentafluorocyanobenzene + aromatic amine systems	136
8.3.1	Excess volumes of mixing	136
8.4	Suggestions for further study	136
<u>APPENDIX - COMPUTER PROGRAMMES</u>		138
A.1	Programme for the evaluation of vapour pressure	139
A.2	Programme for the calculation of excess Gibbs functions	141
<u>REFERENCES</u>		146

## CHAPTER ONE

### INTRODUCTION

## INTRODUCTION

### 1.1 FLUOROCARBON SOLUTIONS

When aliphatic fluorocarbons became available it was discovered that many solutions involving them deviated from the predictions of molecular theories, whilst other solutions agreed quite well.

Scott ( 1,2 ) made a detailed study and reviewed the results of a range of fluorocarbon systems. He found that in general, when a fluorocarbon is mixed with a hydrocarbon, the deviations from ideal behaviour are often large and positive and may even be so large that partial miscibility will occur.

Aromatic fluorocarbons were not obtained in sufficient quantity or of a high enough purity until 1956, when vapour phase chromatography was used as a purification technique ( 6 ). On investigation of these fluorocarbon systems large positive deviations from ideality were observed, similar to the behaviour of the aliphatic fluorocarbon systems.

However in 1960 Patrick and Prosser ( 3 ) reported the existence of a 1:1 complex in the solid state for hexafluorobenzene and benzene. Interest was then focused on hexafluorobenzene systems in which complexing was thought to exist. The systems have been investigated by spectroscopy, x-ray diffraction, thermodynamic measurements and other techniques. The work has also been extended to include other fluorocarbons and their systems.

Fenby (4) and Swinton (5) have both reviewed the thermodynamic and non-thermodynamic work on some of the systems that have been studied (up to 1971).

The aromatic fluorocarbon mixtures fall into various classes of systems and their behaviour, in these classes, is reviewed in the following sections (incorporating work published up to the present).

## 1.2 AROMATIC FLUOROCARBON + ALICYCLIC HYDROCARBONS SYSTEMS

A number of alicyclic hydrocarbon + hexafluorobenzene mixtures have been studied.

The excess volumes of mixing (7), enthalpies of mixing (9) and excess Gibbs functions (10) for cyclohexane and hexafluorobenzene have been found to be large and positive by Swinton and his co-workers. The phase diagram for this system (8) showed several complexes with incongruent melting points. Various excess volumes of mixing for other alicyclic hydrocarbons with hexafluorobenzene that Swinton has determined (11) have also been found to be large and positive. This is in agreement with what would have been expected from the knowledge of how some alicyclic fluorocarbons behave.

Stubley and co-workers have shown that pentafluorobenzene + cyclohexane, and methyl cyclohexane mixtures give excess volumes (12), and enthalpies of mixing (13) which are smaller than those of the parallel hexafluorobenzene systems but still appreciably large and positive. The difference was suggested to be due to the net dipole moment of the pentafluorobenzene molecule (14) producing dipole - induced dipole forces in the mixtures.

A small amount of work has been carried out on pentafluorocyanobenzene and alicyclic hydrocarbon systems.

Fenby (15) showed that the excess volume of mixing of pentafluorocyanobenzene and cyclohexane was similar to that for hexafluorobenzene and cyclohexane.

Hall, Morcom and Brindley (16) determined the enthalpies of mixing of pentafluorocyanobenzene with isopropylcyclohexane and showed them to be large, positive and greater than the corresponding hexafluorobenzene system (17).

Although there is some variation in the actual numerical value for the excess functions for various systems, when changing from hexafluorobenzene, to pentafluorobenzene, and then to pentafluorocyanobenzene, there is still a marked tendency for the quantities to be quite large and positive, as expected.

### 1.3 AROMATIC FLUOROCARBON + AROMATIC HYDROCARBON SYSTEMS

Patrick and Prosser reported the formation of a 1:1 complex in the solid phase for hexafluorobenzene and benzene (3). The unexpected occurrence of a solid compound in a system composed of two relatively simple, non-polar substances was strong evidence that the intermolecular interactions were unusual. The complete phase diagram was investigated more fully by Duncan and Swinton (8).

This behaviour was in complete contrast to that of alicyclic fluorocarbon + hydrocarbon mixtures and aromatic fluorocarbon + alicyclic hydrocarbon mixtures. Other aromatic hydrocarbon mixtures were investigated to see if this phenomenon persisted.

Duncan and Swinton (9) determined the solid-liquid phase diagrams for hexafluorobenzene with toluene, p-xylene and mesitylene. These all showed the existence of a stable 1:1 complex in the solid.

Interest was then focused on the liquid mixtures of these systems and precise thermodynamic measurements were made to see if any indication of complexing occurred in solution.

Duncan, Sheridan and Swinton (7) studied the excess volume of mixing  $V^E$  as a function of composition at 40°C. Their results progressed from,  $V^E$  being quite small and positive for benzene mixtures, though to  $V^E$  being small and negative for mesitylene mixtures. They concluded that complexing in the liquid phase increased as the electron donating power of the hydrocarbon increased.

Gaw and Swinton (18) studied the vapour pressures of mixtures of hexafluorobenzene with benzene, toluene and p-xylene over a range of temperatures and compositions.

A double azeotrope occurred with benzene and the excess Gibbs functions showed a sign inversion.  $G^E$  was principally negative with a minimum of about  $-100 \text{ J mol}^{-1}$  at 40°C. The other two systems had more negative  $G^E$  minima, toluene being about  $-200 \text{ J mol}^{-1}$  and p-xylene being  $-400 \text{ J mol}^{-1}$ .

The enthalpies of mixing for the above systems were determined by Andrews et al (9). They were all found to be negative, becoming increasingly negative with electron donating power.

Having seen that complexing appeared to persist in the liquid state attention was refocused on the solid state complexes and the forces that bound the molecules in a complex of this type.

Dahl carried out a detailed x-ray study of the equimolar compounds formed between hexafluorobenzene and 1,3,5 -trimethylbenzene (19) and hexafluorobenzene and hexamethylbenzene (20). In both cases he found a similar crystal structure. The molecules were arranged alternately face-to-face in stacks. There was a possible source of interstack bonding because one C-C bond in the hydrocarbon pointed directly at a fluorine atom in an adjacent stack. Dahl noted that the general structure of the compounds was similar to  $\pi - \pi$  donor-acceptor complexes, however the interplane spacing would have been expected to be a lot smaller if this were the case.

Brennan, Brown and Swinton (21) investigated the 1:1 solid compound of hexafluorobenzene and benzene using a differential scanning calorimeter. They estimated the heat of formation of the compound to be  $+1.0 \pm 0.3 \text{ kJ mol}^{-1}$ , which is small and positive, and good evidence that the compound is stabilised by geometrical packing effects and weak electrostatic effects, rather than by the normal specific intermolecular interactions of the charge transfer type.

The nature of the complexing in the liquid state has also been open to much speculation. It was thought, at first, to be charge-transfer in type due to the trend of the excess functions becoming more negative on decreasing ionisation potential of the aromatic hydrocarbon (7,9,18). However Swinton showed that this trend also occurred in systems where charge-transfer complexing was not possible (9,11) so it could not be taken to be conclusive evidence.

Spectroscopic evidence was sought to confirm or deny the existence of charge-transfer complexing. No ultraviolet (22) evidence has been found but Steele et al (23) have shown evidence of a band appearing



in the far-infrared region of the spectrum of hexafluorobenzene and benzene. This at least is proof of enhanced intermolecular interaction.

Much work has been done with hexafluorobenzene and aromatic hydrocarbon systems. Phase diagrams and thermodynamic excess functions have been determined. The natural course for research into this type of mixture was to observe the effects of changing the aromatic fluorocarbon.

Duncan and Swinton (24) determined the solid-liquid phase diagram for pentafluorobenzene + benzene and found that the system formed two weak compounds with incongruent melting points. The mole ratios of the fluorocarbon to hydrocarbon were 1:1 and 3:2. They stated that the latter ratio is unique among binary systems of organic substances. They interpreted the results as being due to weaker specific interactions of pentafluorobenzene owing to the presence of one hydrogen atom.

Fenby, McLure and Scott (25) measured  $H^E$  for the same system at 25°C and 42°C. The excess enthalpies were small and mostly endothermic. They interpreted this as being due to weaker specific interactions than in the case of hexafluorobenzene. This was in agreement with the solid state investigations.

Howell, Skillerne de Bristowe and Stubley (13) performed a parallel study to that of Andrews et al (9), but with pentafluorobenzene. They determined the excess enthalpies of pentafluorobenzene with a series of methyl substituted benzenes in the range 308 to 328 K. The mixtures gave negative enthalpies that decreased with methyl substitution, although their values were less negative than those for the corresponding hexafluorobenzene system. This was in agreement with previous studies made with pentafluorobenzene.

Skillerne de Bristowe and Stubley (12), having found similarities between the excess enthalpies of pentafluorobenzene systems and hexafluorobenzene systems, extended their studies to the excess volumes of the pentafluorobenzene systems. They determined the excess volumes at 298.15K and found them to be quite small and positive and decreasing with increase in methyl substitution. Again this was parallel to the hexafluorobenzene systems although the rate of decrease in excess volumes was larger with hexafluorobenzene than pentafluorobenzene systems. Stubley and Skillerne de Bristowe concluded that the results for  $H^E$  and  $V^E$  suggested that both hexafluorobenzene and pentafluorobenzene had specific interactions which increased in a regular manner with methyl substitution of the aromatic hydrocarbon and that the hexafluorobenzene had the stronger specific interaction in each case.

Kelly and Swinton (26) have recently determined the phase diagrams of pentafluorobenzene with 1,2 - 1,3 - 1,4 dimethylbenzenes, 1,3,5 - trimethylbenzene, pentamethylbenzene and hexamethylbenzene. The first five mixtures showed the existence of a compound in the solid phase.

Fenby and Scott (27) widened the field of research by determining the enthalpies of mixing of 34 of the possible binary systems  $C_6H_mF_{6-m}$  and  $C_6H_nF_{6-n}$ . Their results ranged from positive to negative and through to sign changing excess enthalpies of mixing.

They discussed their results in terms of being made up of three effects:- a physical non-specific interaction  $H_p^E$ , due to the mixing of hydrocarbon with fluorocarbon. (This is large and positive) - a specific chemical interaction  $H_c^E$ , due to charge-transfer complexing.

(This is negative and dependent on the donor, acceptor strengths) - and a specific interaction between matching hydrogen atoms and fluorine atoms on adjacent rings, part of the  $H^E_c$  term (which they called a lock and key effect).

Hanna suggested that the last two effects  $H^E_c$ , could be electrostatic in origin and due to quadrupole - quadrupole, bond dipole interactions. In this case there would be little or no stabilisation of the complexes by charge transfer.

Hanna expanded on this view point in a later paper (28). He suggested that the electrostatic forces were due to C-F bond dipole interacting with hydrocarbon  $\pi$  quadrupole and similar induced secondary effects.

This new approach to the interpretation of the nature of complexing in these aromatic fluorocarbon, aromatic hydrocarbon systems caused Fenby and co-workers to systematically investigate the excess functions of benzene with  $C_6F_5X$  where  $X = I, Br, Cl$  and also with cyclohexane. Essentially the  $\pi$  acceptor strength of the aromatic fluorocarbon was being increased. The heats of mixing (29) were measured at 298.15K and 308.15K. For the benzene, substituted fluorobenzene systems the results were negative and became more negative with the increasing  $\pi$  electron acceptor strength of the fluorocarbon. However the cyclohexane corresponding systems' results were positive becoming less positive. When these results were considered as being the physical interaction  $H^E_p$ , and were subtracted from the benzene results to give the chemical contribution,  $H^E_c$ , no trend could be observed in  $H^E_c$  consistent with increasing  $\pi$  acceptor strength. It was concluded that charge-transfer plays no significant role in complex formation.

The excess volume results (30) for the above systems again showed no trend consistent with the existence of charge transfer complexing. In fact the results were understood in terms of shape (cyclohexane non-planar versus benzene planar) and polarisability differences (on changing X in  $C_6F_5X$  for H, F, Cl, Br, I).

Again with the purpose of varying the aromatic fluorocarbon, the pentafluorocyanobenzene and benzene system was investigated. One fluorine atom had been replaced by a very strong electron withdrawing group so making the fluorocarbon a good electron acceptor.

Hall and Morcom (31) have determined the phase diagram for pentafluorocyanobenzene and benzene and shown the existence of a double maxima corresponding to mole ratios 1:1 and 5:3. Hexafluorobenzene + benzene only gave a single maximum but pentafluorobenzene + benzene showed the existence of two weak compounds with mole ratios of 1:1 and 3:2.

Leong, Jones and Fenby (15) have determined the excess volumes of mixing for this system as well as for pentafluorocyanobenzene with cyclohexane. This formed a part of their programme to see if complexing were due to charge-transfer effects. The excess volume, although negative for pentafluorocyanobenzene + benzene, when altered to take account of  $V_p^E$  it did not have a particularly increased chemical contribution  $V_c^E$ , over those for the benzene +  $C_6F_5X$  (X=H, F, Cl, Br, I) systems. He therefore concluded that charge-transfer was insignificant.

#### 1.4 AROMATIC FLUOROCARBON AND AROMATIC AMINE SYSTEMS

Interest in Leicester has been centred on substituting more powerful electron donors, in fact aromatic amines, for aromatic hydrocarbons. These systems have then been investigated by spectroscopic and thermodynamic measurements, to see if hexafluorobenzene and aromatic amines form charge-transfer complexes.

Beaumont and Davis (32) showed that hexafluorobenzene could act as a strong electron acceptor with powerful n-donor aromatic amines. Prominent new ultraviolet absorption bands, characteristic of a charge-transfer band, were found for mixtures of hexafluorobenzene with N,N,N',N'-tetramethyl-p-phenylenediamine, N,N-diethylaniline and N,N-dimethylaniline. Analysis of the spectra gave values for  $K_x$ , the equilibrium constant of complexing, and  $\Delta H^{\circ}_{\text{comp}}$ , the standard heat of formation of the complex.

Beaumont and Davis (33) found that on closer examination of the spectra of the amines many of the absorption bands had double maxima. They could not satisfactorily explain this but attributed it to the effect of the hexafluorobenzene.

Armitage, Brindley, Hall and Morcom (34) have determined the solid-liquid phase diagram of hexafluorobenzene and N,N-dimethylaniline. They found the existence of a well-defined 1:1 complex.

Armitage and Morcom (35) determined the enthalpies of mixing for a range of aromatic amines with hexafluorobenzene at 25°C, 50°C and 70°C.

The large exothermic heats and positive excess heat capacities which they obtained indicated strong complexing in solution.

Morcom, Davis and co-workers (17) carried out ultraviolet spectrophotometric measurements of  $K_x$  and  $\Delta H_{\text{comp.}}^\ominus$ . They could then obtain the quantity  $H_c^E$ , the chemical contribution to the enthalpy of mixing. They also obtained  $H_c^E$  thermodynamically by using results from reference (35) and the system hexafluorobenzene with isopropylcyclohexane to determine  $H_p^E$ , the physical contribution. They obtained good agreement between the two  $H_c^E$  values calculated.

The spectroscopic and thermodynamic evidence for the complexing in these systems being due to charge transfer interactions, was far greater than with hexafluorobenzene + benzene and benzene derivative systems.

Morcom and co-workers (34) have extended their field of study to include pentafluorocyanobenzene and aromatic amine systems. The phase diagram for pentafluorocyanobenzene with N,N-dimethylaniline has been determined and shows the existence of a well defined 1:1 complex in the solid state.

It must be noted here that since Mulliken (36) showed that the prominent absorption spectra of a donor-acceptor complex was due to a charge transfer complex, it has become apparent that the presence or absence of a charge transfer band, in the ultraviolet region, neither confirms nor denies the existence of molecular complexing.

Furthermore the suggestion has been made that charge transfer contributions have been greatly overestimated and that classical electrostatic and polarisation effects could adequately provide the intermolecular binding energy (37).

Therefore even in the case of fluorocarbon + amine systems there is still the possibility that the stability of the complex is, to a large extent, determined by factors other than charge transfer.

#### 1.5 AROMATIC FLUOROCARBON + SUBSTANCES OTHER THAN PREVIOUSLY MENTIONED

Many workers have investigated the interactions of hexafluorobenzene with a range of substances both in the liquid and solid state, again with the hope of resolving the problem of the type of complexing that hexafluorobenzene enters into.

Morcom and Andrews (38) found that hexafluorobenzene with 1,4 dioxan gave an s shaped curve for the enthalpies of mixing measured at 298.15K. As 1,4 dioxan has been known to form charge transfer complexes they suggested that this may also be the case with this system.

Martin and Murray (39) extended this investigation into the reaction of hexafluorobenzene with ethers and measured the excess volumes of mixing of hexafluorobenzene with diethyl, di-n-propyl, di-isopropyl and di-n-butyl ethers. However they obtained positive excess volumes of mixing so could not comment on the existence, or non-existence, of complexing.

Reeder and co-workers have determined solid-liquid phase diagrams for hexafluorobenzene with cyclic hydrocarbons containing one or two  $\pi$  bonds (40). In the case of systems where the hydrocarbon had two  $\pi$  bonds then addition compounds were formed, with incongruent melting points. This they suggested was the result of donor-acceptor complexing.

Goates, Ott and Reeder (41) also determined the phase diagrams of hexafluorobenzene with benzene, pyridine, furan and thiophen. The first two systems gave compounds melting congruently and the last two compounds melting incongruently. They concluded that the stability was as expected if bonding resulted from charge transfer.

Fenby and co-workers (42,46) showed that the excess enthalpies, volumes and Gibbs functions of hexafluorobenzene + carbon tetrachloride indicated that the system deviated from ideal solution behaviour.

Fenby and co-workers carried out a detailed investigation into the system triethylamine and hexafluorobenzene where they measured its excess volumes (43), excess enthalpies (44) and excess Gibbs functions (45). This was because of a report that it gave a charge transfer band (32). All of the excess functions were found to be positive but small and were consistent with weak complex formation.

#### 1.6 THE DEVELOPMENT OF THE PRESENT WORK

The previous sections show the great amount of information available for aromatic fluorocarbon mixtures with alicyclic, aromatic hydrocarbons and amines. However in many cases there is a noticeable lack of excess Gibbs functions.

Only Swinton (10,18) and Fenby (45,46) have obtained excess Gibbs functions for hexafluorobenzene systems.

Therefore the main purpose of the present work was to obtain excess Gibbs functions for aromatic fluorocarbon mixtures by measuring the vapour pressures with a static vapour pressure apparatus.



The systems were chosen so that an equilibrium constant of complexing  $K_x$ , could be calculated from an experimental excess Gibbs function of complexing using a non-ideal solution model (47). This quantity could then be compared with a spectroscopically derived  $K_x$ .

This work was intended to complement a study made by Morcom et al. (35).

It was also hoped that the programme of work begun by Armitage and Hall in Leicester could be completed. This involved the measurements of excess volumes of mixing and phase diagrams for hexafluorobenzene and aromatic amines.

In addition a scheme to study the excess enthalpies and volumes of pentafluorocyanobenzene with cyclohexane, benzene, toluene and p-xylene was planned to determine whether a more powerful electron acceptor behaved differently with these hydrocarbons than hexafluorobenzene.

It was hoped that the excess Gibbs functions for some pentafluorocyanobenzene systems could be determined.

## CHAPTER TWO

### MATERIALS

## MATERIALS

### 2.1 INTRODUCTION

During the course of the vapour pressure measurements that were made, it became obvious that greater care had to be taken over the drying of materials.

In particular this was essential with cyclohexane. Wherever possible materials were dried with phosphorus pentoxide or if they reacted with this then freshly activated molecular sieve, type 5A was used.

All samples were required in a degassed state, so when purified, they were collected in ampoules of the type shown in figure (2.2.1) and repeatedly frozen and thawed, then sealed by covering the capillary tubes with mercury when they were still frozen. The liquid was then easily removed with a hypodermic syringe and long needle.

Various criteria of purity of the samples were used. The original and purified materials were analysed by gas liquid chromatography using a Pye Unicam 104 Chromatograph. In some cases the freezing point curve was also determined and the percentage purity calculated from the shape of the curve. Vapour pressure measurements were carried out on a few samples and these are given in chapter (4).

FIGURE (2.2.1)

AN AMPOULE



## 2.2 MERCURY

Two purification procedures were used as the mercury for the manometer in the vapour pressure measurements had to be of higher purity than that normally used in the laboratory.

The mercury used for calorimetry, excess volume measurements, and storage of materials was purified by filtering stock mercury, shaking it firstly with mercurous nitrate in 5% nitric acid, secondly with de-ionised water and thirdly with potassium hydroxide solution. After a number of washings with de-ionised water, it was dried and twice distilled in vacuo.

Higher purity mercury was required in the manometer so that published data for the density of mercury could be used in vapour pressure calculations, and also so that the menisci were not contaminated with oxidised impurities.

Mercury, as purified above, was vigorously shaken with a 5% nitric acid solution containing mercurous nitrate until the acid no longer became discoloured. This was followed by washing with de-ionised water until the aqueous layer remained colourless. The mercury was then shaken with 10% potassium hydroxide solution until there was no discolouration of the aqueous layer. The product was washed three times with de-ionised water, which remained colourless. It was then dried in a current of air at high temperature followed by distillation under reduced pressure in a current of air. The product was finally given two vacuum distillations.

Mercury purified in this way gave a stable foam lasting 15 - 20 seconds when shaken with de-ionised water (48) and showed no tendency to mark the surface of the manometer.

## 2.5 FLUOROCARBONS

### A) Hexafluorobenzene

Two samples of hexafluorobenzene were used. One sample was obtained from Bristol Organics Ltd., and was of stated purity 99+ %. This sample was dried over phosphorus pentoxide and used, without further purification, for the phase diagram measurements. It has a freezing point of 278.05K and a purity of 99.92 mole %, as determined from its freezing point curve.

The other sample of hexafluorobenzene was obtained from Imperial Smelting Ltd., and was of stated purity 99.95%. This was also dried over phosphorous pentoxide. Gas-liquid chromatography using both a PEG 20M column at 323.15K and a 10% APL column at 323.15K gave only one sharp peak. The sample was used for vapour pressure measurements without further purification.

### B) Pentafluorocyanobenzene

Bristol Organics Ltd., pentafluorocyanobenzene, of stated purity 99+%, was purified by continuous fractional freezing using a freezing apparatus. It was dried over freshly activated molecular sieve and its gas liquid chromatograph, using a 10% E30 column at 373.15K, gave one single sharp peak.

## 2.4 AROMATIC AMINES

### A) N,N Dimethylaniline

"Analar" N,N-dimethylaniline was refluxed for seven hours with acetic anhydride under reduced pressure (49) so as to remove any primary or secondary amines as involatile acyl derivatives. The mixture was then distilled under reduced pressure and in a stream of nitrogen using a fractionating column of the type described by Ray (50) with a reflux ratio of about 50:1. The distillate was condensed in a solid carbon dioxide/acetone trap and initially consisted of acetic acid and acetic anhydride. Eventually N,N-dimethylaniline was collected in the trap as a white solid.

This product was then redistilled, as above, using a high reflux ratio, and the middle fraction of three fractions was kept. This was again distilled, as above, and the middle fraction of three kept and stored in an ampoule as described in section (2.1).

Gas liquid chromatography showed no trace of impurity.

### B) N,N Dimethyl p - toluidine

Ralph N. Emmanuel Ltd., N,N-dimethyl p-toluidine, of stated purity 99+%, was purified by the same method as described for N,N-dimethylaniline.

The freezing point of the purified sample was 245.58K and it has a mole percent purity of 99.97%, as determined from its freezing point curve.

## 2.5 CYCLO ALKANES

### A) Cyclohexane

BDH. Chemical Ltd., research grade cyclohexane was dried over phosphorous pentoxide. It had a freezing point of 279.70K and a purity of 99.99%, as determined from its freezing point curve, so it was used without further purification.

### B) Isopropylcyclohexane

The isopropylcyclohexane was required in a higher degree of purity than used previously in this laboratory (17) where a purity of about 99% was adequate. Previous samples were found to blacken mercury slightly and were obviously unsuitable for vapour pressure measurements.

Firstly repeated zone freezings were done but after about thirty passages the gas chromatograph of the sample, on a 3% OV17 column at 376.15K, still showed the presence of secondary peak.

A spinning band distillation was then carried out using a drehbandkolonne system type AG No. 103 as simple fractional distillation had no apparent effect on the sample.

A gas liquid chromatograph was taken on every sample collected and the sample size was restricted to a couple of  $\text{cm}^3$ . The gas chromatographs showed that the small secondary peak was decreasing and at the seventh fraction it disappeared completely. The required sample was collected after this point and was dried over phosphorous pentoxide. The sample did not blacken mercury when shaken with it.



## 2.6 BENZENE AND AROMATICS

### A) Benzene

"Analar" benzene was purified according to the method of Vogel (51).

1000 cm<sup>3</sup> of benzene was stirred for thirty minutes with 150 cm<sup>3</sup> of concentrated sulphuric acid. The acid layer was separated off and more acid added and the same procedure as above followed, until the acid layer no longer became yellow. Four such processes were required.

The benzene was washed twice with de-ionised water, once with a 10% sodium carbonate solution, and again with water. It was left to stand over calcium chloride overnight.

The sample was twice distilled off sodium, in an atmosphere of nitrogen. In each case the middle fraction of the three fractions was collected. The pure sample was collected in an ampoule as described in section (2.1).

Gas chromatography showed no trace of impurity.

### B) Toluene

Ralph N. Emmanuel Ltd., toluene was dried over phosphorus pentoxide and the gas chromatograph taken using a 10% E30 column at 353.15K. The chromatograph showed no trace of impurity.

The freezing point of the sample was 178.31K and its estimated purity was 99.97%.

C) P - Xylene

Ralph N. Emmanuel Ltd., p-xylene of 99+% purity was dried over phosphorus pentoxide. It was used without further purification.

### CHAPTER THREE

#### THE DESIGN AND OPERATION OF AN APPARATUS TO MEASURE VAPOUR PRESSURE

THE DESIGN AND OPERATION OF  
AN APPARATUS TO MEASURE VAPOUR PRESSURE

3.1 INTRODUCTION

Vapour pressure measurements of liquid mixtures are difficult to perform accurately but are of great interest because they allow the calculation of excess Gibbs functions of the mixtures.

There are various methods available for measuring vapour pressure, the two main being the equilibrium still dynamic method, and the static method.

In the dynamic method the mixture is boiled and the equilibrium vapour and liquid are separated. The vapour is condensed and returned to the boiler via a 'hold-up' trap. When equilibrium is attained samples of the boiler liquid and condensate are analysed. The equilibrium temperature and pressure are measured, along with the vapour pressures of the pure components, and with these quantities the excess Gibbs functions can be calculated.

Fowler (52,53) has reviewed the various designs of equilibrium stills developed although Brown (54) describes a more advanced design.

The static method involves allowing a mixture, of known amounts of the two components, to come to equilibrium with its vapour in an air free cell isolated by a cut-off. The temperature and pressure are measured and corrections made to the liquid composition to allow for the amount of each component present in the vapour. The excess Gibbs functions of mixing can then be calculated.

Baxendale (55), Everett and Penney (56) and Williamson and McGlashan (57,58) were the early workers concerned with developing this method.

In the design of Williamson and McGlashan's apparatus the vapour pressure of a liquid in a cell was measured partly on a mercury cut-off, immersed in a thermostat tank, and partly on an external manometer connected in series.

Gaw and Swinton (10,18) improved the ease of operation of a static method apparatus by replacing the second manometer and buffer line, as used above, by a second cell containing a reference liquid in equilibrium with its vapour, and housed in the thermostat bath. The vapour pressure of the reference liquid was known accurately. Pasco and Fenby (46,59) have also used this differential technique of employing a reference liquid.

Marsh (60,61), Valle Colero and Losa (62) and Garrett (63,64) have measured the vapour pressures on a single manometer. This greatly simplifies the number of readings that need to be taken.

### 3.2 GENERAL DESCRIPTION OF THE PRESENT APPARATUS

Various designs of apparatus have been used in this laboratory but without success.

Armitage (65) built an apparatus similar to Williamson and McGlashan (57,58) but unfortunately it developed a leakage through its greaseless taps which were immersed in the thermostat bath.

Andrews (66 ) modified the above apparatus, adopting a design similar to that of Marsh (60,61 ) and also placing the greaseless taps outside the thermostat tank. However leakage still occurred through the greaseless taps. These taps were replaced by a different make of greaseless tap and the apparatus was apparently functioning satisfactorily when the glass blown join between the manometer and cell collapsed and the apparatus imploded.

It was decided to redesign the apparatus for ease of use, but to retain the basic technique of Marsh. A manometer of the type used by Armitage was made in a larger slightly modified form.

All the taps that the samples came into contact with were greaseless taps from J. Young, Acton. The ground glass joints were also greasefree and were prevented from fusing by using PTFE sleeves from Fisons. They were sealed by surrounding them with cups containing mercury.

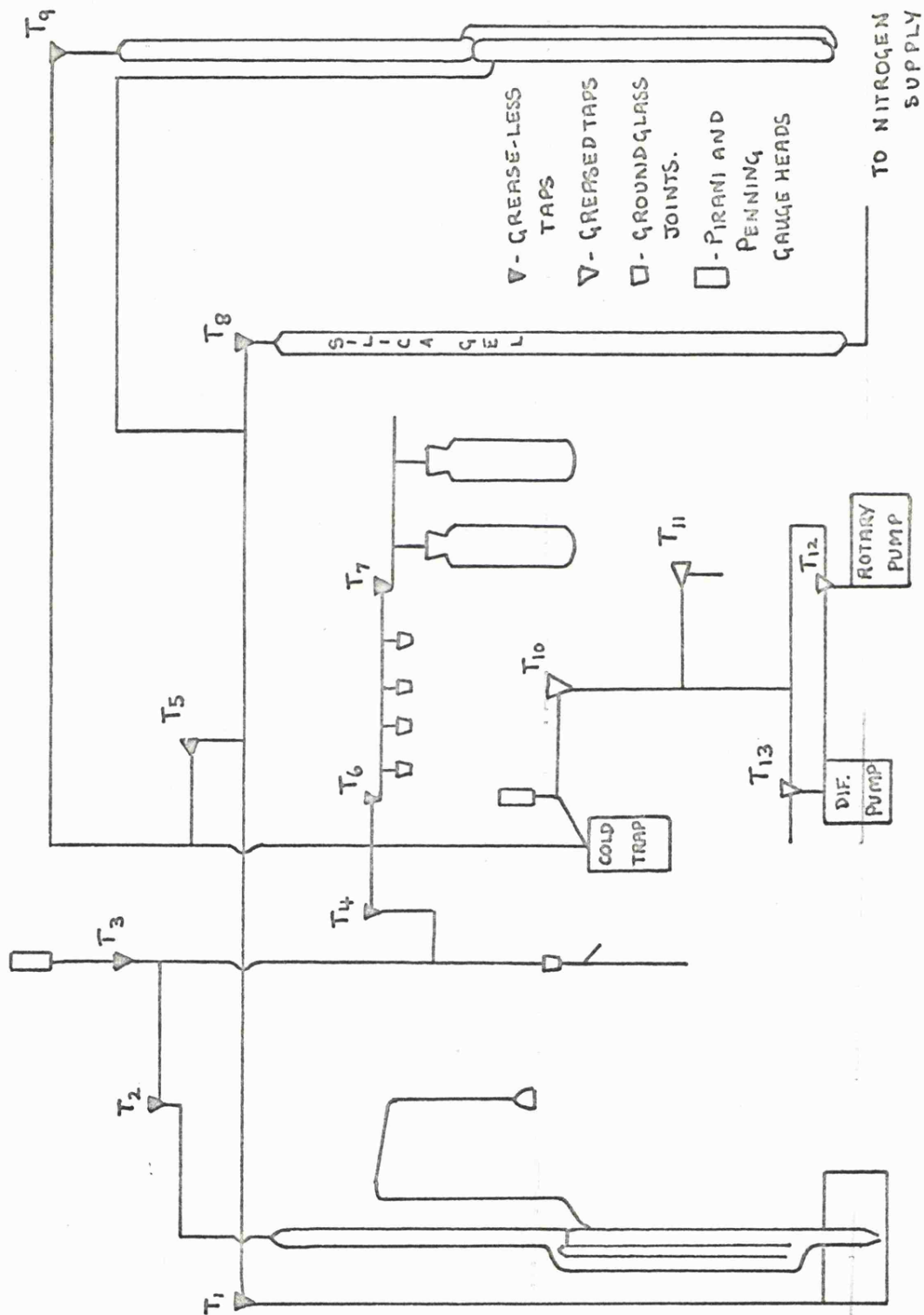
The liquid sample was introduced into the cell by distillation through the mercury manometer, the mercury being removed by lowering it into a reservoir. To be able to do this it was necessary to pump the manometer assembly down to a hard vacuum and also to have a part of the vacuum line available to raise or lower the mercury in the manometer by blowing dry nitrogen through it or pumping on it to create a vacuum.

A number of ground glass sockets and cones were incorporated into the vacuum line in order that the materials to be used could be dried, degassed and stored for a time before being sealed in ampoules.

Figure (3.2.1) shows the apparatus in diagramatic form.

FIGURE (3.2.1)

VAPOUR PRESSURE APPARATUS



### 3.3 THE THERMOSTAT

The thermostat tank, which housed the manometer assembly, was similar to that designed by Williamson (57,58) but was rigidly mounted on a "Dexion" frame.

It was a stainless steel tank which was lagged with 2" sheets of expanded polystyrene and covered with  $\frac{3}{4}$ " block board. A plate glass window was let into the front side of the tank. The tank was fitted with a wooden half-lid, covered with Formica. A frame was fixed on the lower side of this lid to support the regulator and heaters but the stirrers were supported from the top of the lid.

The regulator was constructed from a three metre length of  $\frac{1}{2}$ " diameter copper tubing bent into a coil. A glass to metal seal was attached to one end of the tube (the other end being closed) and a conventional mercury in glass regulator head was attached to this seal. The copper coil was filled with about 400 cm<sup>3</sup> of distilled toluene, and mercury brought the level up to the point of contact with the platinum contact in the regulator head. It was calculated that a temperature change of 0.001K could be detected by a measurable movement of the mercury in the capillary tube of the regulator head.

The two heaters were both made from Pyrotenax mineral insulated resistance cable. They were wound on a nylon frame which also supported the regulator. The intermittent heater was controlled by a variac transformer, regulator and electronic relay. The permanent heater was controlled by a variac transformer. The water was stirred by two Gunn stirrers mounted on the lid of the thermostat.

The stirrers were adjusted so that one drew water from near the bottom of the tank and the other from the centre of the tank.



They were orientated so as to force water in different directions and cause turbulence in all parts of the tank.

In order to prevent excess heat loss and evaporation from the surface of the water, polystyrene was used to cover the surface.

Placed below the thermostat tank was a galvanised steel tank of approximately the same volume. The water in the thermostat tank could be drained off into this lower tank through a stopcock. The lower tank was lagged with polystyrene sheeting and fitted with a wooden lid.

A centrifugal pump (Type 10, Stuart Turner Ltd.) was used to raise the water from the lower to the upper tank, the outlet being slightly above the top of the upper tank.

### 3.4 TEMPERATURE MEASUREMENT

The thermostat temperature was measured using a platinum resistance thermometer (Type 51875A, H. Tinsley and Co.,) a Precision Comparison Bridge (Model VLF 51A, Rosemount Engineering Co.) and a standard resistor (Class 'S' 25 RS, 25.5 ohms).

The temperature was calculated using the expression,

$$T = \left[ \frac{R_t - R_0}{\alpha R_0} + \delta \left( \frac{t}{100} - 1 \right) \frac{t}{100} + \beta \left( \frac{t}{100} - 1 \right) \left( \frac{t}{100} \right)^3 \right] + 273.15$$

(3.4.1)

where T is temperature in K,  $\alpha$ ,  $\delta$ ,  $\beta$ , are constants for the platinum resistance thermometer and  $R_t$  and  $R_0$  are the measured resistances at T K, and 273.15K.

The stability of the thermostat was shown to be  $\pm 0.001\text{K}$  for several hours at the temperatures used.

### 3.5 THE MANOMETER

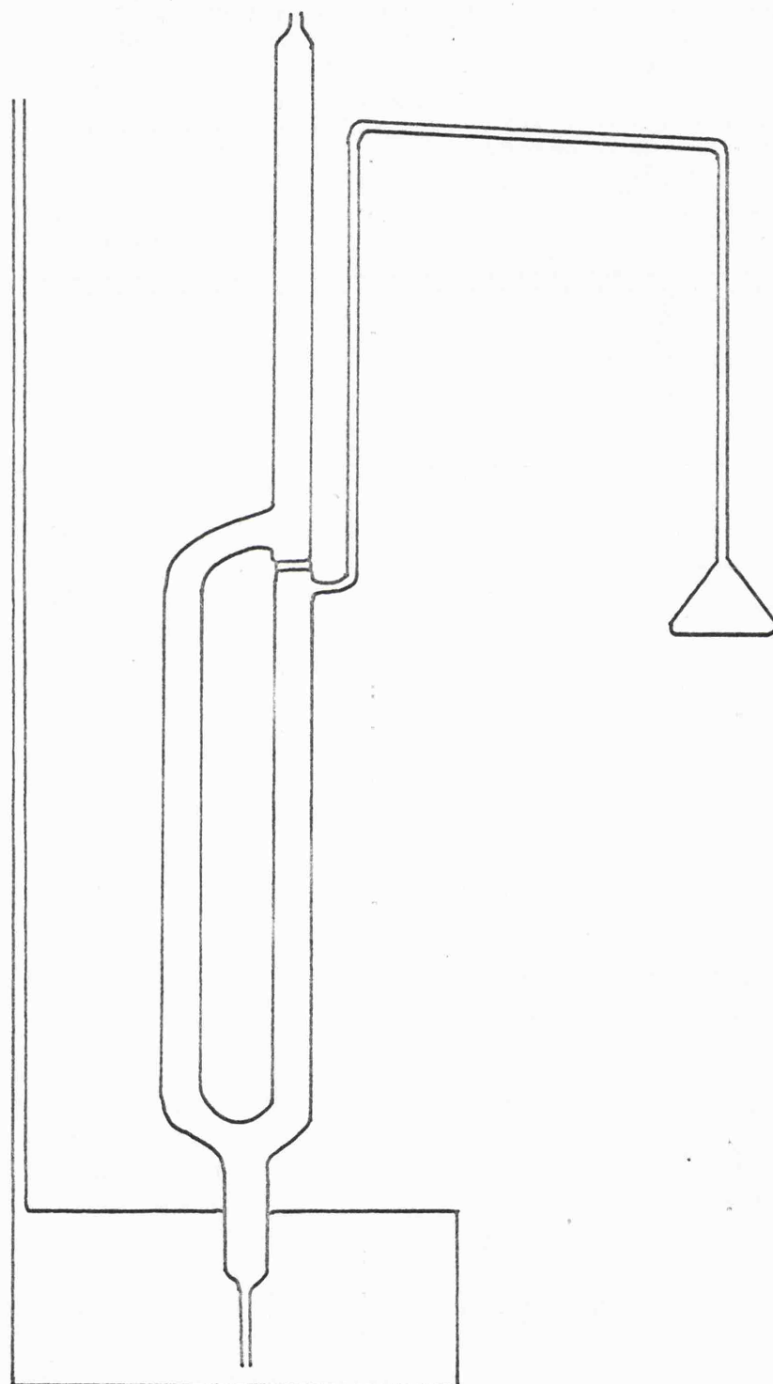
The manometer, figure (3.5.1), was made from 20 mm bore Veridia precision bore tubing. A single cell is shown attached to the manometer in preparation for the measurement of the vapour pressure of a volatile component. A double bulb cell is used for involatile components (Section 3.11). The bulb contained a small stirrer bead made from a piece of soft iron encased in a glass envelope. The metal was thoroughly cleaned and sealed in the glass case under vacuum. The bead was rotated by an electrically driven magnet sealed in a water-proof case and with a long stem up to the stirrer motor so that the motor could be clamped from outside the tank. The height of the magnet could be easily adjusted.

The power supply to the motor was controlled by a Simmerstat so that the liquid was stirred every seven seconds.

The heights of the mercury levels were measured (with an accuracy of  $\pm 0.01$  mm) through the plate glass window of the tank, by using a cathetometer (Precision Tool and Instrument Co.,). The menisci were illuminated by mounting two 9" fluorescent tubes (8W 250 v, housed in a long glass tube and with their light diffused by a translucent roll of paper) in the front corner of the tank and angled so that their light fell onto a white plastic strip mounted behind the manometer. With the lighting arranged in this way it did not have to be disturbed during the distillation process. The menisci also had light shields mounted just above them so that even illumination was achieved. The reference mark, in determining the volume of the vapour space, was taken as the lower part of the glass divider between the upper and

FIGURE (3.5.1)

THE MANOMETER



lower part of the manometer.

The mercury reservoir was placed immediately below the manometer, and in the thermostat tank, so that mercury could be lowered into it, and the temperature of the bulk mercury was the same as that in the manometer.

The manometer was thoroughly cleaned with hot chromic acid before being mounted in the thermostat tank. It was held in place by clamping and by attaching teflon bars.

### 3.6 THE MAIN VACUUM LINE

The final version of the vacuum line is as shown in figure (3.2.1). Throughout the course of the work modifications were made so as to overcome difficulties that arose.

Tap  $T_3$  was introduced so that the pressure gauge head could be isolated from the distilling vapour. Two components which were used were found to be either decomposed by the hot wire in the gauge head or to be reacting with some part of the head.

Tap  $T_{11}$  was also introduced so that air could be introduced to the vacuum line without turning off the pumps.

The vacuum line was periodically cut open and cleaned then glass blown back together.

The line was designed so that the manometer, nitrogen line, and ampoule breaking apparatus, could all be isolated and evacuated as required.

The high vacuum pumping system consisted of a three-stage mercury diffusion pump backed by a single-stage rotary oil pump (Type GRS 2, General Engineering Co.). The pumps were protected by a liquid nitrogen cold trap, as shown in figure (3.2.1), and could be isolated from each other and the vacuum line by taps  $T_{13}$  and  $T_{12}$ .

The pressure in the vacuum line was measured with Pirani and Penning gauges (Types PGH3 and PNH1, General Engineering Co.,) connected to two control units (DR343 and PNG1, General Engineering Co.). The pressure in the system when evacuated was better than  $10^{-2} \text{ Nm}^{-2}$  which was satisfactory for this apparatus.

### 3.7 THE NITROGEN LINE

White spot nitrogen dried over silica gel was used to lower or raise the mercury in the reservoir. It was possible to evacuate this part of the line by opening taps  $T_1$  and  $T_5$ . The pressure was shown by the manometer on the extreme right of the apparatus (figure 3.2.1). The mercury was raised by closing tap  $T_5$ , leaving tap  $T_1$  open and also opening  $T_8$  gradually so that a controlled amount of nitrogen was admitted to the system.

### 3.8 THE AMPOULE BREAKING APPARATUS

The principle of the apparatus was that the composition of the sample in the cell could be changed by lowering the mercury in the manometer and quantitatively distilling a known amount of one component into the cell.

The ampoule breaking equipment is shown in figure (3.8.1). It was designed so that it could be readily assembled without any glass blowing and also so that the sample could be frozen down so that on breaking the ampoule tip no glass splints or liquid splashed into any taps.

The apparatus consists of a vertical glass tube near the top of which is a pocket in which a breaker can be held. The breaker consists of a piece of soft iron sealed, under vacuum, in a glass envelope. The glass envelope broke frequently until the distance the breaker was allowed to fall through was decreased, and also greater care was taken over the annealing of the glass.

One end of the glass tube is attached to the vacuum line via a B19 ground glass socket, with a teflon sleeve between socket and cone, and the whole joint is surrounded by mercury.

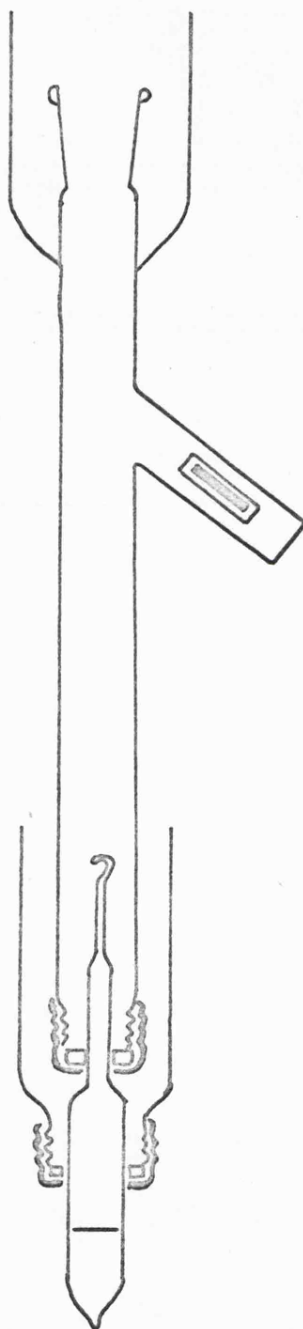
The other end of the tube has a Quickfit screw cap adaptor attached to it so that the ampoule is held rigidly. Again the joint is surrounded with mercury.

### 3.9 THE SAMPLE PREPARATION LINE

For a static method of measuring vapour pressures it is important to ensure that all samples are thoroughly degassed. A section of the vacuum line, figure (3.2.1), was provided for this purpose. It consists of four B10 ground glass sockets to which either ampoules or cells could be attached. These are connected to the main vacuum line by tap T6 and to two storage vessels by tap T7. The two storage vessels are attached to the vacuum line by two B19 sockets.

FIGURE (3.8.1)

THE AMPOULE BREAKING APPARATUS



### 3.10 THE DESIGN AND PREPARATION OF AMPOULES OF VOLATILE COMPONENTS

The ampoules used are shown in figure (3.10.1). They were carefully designed so that:-

- 1) The maximum volume of sample could be taken but the ampoule was still small enough to be weighed on a micro-balance, (Type 146, L. Oertling Ltd. with a sensitivity of 0.00002 g).
- 2) A glass cup, figure (3.10.1), could be attached to the ampoule around the B10 cone so that mercury could seal the joint but there was still an adequate clearance for glass blowing in the necked down region.
- 3) The part of the ampoule that was contained in the ampoule breaking apparatus was long enough.

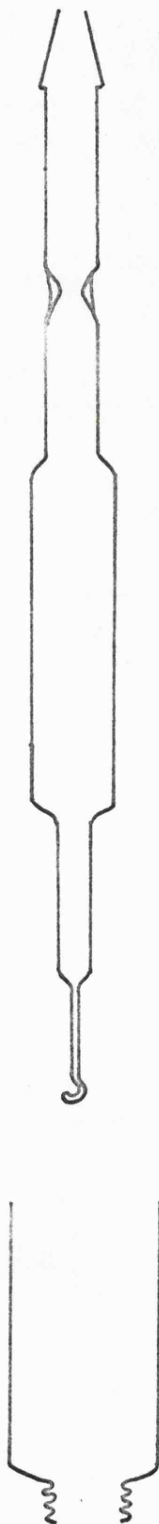
The ampoules were made without the constriction so that they could easily be cleaned. They were cleaned by filling them with freshly prepared hot chromic acid and immersing them completely in the acid. They were left to soak overnight and then washed with deionised water, several times, followed by analar acetone. They were put in an air oven to dry, for a few hours, and then were attached to the sample preparation line and pumped on so as to remove any acetone vapour. The ampoules were wiped with a soft cloth and the inner surfaces were examined before the constrictions were placed near the B10 cones. The outer surfaces then had to be cleaned again, with methylene dichloride. The ampoules were placed in a balance case containing a tray of active silica gel for a short while, were weighed, dried in an air oven for several hours, allowed to cool in a silica gel vacuum desiccator, and re-weighed.

This procedure was continued until two consecutive weights agreed to within  $\pm 0.00001$ g. The temperature of the air in the balance case



FIGURE (3.10.1)

AN AMPOULE AND GLASS CUP



was recorded at the time of the weighings.

Each glass cup that was attached to an ampoule had a number on it so the ampoules were readily identified. The ampoules were attached to the vacuum line and then the storage vessels were also attached. One of the storage vessels contained a drying agent and the liquid to be degassed and ampouled.

Initially only the rotary pump was started. The liquid in the storage vessel was quickly pumped on, to remove some of the air, and then it was isolated by closing tap, T7 and frozen in liquid nitrogen. The mercury diffusion pump was started and in less than an hour a good vacuum was obtained.

The liquid was degassed by repeated vacuum distillation from one storage vessel to the other. Liquid nitrogen was used to cool the collecting vessel and a beaker of cold water surrounded the frozen sample. This section of the line was pumped down to a hard vacuum after each distillation. At least twelve distillations were usually carried out. The final distillation returned the material to the vessel containing the drying agent, and the material was allowed to warm up.

Tap, T6, was closed and tap, T7, was opened. The ampoule to be filled was surrounded with ice and water and the ampoule was over filled so that the excess liquid could be redistilled back into the storage vessel to eliminate the presence of a volatile impurity. The volume of sample required was calculated and this amount of water was syringed into a spare ampoule. The spare ampoule was then held against the ampoule on the vacuum line so that the ampoule could be filled to the required level. The sample was then hard frozen and the ampoule sealed at the constriction, with the apparatus evacuated.

The contents were allowed to thaw and the ampoule was cleaned before weighing.

The ground-glass cones, which had been detached from the ampoules and left on the vacuum line, were removed and washed with methylene dichloride. They were dried in an air oven and weighed in the same way as the ampoules.

The external volume of the filled ampoules were determined by measuring the displacement of their volume of water.

The true weight of material in an ampoule was calculated as follows, if  $W_1$  = the weight recorded for the ampoule before filling  $W_2$  = the weight recorded for the ampoule after filling  $W_3$  = the weight recorded for the detached cone, and  $\rho_1, \rho_2, \rho_3$  are the densities of dry air at the temperatures at which  $W_1, W_2$  and  $W_3$  were recorded.  $\rho_W$  is the density of the balance weights,  $\rho_g$  the density of pyrex glass at the required temperatures, and  $V$  the external volume of the filled ampoule, then

$$W_1 \text{ true} = W_1 \left[ \frac{1 - \rho_1}{\rho_W} \right] \left[ \frac{1 - \rho_1}{\rho_g} \right]^{-1} \quad (3.10.1)$$

$$W_2 \text{ true} = W_2 \left[ \frac{1 - \rho_2}{\rho_W} \right] + V \rho_2 \quad (3.10.2)$$

$$W_3 \text{ true} = W_3 \left[ \frac{1 - \rho_3}{\rho_W} \right] \left[ \frac{1 - \rho_3}{\rho_g} \right]^{-1} \quad (3.10.3)$$

and the true weight of the sample taken,  $W_1$  was given by

$$W = W_{2\text{true}} + W_{3\text{true}} - W_{1\text{true}} \quad (3.10.4)$$

### 3.11 THE DESIGN AND PREPARATION OF CELLS FOR INVOLATILE COMPONENTS

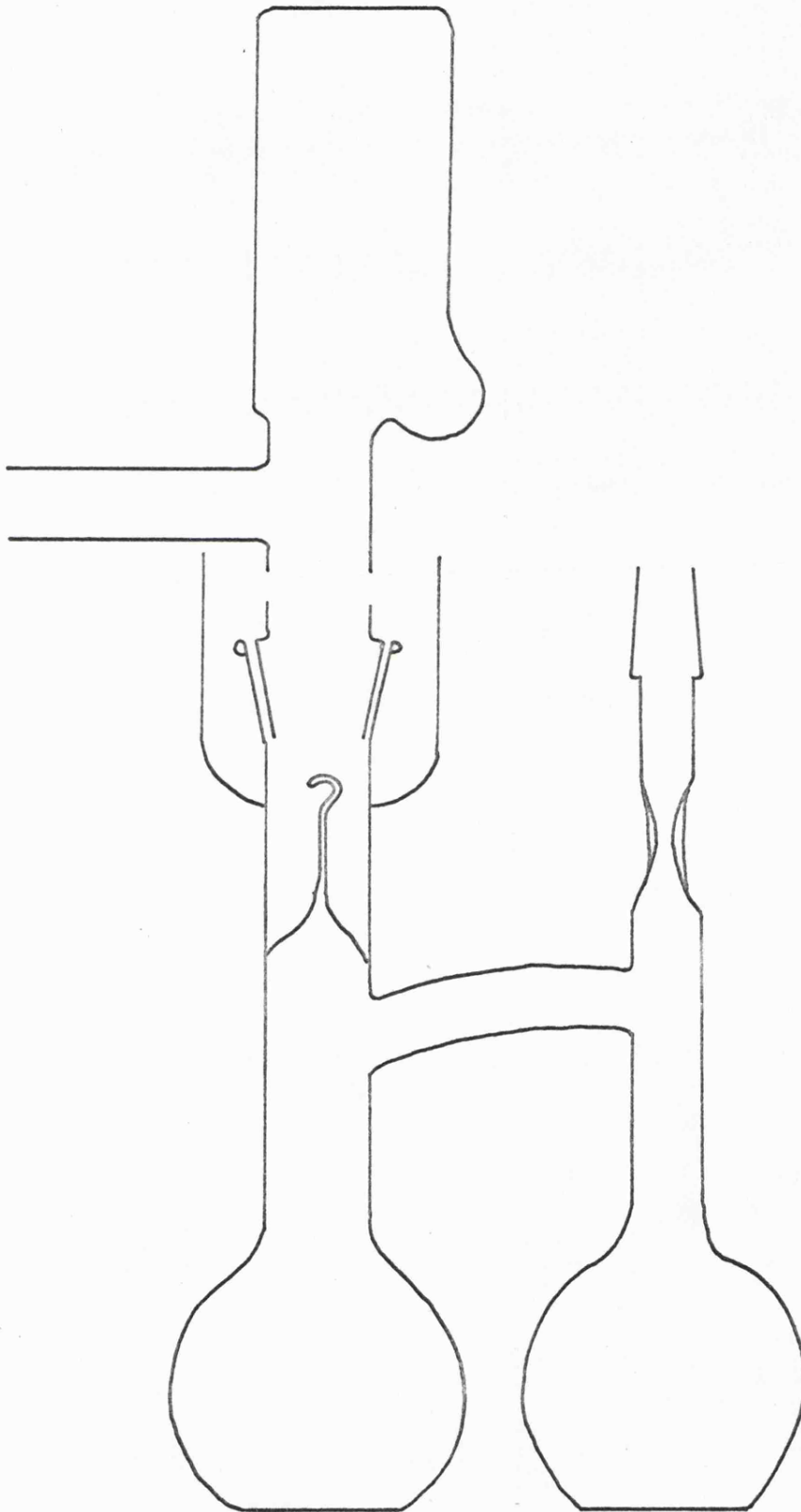
If one component of a mixture is relatively involatile it is necessary to use a cell having a break seal. The cell can then be directly attached to the manometer in place of the bulb. The bulb has to be removed and a breaker housing attached to the manometer, as shown in figure (3.11.1). The cell can then be attached via a B19 socket.

The cell was made as shown in figure (3.11.1). It was thoroughly cleaned using freshly prepared hot chromic acid, being allowed to soak overnight in the acid. The cell was then washed in deionised water following by analar acetone and put to dry in an air oven. A magnetic stirrer bead was made and put into the cell before a constriction was put in the stem of the cell below the B10 cone. Water was syringed into the cell to a point halfway up the constriction in the stem. The cell was placed on a weighed strip of aluminium, so that it was steady on the balance pan, and its weight was noted. After a further half an hour the weight and temperature were again recorded. This was repeated to constant weight. The water was removed and the cell dried. It was pumped on the vacuum line and then it was weighed to constant weight.

The desired quantity of involatile component was syringed into the cell and the cell attached to the sample preparation line. The sample was quickly pumped on, with only the rotary pump, and then it was hard frozen in liquid nitrogen. When the sample was completely frozen a hard vacuum was used to remove all traces of air. The sample was thawed and frozen and again pumped on a few more times before twelve vacuum distillations were carried out by distillation from one bulb of the cell to the other. The sample was completely degassed by this process. The pressure gauges showed no change in pressure, when tap T6 was opened, after four vacuum distillations.

FIGURE (3.11.1)

CELL AND BREAKER HOUSING



The cell was removed by sealing it, under vacuum, at the constriction with the sample frozen in liquid nitrogen. When the sample had thawed the cell surface was cleaned and the cell weighed to constant weight. The B10 cone was removed from the vacuum line, cleaned, and also weighed, to constant weight, as described previously.

The weight of the component was calculated by applying the necessary buoyancy corrections in a similar manner to the method used in section (3.10).

### 3.12 OPERATION OF THE APPARATUS

#### 3.12.1 Determination of the Vapour Volume

When static vapour pressure measurements, with total composition data, are used to determine activity coefficients and the excess Gibbs functions on mixing, it is necessary to know the composition of the vapour. When only the total composition (liquid and vapour) is known the volume of the vapour space is required as well.

The method used for determining this vapour space was by carrying out isothermal compressions on a sample of nitrogen, assuming the nitrogen to behave ideally (65).

#### 3.12.2 Introduction of a Volatile Sample and Measurement of Vapour Pressure

The introduction of a sample into the cell of the manometer is greatly simplified when no sample is present in the cell. Therefore the more complicated case of addition of material to a sample in a cell will be considered here.

An ampoule was inserted into the ampoule breaking apparatus, figure (3.8.1), and attached to the vacuum line. The main vacuum line was then evacuated with taps T3, T2 and T4 open.

The thermostat electrical equipment was then switched off, and the water from the thermostat tank was drained into the lower tank. The water level was lowered until the cell was adequately uncovered. The stirrer motor was completely removed from the tank and a small dewar (with a long side arm attached) of liquid nitrogen was clamped below the cell. The rate of cooling of the sample was slow enough not to cause oscillations in the mercury of the manometer.

Tap T4 was closed and T5 opened so that the nitrogen line, up to tap T1, could be evacuated. The lowering of the mercury in the manometer was controlled by T1. The mercury levels were lowered until they were within 10 cm of the mercury reservoir. The sample was still isolated from the evacuable side arm of the manometer.

Taps T1, and T5 were closed and Tap T4 opened again. The vacuum line was evacuated until a satisfactory vacuum had been achieved. The dewar around the cell was raised, so that the sample was hard frozen, and the ampoule sample was also frozen in liquid nitrogen. When the mercury levels in the manometer were at the same height the preparations for breaking the ampoule tip were complete.

Taps T2, T3 and T4 were closed and the breaker was removed from its pocket, by a horse-shoe magnet, and allowed to fall on the ampoule hook. The dewar of liquid nitrogen was removed from about the ampoule.

The breaker was replaced in its pocket and checked to be intact. Tap T1 was then opened, so as to lower the mercury completely, and T2 could then be opened to allow distillation of the sample into the cell. The dewar of liquid nitrogen, around the cell, was lowered slightly so that the sample did not freeze in the neck of the cell but in the bulb. The sample readily distilled and was seen to have completely gone from the ampoule in about ten minutes, if the sample was cyclohexane or hexafluorobenzene, or in the case of pentafluorocyanobenzene or isopropylcyclohexane, in about forty minutes. The liquid nitrogen was raised around the cell at this point and left for a further ten minutes. When it was thought that no vapour was left unfrozen Tap T3 was opened and a check was made, on the pirani gauge, to see that no leakage had occurred and that distillation was complete.

Nitrogen was introduced to the nitrogen line up to Tap T1. The nitrogen was slowly allowed into the mercury reservoir by turning Tap T1.

The mercury level in the manometer was raised to half way up the manometer. The dewar of liquid nitrogen was removed from around the cell and the stirrer motor clamped into position. The thermostat was then filled with water and the electrical equipment switched on again.

It was found that with pure cyclohexane and pure hexafluorobenzene traces of liquid were found on the mercury surface, in contact with the sample, unless care was taken on filling the thermostat. The mercury surface was kept surrounded with hot water whilst the cell was kept cool to reduce distillation onto the mercury. The top of the thermostat was filled with cold water and the bottom with hot. Any liquid which left the cell condensed on the sloping arm of the manometer and ran back into the cell.



Tap T4, of the main vacuum line, was opened and the manometer side arm evacuated. The mercury levels in the manometer were raised further, if required, by opening Tap T1, and allowing more nitrogen into the mercury reservoir. When the sample in the cell had thawed completely the stirrer motor was switched on.

The thermostat was set to a suitable temperature and the apparatus was left overnight to achieve equilibrium.

The thermostat was altered to the correct temperature the following morning, and the apparatus was evacuated while the equipment re-established equilibrium. The cathetometer was levelled before the heights of the mercury levels and reference mark were taken. The readings were taken on rising menisci. The thermostat temperature, menisci heights, and reference mark, were taken four times. The temperature of the thermostat was measured with a platinum resistance thermometer and the temperature of the cathetometer scale with a mercury in glass thermometer.

The thermostat was then reset, by removing mercury from the regulator, and allowed to reach equilibrium at its new temperature.

More ampoules of the volatile component were added to the cell in the manner described above.

### 3.12.3 Introduction of an Involatile Sample

A cell was prepared as described in section (3.11). The manometer was altered to accommodate the breaker housing, shown in figure (3.11.1). The breaker, a piece of soft iron in an envelope of glass, was placed in the housing and the cell attached to the B19 cone. A teflon sleeve was inserted between cone and socket and the joint was surrounded with mercury.

The manometer was evacuated, making sure that the nitrogen line was evacuated at the same time with Tap T1, open so that the mercury did not rise up the manometer. The sample in the cell was frozen in liquid nitrogen. When the sample was completely frozen Tap T4 was closed, so isolating the pumping system, and the breaker was moved from the housing, by a horse-shoe magnet, and allowed to fall on the delicate hook. The pressure gauge was observed to ensure that there was no leakage in the cell. The mercury in the manometer was raised before the liquid nitrogen was moved from around the cell. The stirrer was placed under the cell and the thermostat filled with water, as described in the previous section.

The pressure measurements were recorded when the equipment had achieved equilibrium.

### 3.13 CALCULATION OF THE VAPOUR PRESSURE

Consider the diagrammatic representation of the manometer and cell shown in figure (3.13.1).

The vapour pressure,  $P$ , at the surface of the liquid can be written as

$$P = P_1 - P_2 \quad (3.13.1)$$

Where  $P_1$  and  $P_2$  are given by

$$P = h_1 \rho_1 g - h_2 \rho_2 g \quad (3.13.2)$$

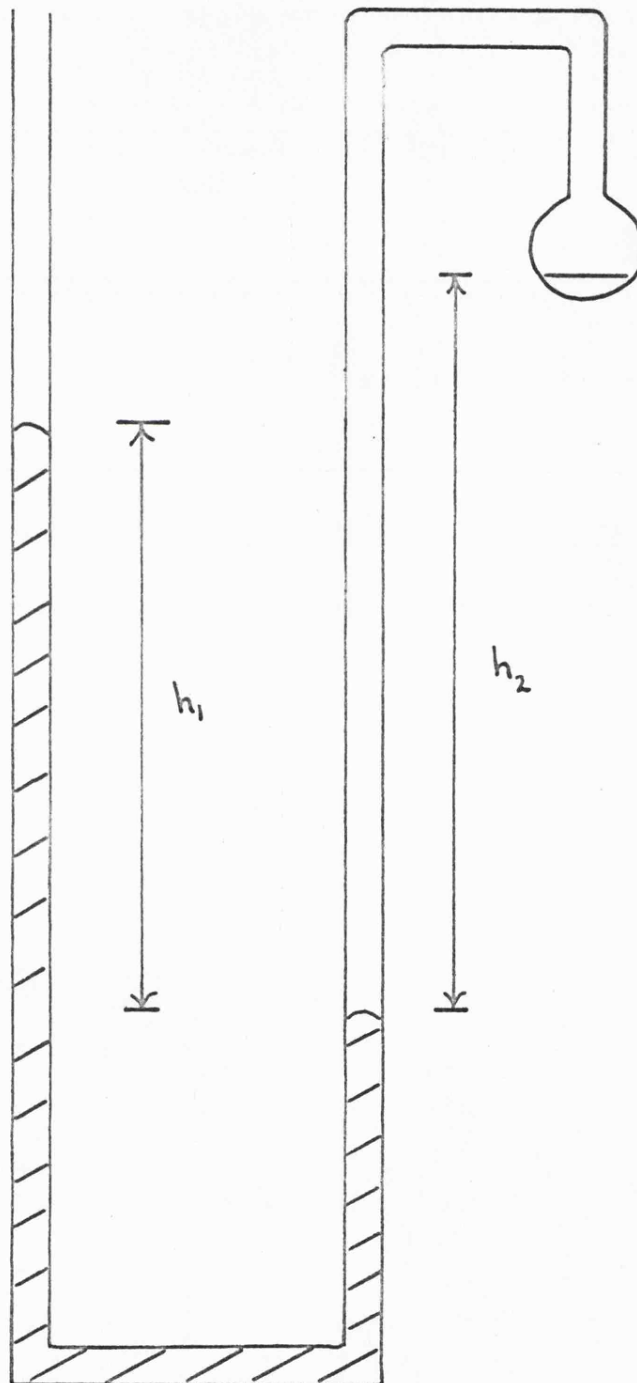
$\rho_1$  = density of mercury at the thermostat temperature

$\rho_2$  = density of the equilibrium vapour at the thermostat temperature.

$g$  = acceleration due to gravity.

FIGURE (3.13.1)

DIAGRAMATIC REPRESENTATION OF THE MANOMETER



If the vapour is treated as being ideal, then  $P_{\text{vap}} V_m = RT$  will apply. If the molecular weight of the vapour is  $M_{\text{vap}}$ ,  $\rho_2$  can be derived as follows,

$$\rho_2 = \frac{M_{\text{vap}}}{V_m} = \frac{P_{\text{vap}} M_{\text{vap}}}{RT} \quad (3.13.3)$$

If it is assumed that  $P_{\text{vap}} \approx P_1$  equation (3.13.3) becomes

$$\rho_2 = \frac{P_1 M_{\text{vap}}}{RT} \quad (3.13.4)$$

and on substitution in equation (3.13.2)

$$P = h_1 \rho_1 g \left( 1 - \frac{h_2 M_{\text{vap}} g}{RT} \right) \quad (3.13.5)$$

The local value of the acceleration due to gravity was calculated to be  $9.81288 \text{ ms}^{-2}$  by using the expression from Kaye and Laby (67) and on substituting for the laboratory latitude and height above sea level.

The density of mercury at the thermostat temperature was calculated from the equation in reference (68).

The scale of the cathetometer was ruled at 293.15K and so only at this temperature was the reading of the instrument giving the true height. In fact the true height,  $h_{\text{true}}$ , at temperature T, is given by,

$$h_{\text{True}} = h_{\text{Read}} (1 + \alpha (T - 293.15)) \quad (3.13.6)$$

where  $h_{\text{read}}$  is the observed height,  $\alpha$  the coefficient of linear expansion of brass =  $1.9 \times 10^{-5} \text{ K}^{-1}$ , and T the temperature of the scale in Kelvin.

A computer programme was used to take into account all these various corrections when calculating the vapour pressures. In this manner accuracy was ensured and tedium avoided. The programme used was a modified form of the one used by Armitage (65) and is listed in the appendix.

## CHAPTER FOUR

### THE VAPOUR PRESSURE RESULTS AND THE CALCULATIONS OF THE EXCESS GIBBS FUNCTIONS

THE VAPOUR PRESSURE RESULTS AND  
CALCULATIONS OF THE EXCESS GIBBS FUNCTIONS

4.1 THE THERMODYNAMICS OF LIQUID - VAPOUR EQUILIBRIUM

Consider the definition of the chemical potential,  $\mu_i$ , of a component  $i$  of a mixture given by,

$$\mu_i = \left( \frac{\partial G}{\partial n_i} \right)_{T, P, n_j} \quad j \neq i \quad (4.1.1)$$

$\mu_i$  is the chemical potential or the partial molar Gibbs function and is an intensive property of a system.

It can be shown that for any system

$$\mu_i = \mu_i^* + RT \ln a_i \quad (4.1.2)$$

where  $a_i$  is the activity of component  $i$ , and  $\mu_i^*$  is the chemical potential of pure  $i$ . For a liquid we can write  $a_i = x_i f_i$ , where  $x_i$  is the mole fraction of component  $i$ , and  $f_i$  is the activity coefficient.

then,

$$\mu_i = \mu_i^* + RT \ln x_i f_i \quad (4.1.3)$$

The Gibbs function,  $G$ , for a two component system is given by,

$$G = n_1 \mu_1 + n_2 \mu_2 \quad (4.1.4)$$

at constant temperature and pressure.

For a process of mixing  $n_1$  moles of component 1, with  $n_2$  moles of component 2, at some temperature,  $T$ , and pressure,  $P$ , we can write

$$\Delta G = n_1 \mu_1 + n_2 \mu_2 - n_1 \mu_1^* - n_2 \mu_2^* \quad (4.1.5)$$

$$\Delta G = n_1 (\mu_1 - \mu_1^*) + n_2 (\mu_2 - \mu_2^*) \quad (4.1.6)$$

by substituting 4.1.3.

$$\Delta G = n_1 RT \ln x_1 f_1 + n_2 RT \ln x_2 f_2 \quad (4.1.7)$$

If the change in Gibbs function per mole of mixture is defined by

$$\Delta_{mG} = \frac{\Delta G}{(n_1 + n_2)}$$

then (4.1.7) becomes

$$\Delta_{mG} = x_1 RT \ln x_1 f_1 + x_2 RT \ln x_2 f_2 \quad (4.1.8)$$

An ideal mixture is one where  $f_i = 1$  so  $\Delta_{mG}(\text{ideal})$  is

$$\Delta_{mG}(\text{ideal}) = x_1 RT \ln x_1 + x_2 RT \ln x_2 \quad (4.1.9)$$

If we define the excess Gibbs function for mixing,  $G^E$ , by

$$G^E = \Delta_{mG} - \Delta_{mG}(\text{ideal}) \quad (4.1.10)$$

then

$$G^E = x_1 RT \ln f_1 + x_2 RT \ln f_2 \quad (4.1.11)$$

An expression for  $\ln f_1$  and similarly  $\ln f_2$  can be derived in terms of the liquid mole fraction of ①  $x_1$ , the vapour mole fraction of ①  $y_1$ , total vapour pressure  $P$ , the vapour pressure of pure ①  $P_1^*$ , and temperature  $T$ , by treating the vapour as being non-ideal and using the fact that the chemical potential of component ① in the liquid will equal the chemical potential of ① in the vapour at equilibrium. Then  $\ln f_1$  is given by,

$$\ln f_1 = \ln \frac{y_1 P}{x_1 P_1^*} + \frac{(B_{11} - V_1^*)(P - P_1^*)}{RT} + \frac{(V_1 - V_1^*)(P^\ominus - P)}{RT} + \frac{B_{11}^2 (P_1^{*2} - P^2)}{2(RT)^2} + (1 - y_1)^2 \frac{\delta_{12} P}{RT} \quad (4.1.12)$$

$\delta_{12}$  is defined by,

$$\delta_{12} = 2B_{12} - B_{11} - B_{22}$$



Where  $B_{11}$ ,  $B_{22}$  and  $B_{12}$  are the second virial coefficients of pure ①, pure ② and the equimolar mixture respectively,  $V_1$  is the partial molar volume of component ① of the mixture and  $V_1^*$  is the molar volume of pure ①.

$\ln f_2$  can be represented similarly.

$$G^E = x_1 \left[ RT \ln (P_{y1} / P_1^* x_1) + (P - P_1^*) (B_{11} - V_1^*) + P \delta_{12} y_1^2 + B_{11}^2 (P_1^{*2} - P^2) / 2RT \right] + x_2 \left[ RT \ln (P_{y2} / P_2^* x_2) + (P - P_2^*) (B_{22} - V_2^*) + P \delta_{12} y_1^2 + B_{22}^2 (P_2^{*2} - P^2) / 2RT \right] + (P^* - P) V^E \quad (4.1.13)$$

Equation (4.1.13) could not be used directly to calculate  $G^E$

because  $y$ , the vapour composition was not measured, so a modification of the procedure by Barker (69) was used to calculate  $G^E$  from the total vapour pressure, composition data.

#### 4.2 THE BARKER METHOD (AND ITS MODIFICATION) FOR CALCULATING $G^E$

In the Barker method,  $G^E$  is expressed as an expansion of the form,

$$\frac{G^E}{RT} = x_1 x_2 (G_0 + G_1 (x_2 - x_1) + G_2 (x_2 - x_1)^2 + \dots)$$

where  $G_0$ ,  $G_1$  ... are constants chosen by a least mean squares procedure so as to minimise errors in the total pressure. It is essential that the mole fraction of the liquid phase be known for the application of the original Barker method. With the present apparatus only the overall mole fraction of the mixture was known precisely and so it was necessary to modify the calculation to allow for the material present in the vapour state. Also it was decided to use the more accurate representation of  $G^E$  given in 4.1.13 than the one used by Barker.

Initially the mole fraction of fluorocarbon in the liquid state  $x_1$ , was set equal to the overall mole fraction of fluorocarbon present and by using the modified Barker technique, a preliminary value for the mole fraction of the fluorocarbon in the vapour state  $y_1$ , was found. This value of  $y_1$  was then used to determine a better value of  $x_1$  by also using a knowledge of the volume of the apparatus occupied by the vapour and by allowing for vapour imperfections.

The data were re-cycled and new values for  $x_1$  and  $y_1$  were calculated until consistency was achieved.

The programme used for the calculation of  $G^E$  was not significantly different from the programme used by Armitage (65). Armitage rigorously tested the programme by recalculating the Gaw and Swinton (18) results for hexafluorobenzene + benzene at 303.15K, 313.15K, 343.15K and also by recalculating the results of Brown (54) for benzene + n-heptane at 353.15K. The programme is listed in the appendix.

#### 4.3 TEST MEASUREMENTS

Workers in this laboratory have previously taken as a test of their vapour pressure apparatus the ability to reproduce the vapour pressure results of pure substances. This is necessary but does not effectively test the technique employed to produce a set of vapour pressures for a mixture of two components. Accordingly it was decided to attempt to reproduce the results of Gaw and Swinton (10) for hexafluorobenzene and cyclohexane at 323.15K.

The vapour pressure results and calculated values of the excess Gibbs functions are given in table (4.3.1). The root mean square deviation (R.M.S./kPa) is defined by,

$$\text{R.M.S.} = \frac{(\sum \text{SP}^2)^{\frac{1}{2}}}{m}$$

where SP is the deviation of the calculated from the experimental vapour pressure, and m is the number of vapour pressure measurements.

The standard deviation (S.D./kPa) is defined by,

$$\text{S.D.} = \frac{(\sum \text{SP}^2)^{\frac{1}{2}}}{m-n}$$

where n is the number of parameters.

The values for these two quantities for the hexafluorobenzene + cyclohexane system are quoted in table (4.3.1).

For the sake of comparison the data used in the calculation of the excess Gibbs functions were the same as those used by Gaw and Swinton (10). They include the second virial coefficients of pure hexafluorobenzene  $B_{11}$ , pure cyclohexane  $B_{22}$ , and the equimolar mixture  $B_{12}$ , the molar volume of pure hexafluorobenzene  $V_{11}$  and pure cyclohexane  $V_{22}$ , and the excess volume of mixing  $V^E$  at  $X_F = 0.5$ . The quantities are quoted in table (4.3.1).

The excess Gibbs functions are represented in figure (4.3.1) together with the results of Gaw and Swinton (10). They are seen to be in excellent agreement.

TABLE (4.3.1)

RESULTS FOR HEXAFLUOROBENZENE AND CYCLOHEXANE AT 323.15K

$X_F$	$Y_F$	$P_{exp}/kPa$	$P_{cal.}/kPa$	$G^E/J \text{ mol}^{-1}$
0	0	36.269	-	-
0.0925	0.2062	42.298	42.318	295
0.1926	0.3076	45.216	45.164	522
0.4554	0.4474	47.043	47.104	769
0.7234	0.5890	45.023	44.989	587
0.8686	0.7332	40.954	40.961	322
1.0000	1.0000	34.103	-	-

R.M.S. = 0.041 kPa

S.D. = 0.091 kPa

$G_0 = 1.1437$

$G_1 = -0.1192$

$G_2 = 0.0456$

$G_3 = -0.0719$

$B_{11} = -0.001975 \text{ m}^3 \text{ mol}^{-1}$

$V_{11} = 0.000120 \text{ m}^3 \text{ mol}^{-1}$

$B_{22} = -0.001380 \text{ m}^3 \text{ mol}^{-1}$

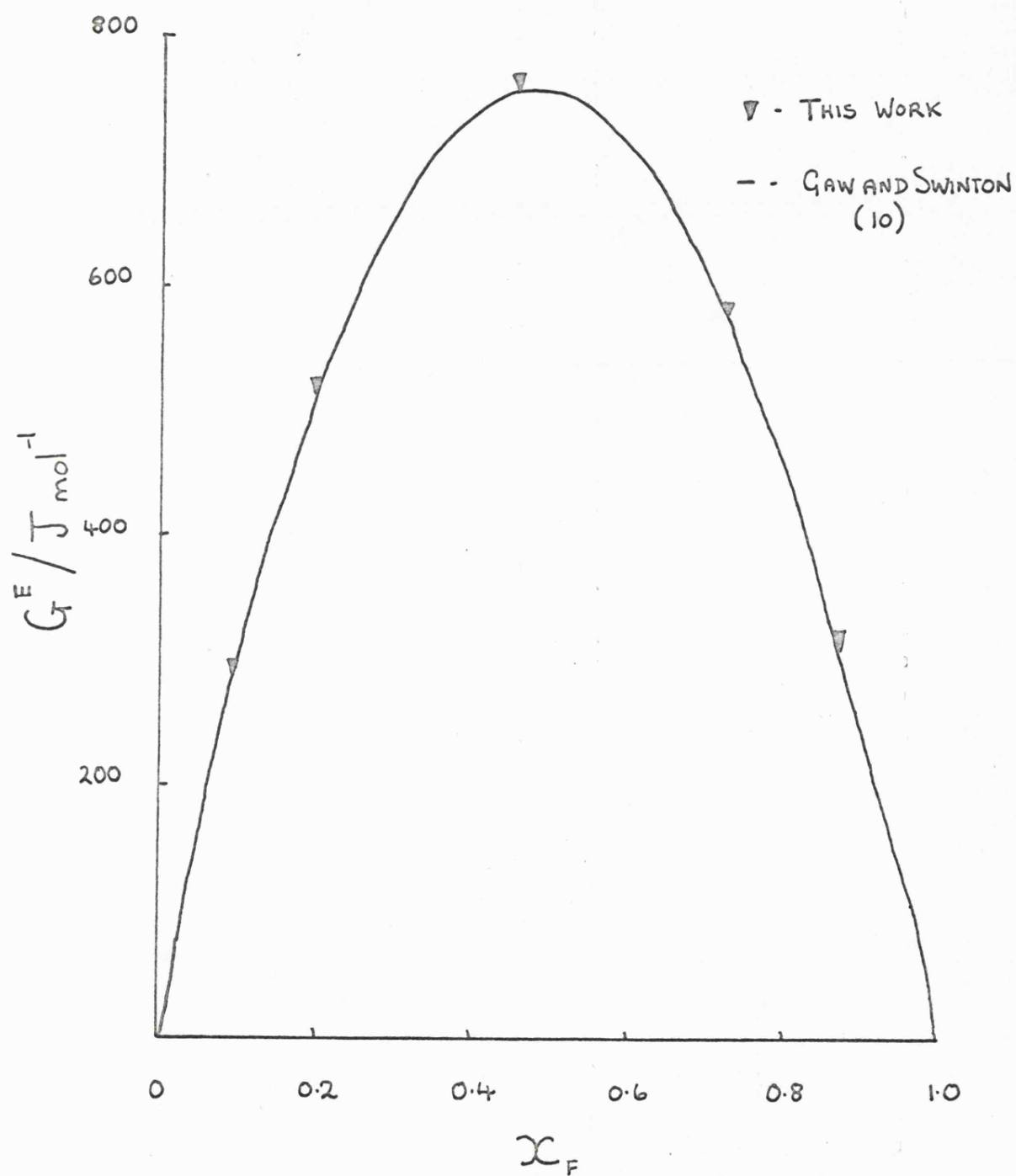
$V_{22} = 0.000112 \text{ m}^3 \text{ mol}^{-1}$

$B_{12} = -0.001100 \text{ m}^3 \text{ mol}^{-1}$

$V^E = 2.56 \times 10^{-6} \text{ m}^3 \text{ mol}^{-1}$

FIGURE (4.3.1)

$G^E$  FOR HEXAFLUOROBENZENE AND CYCLOHEXANE AT 323.15K



#### 4.4 THE VAPOUR PRESSURE RESULTS FOR THE PURE COMPONENTS

##### 4.4.1 Cyclohexane

Some difficulties were encountered when measuring the vapour pressures of the pure components used. These difficulties were wholly due to the presence of moisture in the sample and the choice of the drying agent.

This is well illustrated by the range of vapour pressures obtained for cyclohexane at 323.15K. The results are given in table (4.4.1) together with the drying agent used. The vapour pressure of cyclohexane at 312.58K is also quoted together with the vapour pressure results of other workers.

The results for cyclohexane are in good agreement with literature results.

##### 4.4.2 Hexafluorobenzene

The vapour pressures of hexafluorobenzene at 323.15K and 322.52K are given in table (4.4.2) together with those of other workers. They are seen to be in good agreement.

##### 4.4.3 N,N-Dimethylaniline

The vapour pressure result for N,N-dimethylaniline at 322.52K is given in figure (4.4.1) together with the results of other workers. It was considered to be in good agreement.

##### 4.4.4 Isopropylcyclohexane

The vapour pressure result for isopropylcyclohexane at 323.15K is given in table (4.4.3) together with the vapour pressure for isopropylcyclohexane at this temperature calculated from the Antoine constants of Forziati, Norris and Rossini (77).

TABLE (4.4.1)

VAPOUR PRESSURE OF PURE CYCLOHEXANE AT 323.15K

VAPOUR PRESSURE/kPa

39.366	Sample not stood over drying agent
37.761	Sample stood over phosphorus pentoxide and syringed into vessel
36.683	Sample stood over molecular sieve in vacuum line.
36.269	Sample stood over phosphorus pentoxide in vacuum line.
36.248	Gaw and Swinton (10).
36.237	A.P.I. Project 55 ( 70 )
36.266	Brown ( 54 )

---

VAPOUR PRESSURE OF PURE CYCLOHEXANE AT 312.58K.

VAPOUR PRESSURE/kPa

Worker

24.078	This work
24.064	A.P.I. Project 55 ( 70 )

---

TABLE (4.4.2)

VAPOUR PRESSURE OF PURE HEXAFLUOROBENZENE AT 323.15K

<u>VAPOUR PRESSURE/kPa</u>	<u>WORKER</u>
34.103	This work
33.970	Patrick and Prosser ( 71 )
34.089	Gaw and Swinton ( 10 )
34.090	Counsell et al ( 72 )
34.106	Armitage ( 65 )

VAPOUR PRESSURE OF PURE HEXAFLUOROBENZENE AT 322.52K

<u>VAPOUR PRESSURE/kPa</u>	<u>WORKER</u>
33.245	This work
33.224	Counsell et al ( 72 )
33.117	Patrick and Prosser ( 71 )



FIGURE (A.4.1)

THE VAPOUR PRESSURES OF N,N-DIMETHYLANILINE AT VARIOUS  
TEMPERATURES

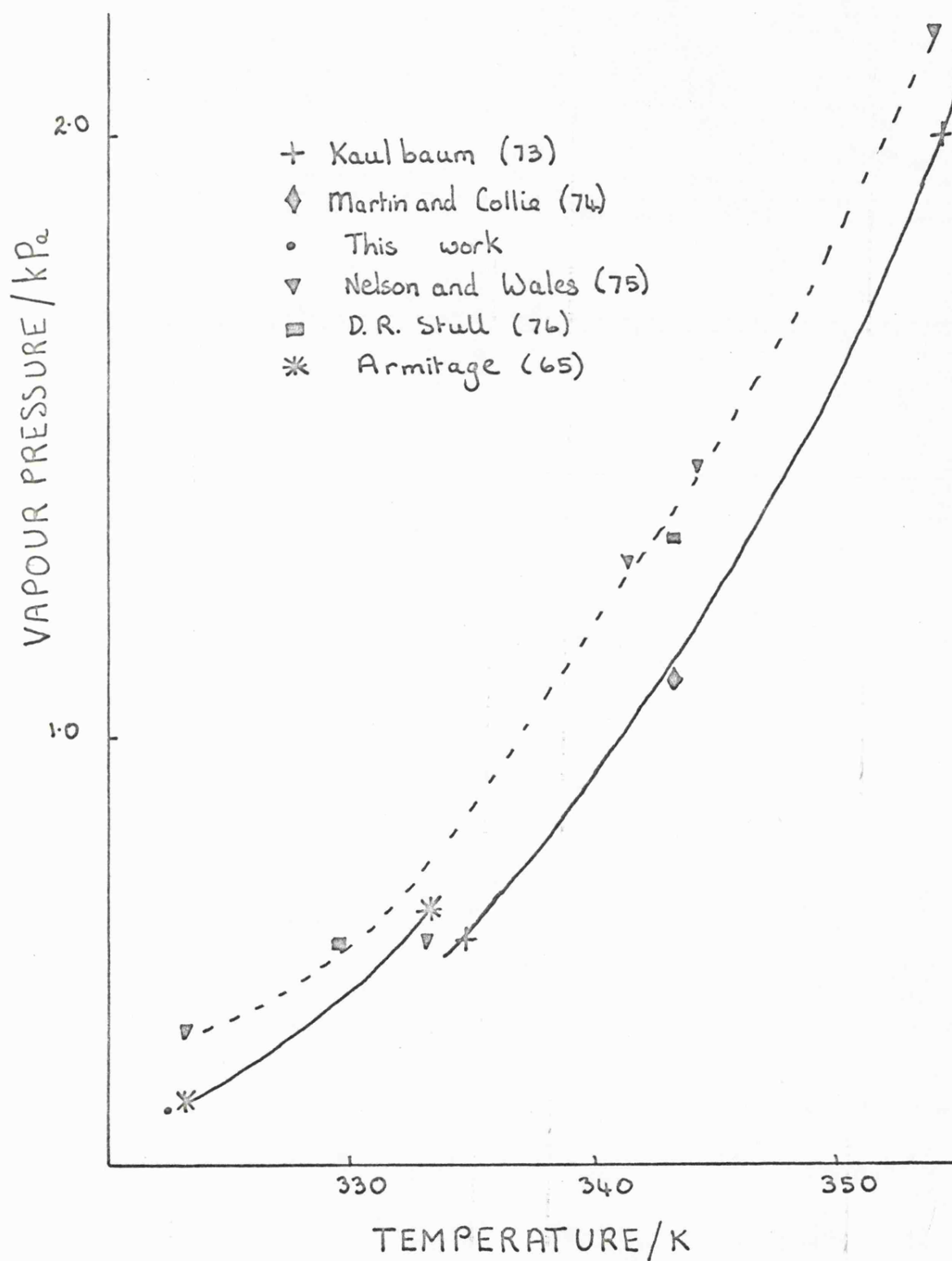


TABLE (4.4.3)

THE VAPOUR PRESSURE OF ISOPROPYLCYCLOHEXANE AT 323.15K

<u>VAPOUR PRESSURE/kPa</u>	<u>WORKER</u>
2.773	This work
2.492	Forziati, Norris, Rossini (77 ) (calculated from the Antoine constants based on experimental data above 343.15K)

Their experimental results were determined above 343.15K. The results are seen to be reasonably close.

#### 4.4.5 Pentafluorocyanobenzene

There were no literature data available for pentafluorocyanobenzene. The only test for the vapour pressure results obtained was that they predicted a boiling point in agreement with the literature value of 435.15K. The vapour pressure results are given in table (4.4.4). They were determined at four temperatures, 308.08K, 312.58K, 317.64K and 323.15K. Figure (4.4.2) is a plot of the vapour pressures against temperature, and figure (4.4.3) is a plot of  $\log_{10}$  vapour pressure against the reciprocal of the temperature including the literature boiling point (78). The vapour pressure results extrapolate well to the literature boiling point. The heat of vapourization, calculated from figure (4.4.3), is given in table (4.4.4)

### 4.5 THE VAPOUR PRESSURE RESULTS AND THE CALCULATED $G^E$ VALUES FOR THE MIXTURES STUDIED

#### 4.5.1 N,N-Dimethylaniline + Hexafluorobenzene

The results for the system N,N-dimethylaniline (DMA) + hexafluorobenzene (F) at 322.52K are given in table (4.5.1). The excess Gibbs functions are represented in figure (4.5.1). The R.M.S. deviation and standard deviation are quoted in table (4.5.1)

The data used in the modified Barker programme is listed in table (4.5.1). The second virial coefficient for hexafluorobenzene  $B_{11}$ , was taken from the values calculated by Douslin, Harrison and Moore (79) from enthalpies of vapourisation and vapour pressure measurements. There was no second virial coefficient data available for N,N-dimethylaniline or any related compound so values of 0.0 and -0.002 were substituted in turn.

TABLE (4.4.4)

THE VAPOUR PRESSURE RESULTS FOR PURE PENTAFLUOROCYANOBENZENE AT  
SEVERAL TEMPERATURES

<u>Temperature/K</u>	<u>Vapour Pressure/kPa</u>
308.08	0.529
312.58	0.685
317.64	0.897
323.15	1.244
435.15	101.325 (78)

The heat of vapourisation =  $4.760 \times 10^4 \text{ J mol}^{-1}$

FIGURE (1.1.2)

THE VAPOUR PRESSURE RESULTS OF PURE PENTAFLUOROCYANOBENZENE

PLOTTED AGAINST TEMPERATURE

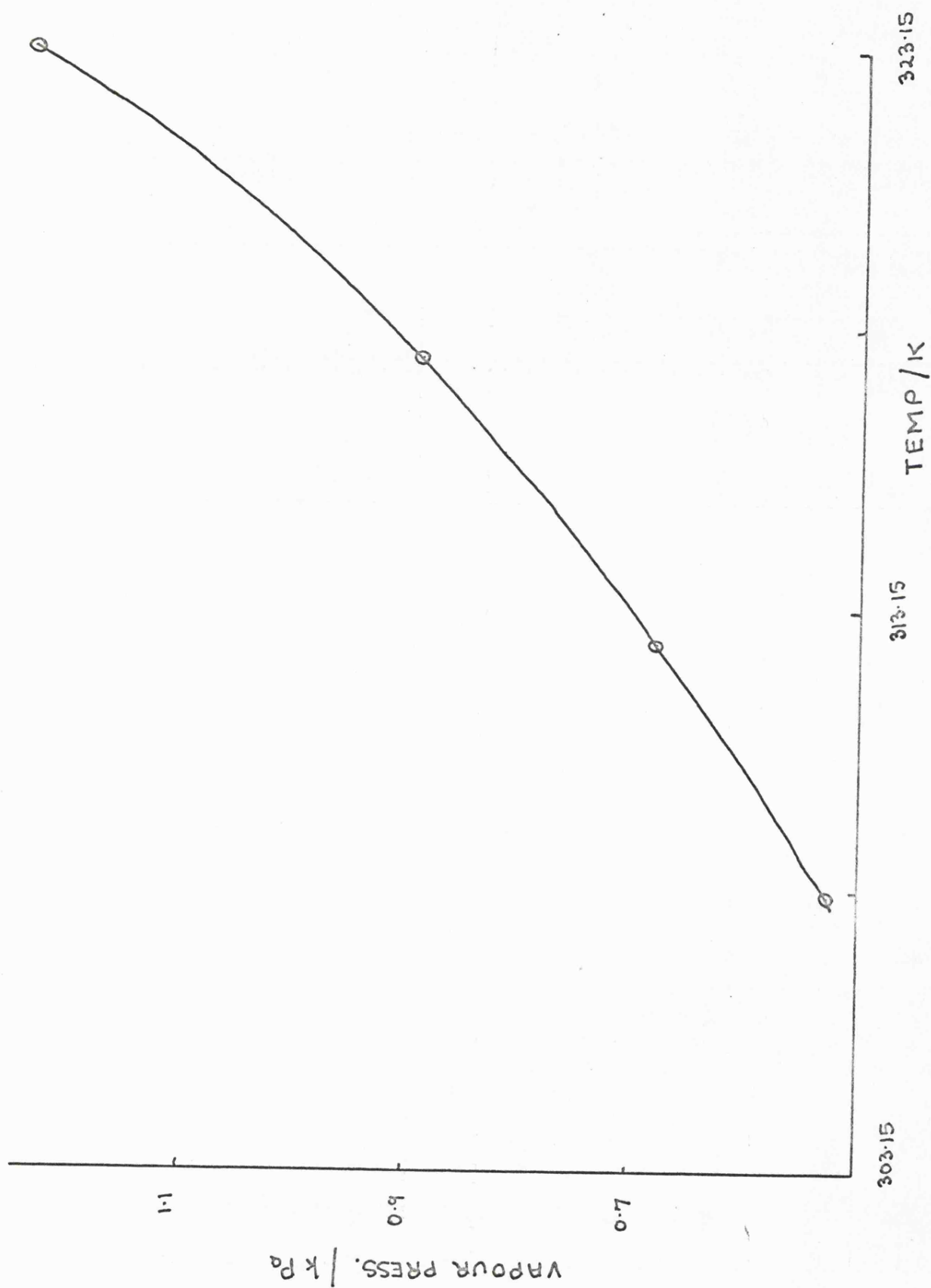


FIGURE (4.4.3)

$\text{LOG}_{10}$  VAPOUR PRESSURE AGAINST RECIPROCAL TEMPERATURE FOR

PENTAFLUOROCYANOBENZENE

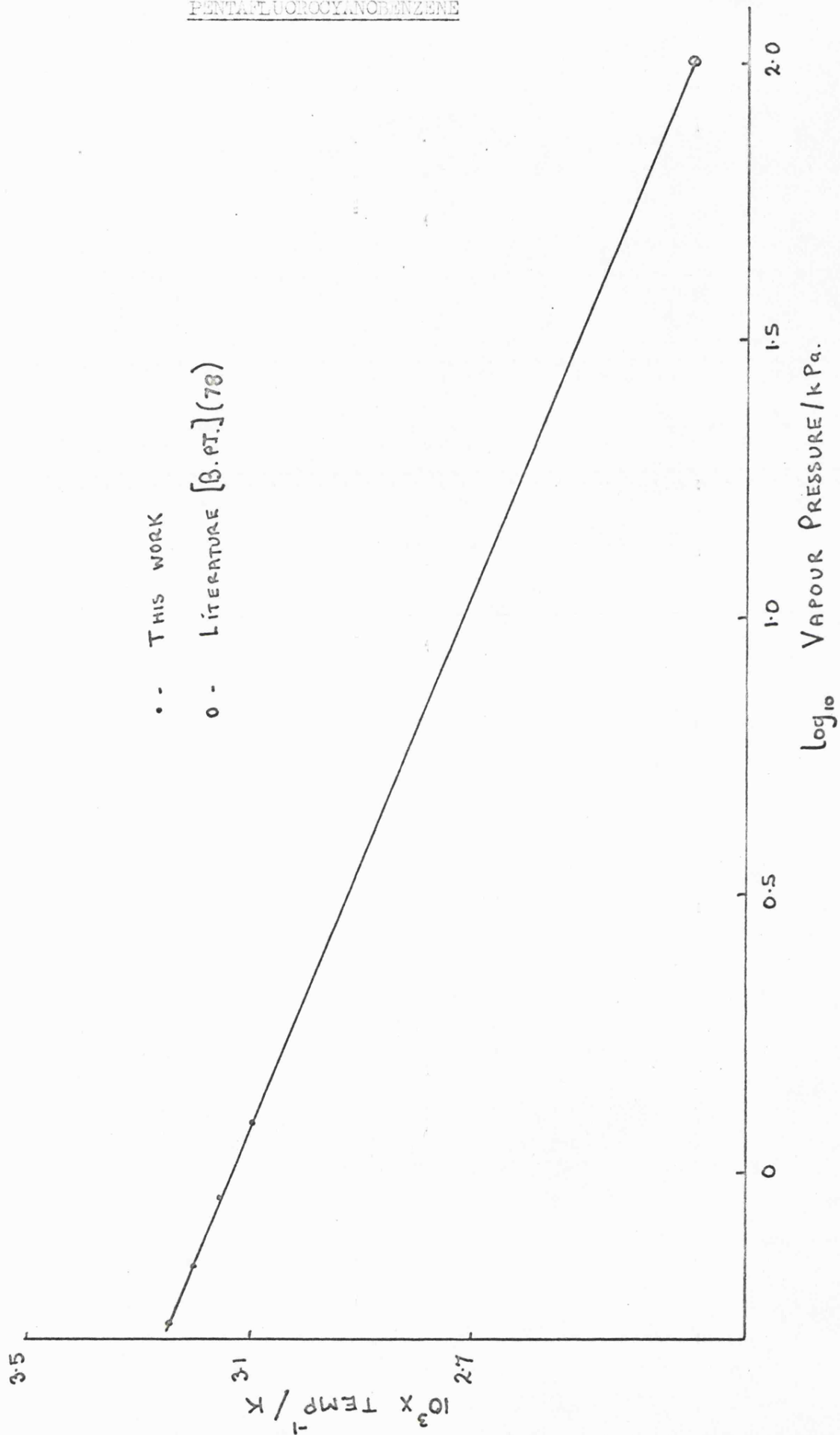


TABLE (4.5.1)

THE RESULTS FOR N,N-DIMETHYLANILINE AND HEXAFLUOROBENZENE (F) AT 322.52K

$X_F$	$Y_F$	$P_{exp}/kPa$	$P_{cal.}/kPa$	$G^E/J \text{ mol}^{-1}$
0.0	0.0	0.387	-	-
0.1351	0.9195	4.135	4.117	-68
0.3197	0.9710	9.077	9.141	-141
0.4166	0.9813	11.979	11.941	-181
0.5010	0.9874	14.808	14.742	-207
0.5892	0.9919	18.063	18.085	-217
0.6759	0.9951	21.582	21.668	-200
0.7973	0.9977	26.671	26.596	-132
1.0	1.0	33.245	-	-

R.M.S. = 0.058 kPa

S.D. = 0.089 kPa

$G_0 = -0.3092$

$G_1 = -0.1735$

$G_2 = 0.1389$

$G_3 = 0.2793$

$B_{11} = -0.001990 \text{ m}^3 \text{ mol}^{-1}$        $V_{11} = 0.0001199 \text{ m}^3 \text{ mol}^{-1}$

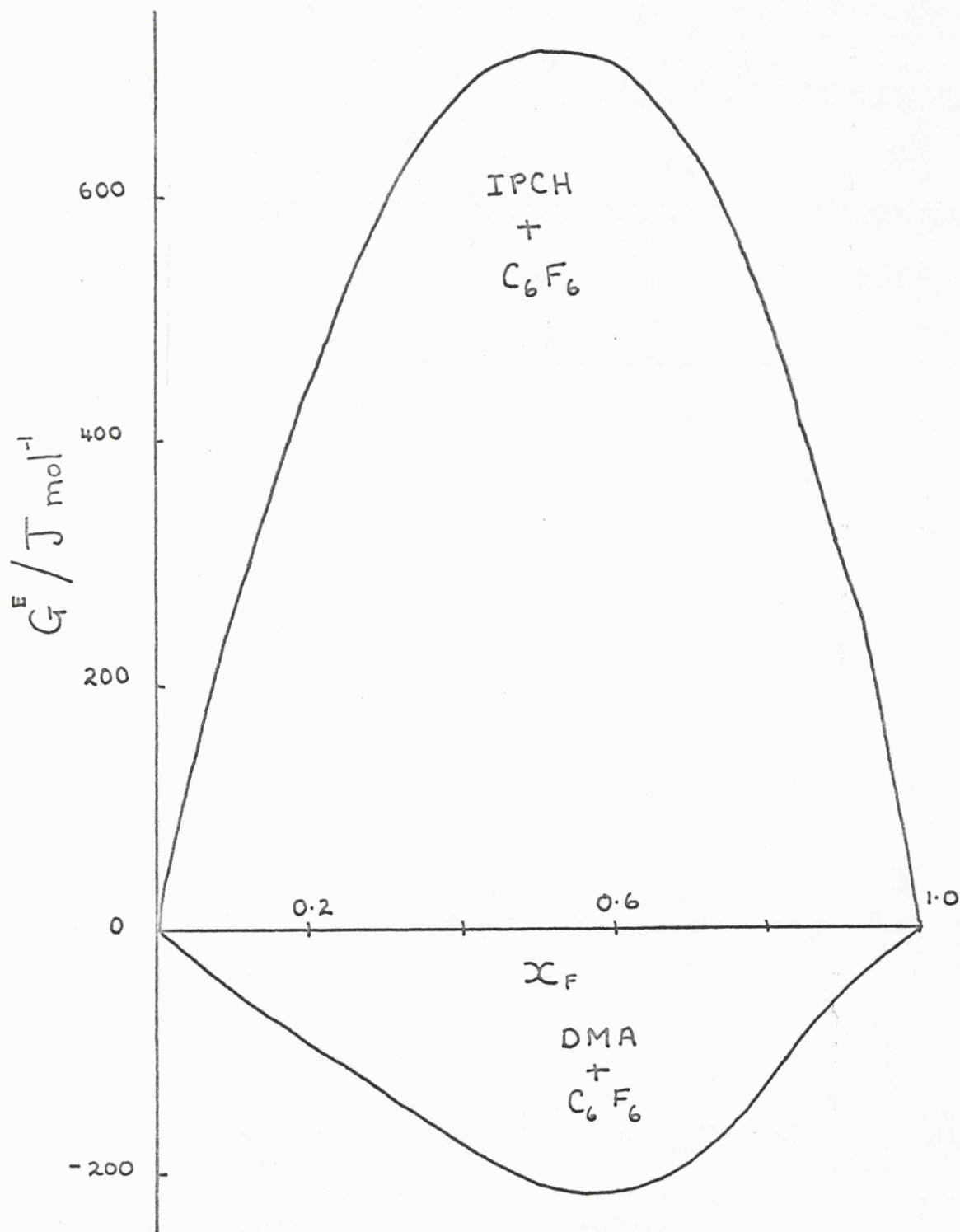
$B_{22} = 0.0 \text{ m}^3 \text{ mol}^{-1}$        $V_{22} = 0.0001298 \text{ m}^3 \text{ mol}^{-1}$

$B_{12} = -0.000998 \text{ m}^3 \text{ mol}^{-1}$        $V^E = -4.86 \times 10^{-7} \text{ m}^3 \text{ mol}^{-1}$

FIGURE (4.5.1)

EXCESS GIBBS FUNCTIONS FOR HEXAFLUOROBENZENE + N,N-DIMETHYLANILINE

AT 322.52K AND ISOPROPYLCYCLOHEXANE AT 323.15K





The difference in the excess Gibbs functions was  $0.1 \text{ J mol}^{-1}$ , which was within the experimental error, so  $B_{22}$  was put equal to zero. The crossed virial coefficient was estimated as being equal to the arithmetic mean of  $B_{11}$  and  $B_{22}$ . The molar volumes of pure hexafluorobenzene  $V_{11}$ , and pure N,N-dimethylaniline  $V_{22}$  are quoted together with the excess volume of mixing  $V^E$  at  $X_F = 0.5$  (chapter 6).

Four coefficients were required to obtain a satisfactory fit to the data and these are also given in table (4.5.1).

During the series of measurements the outer coating of glass around a metal breaker smashed at the third experimental point. There was no apparent increase in pressure due to the presence of air as the frozen sample was quickly pumped on to remove any air. The system was continued as it was thought that any contamination was due to air and this had been removed. However, for this reason the results are not considered to be of the highest precision, the uncertainty on the excess Gibbs functions is probably about  $\pm 20 \text{ J mol}^{-1}$ . The excess Gibbs function for the system is seen to be negative.

#### 4.5.2 Isopropylcyclohexane + Hexafluorobenzene

The results for isopropylcyclohexane (IPCH) and hexafluorobenzene (F) at 323.15K are given in table (4.5.2) together with the R.M.S. and standard deviations and coefficients for the excess Gibbs function fit. The data for the modified Barker programme is also quoted. The second virial coefficient for hexafluorobenzene  $B_{11}$ , was taken from reference (79). No data were available for the second virial coefficient of isopropylcyclohexane  $B_{22}$ , so the data for cyclohexane determined by Hajjar, Kay and Leverett (80) was used.  $V_{11}$  and  $V_{22}$  are the molar volumes of hexafluorobenzene and isopropylcyclohexane and these are given together with the excess volume at  $x_F = 0.5$  (chapter 6).

TABLE (4.5.2)

THE RESULTS FOR ISOPROPYLCYCLOHEXANE AND HEXAFLUOROBENZENE (F) AT 323.15K

$X_F$	$Y_F$	$P_{exp}/kPa$	$P_{cal.}/kPa$	$G^E/J \text{ mol}^{-1}$
0.0	0.0	2.773	-	-
0.1111	0.7724	11.020	11.043	278
0.2076	0.8549	15.936	15.892	464
0.3249	0.8950	20.025	20.041	623
0.4277	0.9153	22.741	22.787	702
0.5787	0.9367	26.122	26.041	716
0.7183	0.9527	28.545	28.614	617
0.7772	0.9599	29.675	29.655	540
1.0	1.0	34.103	-	-

R.M.S. = 0.048 kPa

S.D. = 0.074 kPa

$G_O = 1.0781$

$G_1 = 0.0847$

$G_2 = 0.0902$

$G_3 = 0.0427$

$B_{11} = -0.001975 \text{ m}^3 \text{ mol}^{-1}$

$V_{11} = 0.0001200 \text{ m}^3 \text{ mol}^{-1}$

$B_{22} = -0.001380 \text{ m}^3 \text{ mol}^{-1}$

$V_{22} = 0.0001622 \text{ m}^3 \text{ mol}^{-1}$

$B_{12} = -0.001677 \text{ m}^3 \text{ mol}^{-1}$

$V^E = 2.11 \times 10^{-6} \text{ m}^3 \text{ mol}^{-1}$

The excess Gibbs energies are represented in figure (4.5.1). They are seen to be quite large and positive.

#### 4.5.3 Pentafluorocyanobenzene + Cyclohexane

The results for pentafluorocyanobenzene + cyclohexane at 312.58K and 323.15K are given in tables (4.5.3) and (4.5.4). There was no data available on the second virial coefficient of pentafluorobenzonitrile  $B_{11}$ , and as on using values of 0 and -0.002 a change of only  $0.1 \text{ J mol}^{-1}$  was seen in the excess Gibbs functions  $B_{11}$  was put equal to zero at both temperatures. The second virial coefficient of cyclohexane  $B_{22}$ , for both temperatures was taken from Hajjar, Kay and Leverett (80) and  $B_{12}$  for the equimolar mixture was assumed to be the arithmetic mean of  $B_{11}$  and  $B_{22}$ . The excess volume of mixing at  $X_F = 0.5$  was taken to be the same at both temperatures and was determined by Fenby (15).

The excess Gibbs functions are represented in figure (4.5.2).

Eight coefficients were required to obtain a satisfactory fit for the excess Gibbs functions. The results were determined by successive addition of cyclohexane samples to an initial sample of pentafluorocyanobenzene. It was intended to then determine the vapour pressures from the cyclohexane rich region to the equimolar part of the vapour pressure curve but the barrel of tap  $T_2$ , positioned on the top of the manometer, broke and there was not enough time to allow repair of the apparatus and continuation of vapour pressure work. There is thus a small but accumulating error on the compositions of the mixtures.

TABLE (4.5.3)

THE RESULTS FOR PENTAFLUOROCYANOBENZENE (F) AND CYCLOHEXANE AT 312.58K

$X_F$	$Y_F$	$P_{exp}/kPa$	$P_{cal.}/kPa$	$G^E/J \text{ mol}^{-1}$
0.0	0.0	24.078	-	-
0.1484	0.0233	23.446	23.413	868
0.1837	0.0203	23.356	23.395	994
0.2423	0.0223	23.269	23.273	1159
0.3379	0.0247	23.038	23.009	1335
0.4404	0.0232	22.892	22.906	1413
0.5062	0.0225	22.740	22.776	1405
0.5532	0.0253	22.592	22.574	1374
0.5889	0.0266	22.398	22.360	1336
0.6968	0.0247	21.318	21.363	1149
0.7705	0.0315	19.696	19.665	956
0.8467	0.0389	15.699	15.709	709
0.9572	0.0837	7.995	7.994	262
1.0	1.0	0.685	-	-

R.M.S. = 0.028 kPa

S.D. = 0.049 kPa

$G_0 = 2.1663$        $G_1 = -0.2934$        $G_2 = 0.3022$

$G_3 = -0.0043$        $G_4 = -0.0209$        $G_5 = -0.8928$

$G_6 = 0.5324$        $G_7 = 1.0994$

$B_{11} = 0.0 \text{ m}^3 \text{ mol}^{-1}$        $V_{11} = 0.0001253 \text{ m}^3 \text{ mol}^{-1}$

$B_{22} = -0.001531 \text{ m}^3 \text{ mol}^{-1}$        $V_{22} = 0.0001110 \text{ m}^3 \text{ mol}^{-1}$

$B_{12} = -0.000765 \text{ m}^3 \text{ mol}^{-1}$        $V^E = 1.87 \times 10^{-6} \text{ m}^3 \text{ mol}^{-1}$

TABLE (4.5.4)

THE RESULTS FOR PENTAFLUOROCYANOBENZENE (F) AND CYCLOHEXANE AT 323.15K

$\underline{X_F}$	$\underline{Y_F}$	$\underline{P_{exp}/kPa}$	$\underline{P_{cal.}/kPa}$	$\underline{G^E/J \text{ mol}^{-1}}$
0.0	0.0	36.269	-	-
0.1492	0.0249	35.028	34.999	839
0.1822	0.0239	34.831	34.860	954
0.2421	0.0254	34.555	34.570	1120
0.3374	0.0282	34.171	34.130	1291
0.4396	0.0265	33.723	33.769	1362
0.5131	0.0291	33.362	33.344	1347
0.5576	0.0292	32.941	32.943	1312
0.5940	0.0304	32.555	32.539	1271
0.7198	0.0322	30.412	30.441	1028
0.7913	0.0387	27.628	27.598	820
0.8510	0.0469	22.820	22.835	612
0.9320	0.0940	12.443	12.441	296
1.0	1.0	1.244	-	-

R.M.S. = 0.026 kPa

S.D. = 0.045 kPa

$$G_0 = 2.0148$$

$$G_1 = -0.3239$$

$$G_2 = 0.2325$$

$$G_3 = -0.1021$$

$$G_4 = -0.1059$$

$$G_5 = -0.6334$$

$$G_6 = 0.2153$$

$$G_7 = 0.4644$$

$$B_{11} = 0.0 \text{ m}^3 \text{ mol}^{-1}$$

$$V_{11} = 0.0001255 \text{ m}^3 \text{ mol}^{-1}$$

$$B_{22} = -0.001380 \text{ m}^3 \text{ mol}^{-1}$$

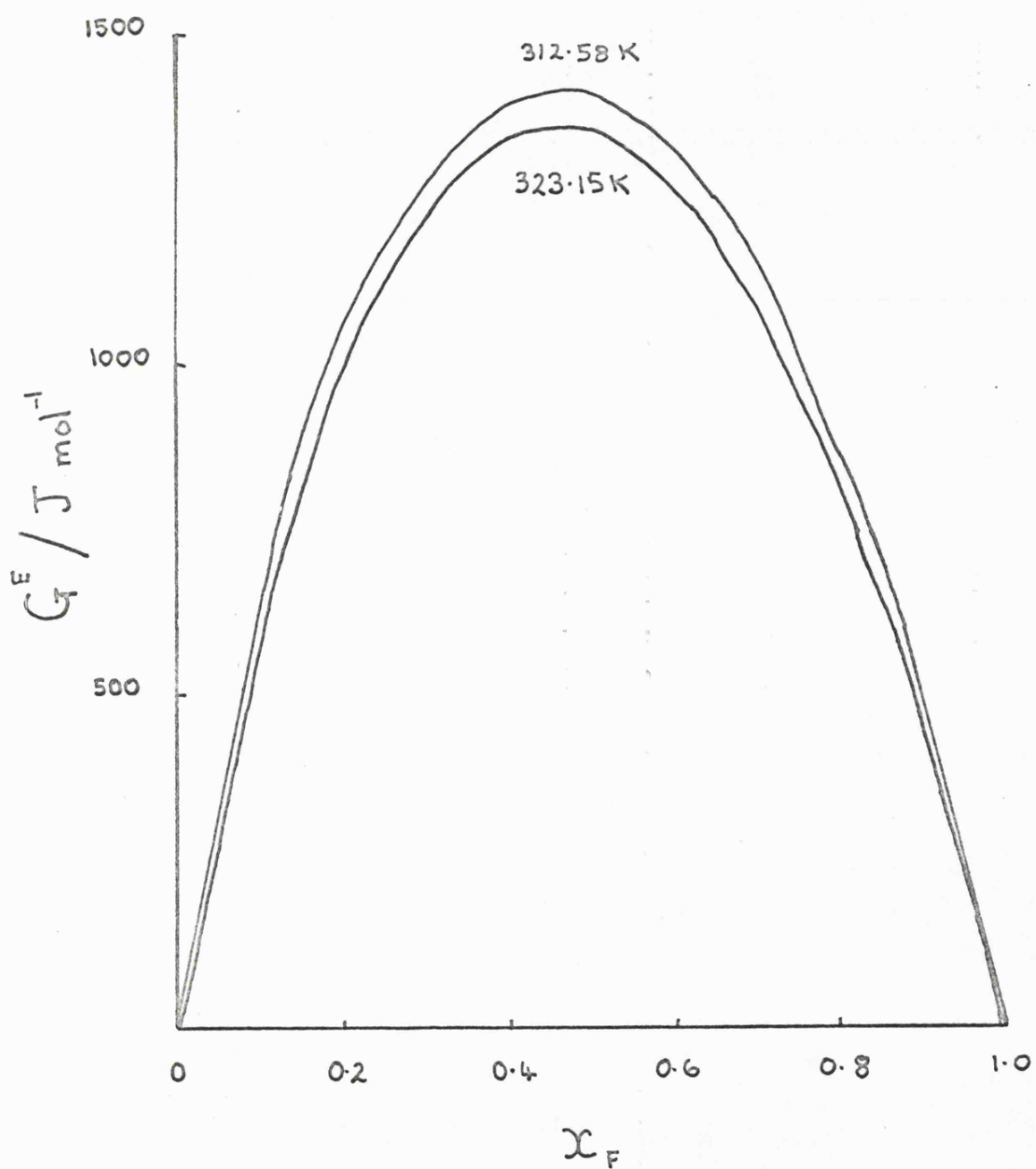
$$V_{22} = 0.0001120 \text{ m}^3 \text{ mol}^{-1}$$

$$B_{12} = -0.00069 \text{ m}^3 \text{ mol}^{-1}$$

$$V^E = 1.87 \times 10^{-6} \text{ m}^3 \text{ mol}^{-1}$$

FIGURE (4.5.2)

$G^E$  FOR PENTAFLUOROCYANOBENZENE AND CYCLOHEXANE AT 323.15K AND 312.58K



#### 4.6 CORRELATION OF VAPOUR PRESSURES WITH MOLAR EXCESS ENTHALPIES

Since the excess Gibbs functions have been measured at two temperatures for pentafluorocyanobenzene + cyclohexane it is possible to calculate the molar excess enthalpies. However the temperature interval is small, because at lower temperatures the system phase separates, so the calculation of  $H^E$  is very imprecise.

Assuming that the excess Gibbs function at  $X_F = 0.5$  is reliable to  $\pm 20 \text{ J mol}^{-1}$ , then the excess enthalpy for  $X_F = 0.5$  at 323.15K is calculated to be  $3.0 \pm 1.2 \text{ kJ mol}^{-1}$ . The experimental value of the excess enthalpy (chapter 5) is  $2.12 \text{ kJ mol}^{-1}$ . Therefore the calculated excess enthalpy is of the same order of magnitude as the experimental excess enthalpy.

CHAPTER FIVE

EXCESS ENTHALPIES OF MIXING



## EXCESS ENTHALPIES OF MIXING

### 5.1 INTRODUCTION

For the process of mixing  $N_1$  moles of component 1 with  $N_2$  moles of component 2 in a calorimeter and applying the first law, the change in thermodynamic energy  $\Delta U$  is given by,

$$\Delta U = U(\text{mixture}, T_f) - U(\text{unmixed}, T_i) = q + W_s + W_{\text{exp}} \quad (5.1.1)$$

where  $T_i$  and  $T_f$  are the initial and final temperatures,  $-q$  represents any heat losses,  $W_s$  is the work of stirring, and  $W_{\text{exp}}$  is a term which allows for the work done due to a change in volume of the calorimeter or its contents.

However the energy change at a given temperature,  $T_i$ , is required. If it is assumed that the mixing process is exothermic, ie.  $T_f > T_i$ , then the calorimeter and contents will cool back to  $T_i$  and the measure of the quantity of electrical energy,  $W_{el}$ , needed to raise the temperature of the calorimeter from  $T_i$  to  $T_f$  is,

$$\begin{aligned} U(\text{mixture}, T_f) - U(\text{mixture}, T_i) &= \int_{T_i}^{T_f} C_f dT \\ &= -q + W_{el} \end{aligned} \quad (5.1.2)$$

where  $C_f$  is the heat capacity of the calorimeter and its contents after mixing and it is assumed that any heat losses,  $-q$ , are the same as in the previous stage.

On subtracting (5.12) from (5.11) the following is obtained.

$$\Delta U(T_i) = U(\text{mixture}, T_i) - U(\text{unmixed}, T_i) = W_s + W_{\text{exp}} - W_{el} \quad (5.1.3)$$

If the calorimeter is of the constant pressure type (89), in which the components are subjected to a constant pressure,  $P$ , throughout the mixing process then,

$$W_{\text{exp}} = - P \Delta V \quad (5.1.4)$$

where  $\Delta V$  is the change in volume of the liquid mixture. The enthalpy change on mixing,  $\Delta H (T_i)$  is then given by,

$$\Delta H (T_i) = W_s - W_{el} \quad (5.1.5)$$

Most modern calorimeters, designed to study mixtures, involve a sealed system incorporating an expansion bulb and are neither constant pressure nor constant volume calorimeters. However if the expansion bulb is sufficiently large, (as in the Larkin and McGlashan type calorimeter described in section (5.2)), the mixing process approximates to a constant pressure process with negligible error.

The quantities measured in the present work can thus be regarded as enthalpies of mixing.

The above describes the basic principles of the calorimeter. In practice a nulltechnique was used for all of the measurements and the experimental technique is described in detail in sections (5.9) and (5.10).

The molar excess enthalpy  $H^E$ , which is the quantity tabulated in the section containing the experimental results (5.14), is defined by

$$H^E = \Delta H / (N_1 + N_2)$$

where  $\Delta H$  is the enthalpy change of mixing,  $N_1$  is the number of moles of component 1, and  $N_2$  is the number of moles of component 2..

For an ideal solution there is no change in enthalpy on mixing components 1 and 2 so  $\Delta H$  is zero. Therefore any measured enthalpy change directly gives the excess enthalpy of mixing.

Larkin and McGlashan (81,82) were responsible for the design of a calorimeter which allowed high accuracy combined with ease of loading and absence of vapour spaces.

The basic design was adopted by Marcom and Travers (83 ) although they used a polystyrene jacket rather than a vacuum for thermal insulation.

A single calorimeter, of the above type, is ideally suited to measurement of endothermic enthalpies of mixing. However, use of such a calorimeter for exothermic enthalpies gives rise to errors of the galvanometer being operated on too low a sensitivity and indefinite cooling curves.

Atwin calorimeter, utilising a null technique, was developed by Armitage (65). It comprised two calorimeter vessels, of the type used by Marcom and Travers (83), thermally insulated from one another and the thermostat bath by a polystyrene jacket. The null technique enables the galvanometer recorder to be used at a high sensitivity and makes the extrapolation of the cooling curves more accurate as the overall temperature differences are small. This was the type of apparatus used for the present measurements so will be described more fully in section (5.2).

Several workers have adopted similar designs (84-86).

## 5.2 CALORIMETER VESSELS

The vessels used are shown in figure (5.2.1) and were made by Messrs. Jencons (Scientific) Ltd. They contained a glass partition to separate the two components, a pocket to accommodate an electric heater and had a neck with a B7 socket.

The calorimeter thermometer consisted of three thermistors (Standard Telephones and Cables type M52 with a resistance at room temperatures of 450  $\Omega$ ) wired in parallel on the surface of the vessel such that they were adjacent to the mercury rather than the liquids. This was done so that the thermistors did not record any instantaneous non-equilibrium temperatures which can occur in the liquid after mixing. The copper discs of the thermistors were stuck to the surface of the vessel with a little Araldite.

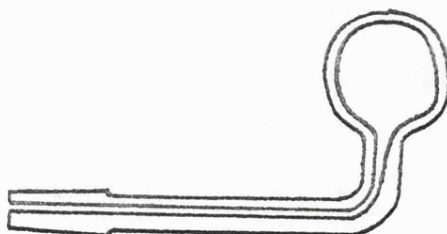
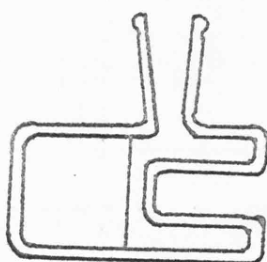
The calorimeter heater consisted of a length of eureka wire (cotton covered constantan of 38SWG) wound onto a teflon plug, of the type shown in figure (5.2.1), machined such that the heater was a push fit into the glass pocket of the vessel. The teflon plug contained two holes from which the heater wires protruded.

The thermistors and heater wires were soldered to copper wires which were sheathed and soldered to a four way, non-reversible plug. The wires were bent until the plug was in a suitable position and then all the exposed wires were thickly coated with Araldite.

The calorimeters were sealed, when loaded, by gently pushing into the socket the bulb attachment shown in figure (5.2.1)

FIGURE (5.2.1)

HEAT OF MIXING CALORIMETER AND EXPANSION BULB



### 5.3 HEATER CIRCUIT

The heater circuit is shown in figure (5.3.1). It was designed so that heat could be put into both or either calorimeter, as necessary,

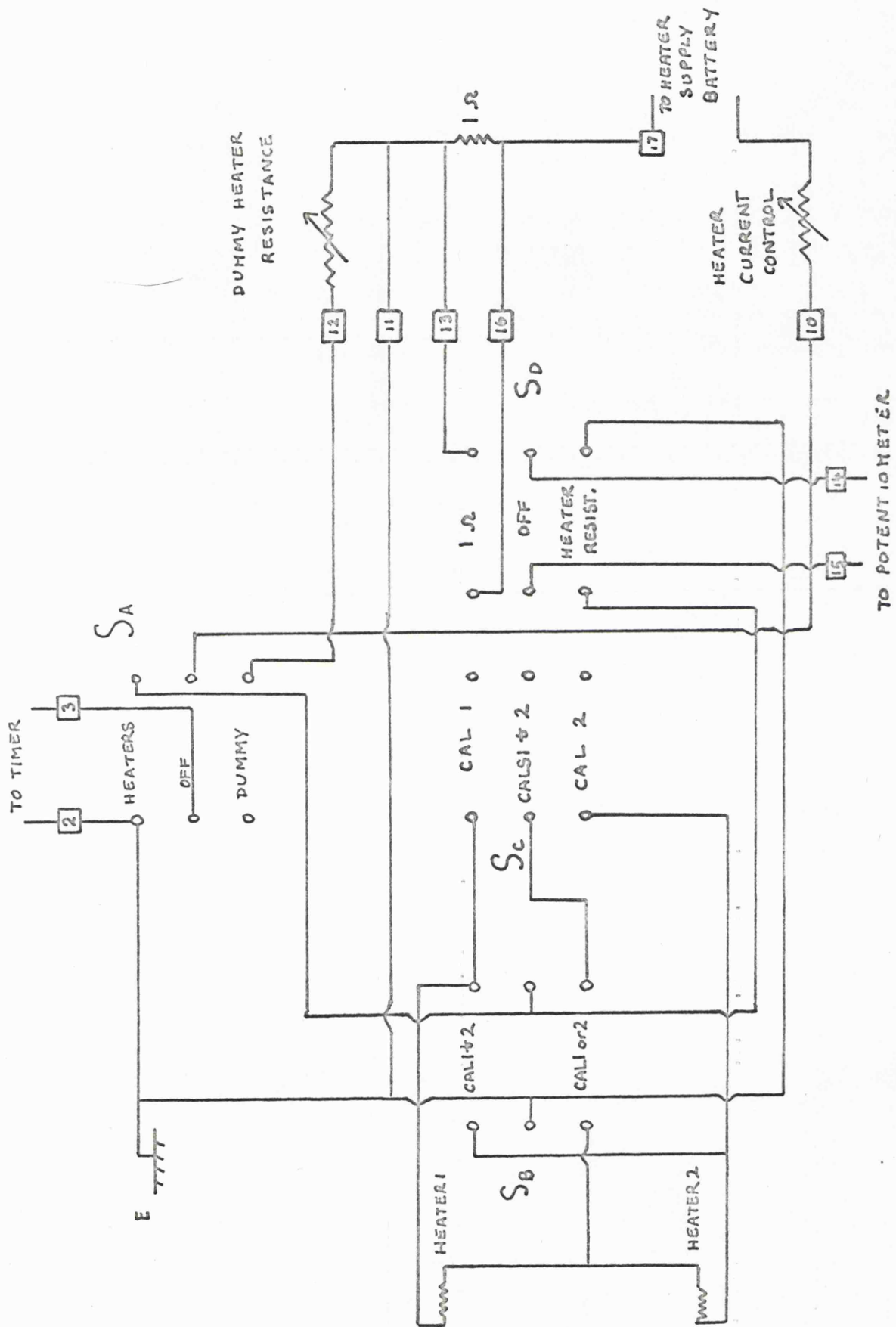
Two four-decade resistance boxes were used. One was the heater current control, which was set to give the required current through the heater (the value of which was calculated from an estimated enthalpy change), and the other was the dummy heater resistance. The dummy heater resistance was set equal to the total resistance at the part of the heater circuit to be used in the measurement. The heater supply battery was connected through the dummy heater resistance so as to allow the battery to stabilise before heating was commenced.

The heating times were measured using a 50 MHz timer Counter TC98 (from Advance Instruments). The instrument was wired so that on closing switch  $S_A$  the counter was triggered and on opening it the counter stopped. The time was displayed digitally so it could be readily noted.

The heating currents were determined by measuring the potential drop across a one ohm standard resistance (type 1659, Tinsley and Co. Ltd.) using a potentiometer (type 4025, H. Tinsley and Co.). The standard cell for the potentiometer, (a Western cell type 1268 from H. Tinsley and Co.) was housed in a vacuum flask to minimise temperature variations. A two volt constant voltage supply connected to the mains supply was the driving cell for the potentiometer. The potentiometer reading, for the balance point as observed on the spot galvanometer, represented the current flowing in the heater circuit as the standard resistance was exactly one ohm.

FIGURE (5.1.1)

THE HEATER CIRCUIT



The resistance of the calorimeter heater,  $R_H$ , was obtained in the following way. A small current was passed through the heater and its leads and the potential drop,  $V_s$ , across the standard one ohm resistance,  $R_s$ , and the potential drop across the heater and its leads,  $R_{H+L}$ , were noted.

$$\text{Then, } R_{H+L} = \frac{V_{H+L}}{V_s} \times R_s = \frac{V_{H+L}}{V_s}$$

$$\text{As } R_s = 1$$

The resistance of the leads,  $R_L$ , were determined in a similar way to the resistance,  $R_{H+L}$ , with the difference that the calorimeter was replaced by a four way connector with its heater terminals joined by a short piece of wire.

$$\text{Then, } R_H = R_{H+L} - R_L$$

The resistance of the leads,  $R_L$ , and the resistance of the heater,  $R_H$ , were both redetermined at each new temperature at which measurements were done.

#### 5.4 THERMISTOR CIRCUIT

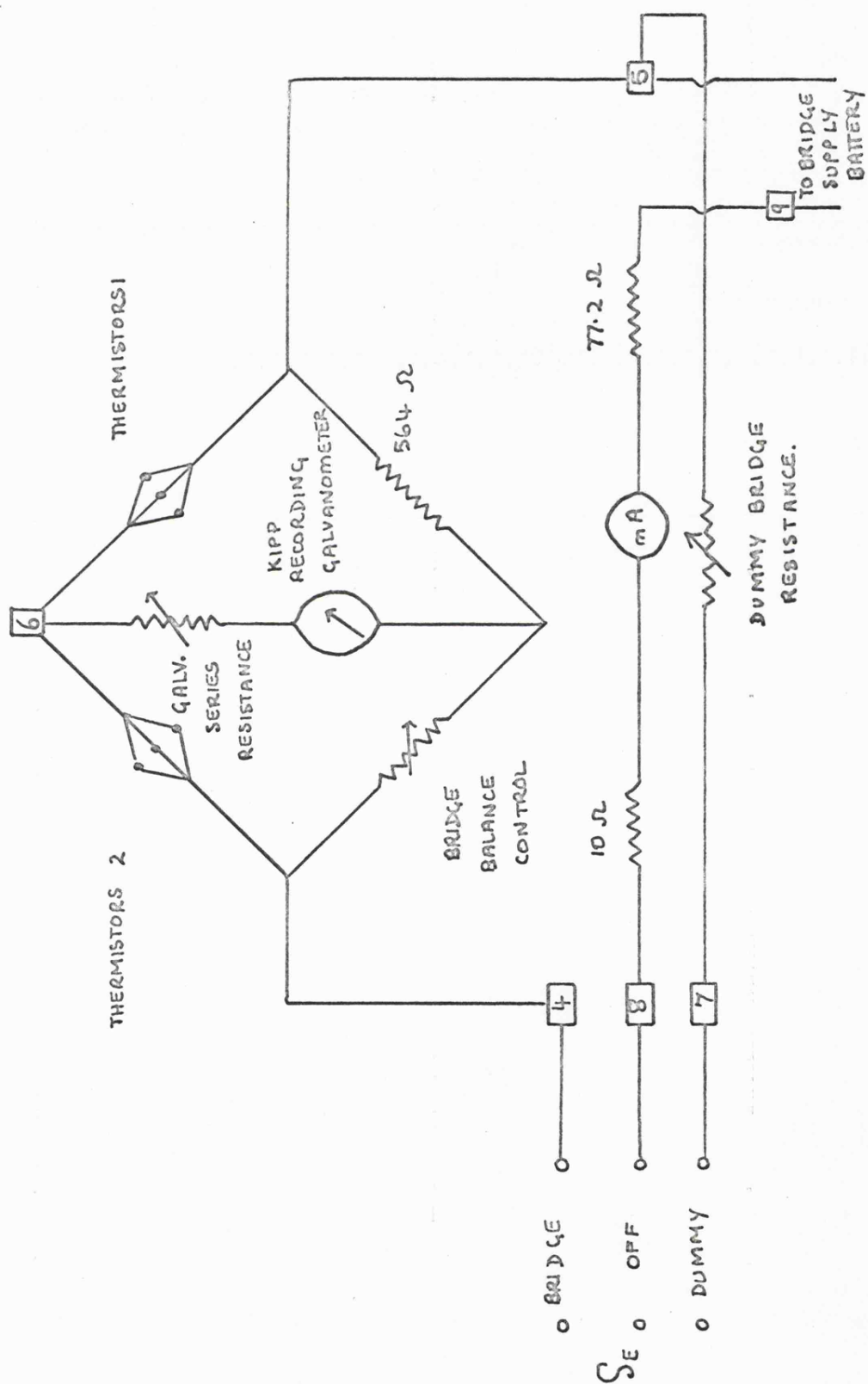
The two sets of thermistors formed two arms of a Wheatstone bridge network, as shown in figure (5.4.1). The out of balance current was measured using a recording galvanometer (Type B.D.2 from Kipp and Zonen).

The galvanometer series resistance and the dummy bridge resistance were both four-decade resistance boxes. The dummy bridge resistance was used to stabilise the six volt battery, which supplied the current to the bridge and the galvanometer series resistance protected the recorder, in between experiments by being set at a high value.



FIGURE (5.4.1)

THE THERMISTOR CIRCUIT



The bridge balance control was a six-decade resistance box ranging from 0.01 to 9999.99 ohms. This resistance was altered until the pen of the recording galvanometer had been centred on the chart paper prior to doing an experiment.

### 5.5 CALORIMETER JACKET

The calorimeter jacket consisted of a brass cylinder, (diameter 11 cm and length 15 cm), fitted with a removable end plate held in place by eight 2BA bolts and made water tight by an 'O' ring inset between the cylinder and end plate.

A short piece of brass tubing was soldered to the sides of a hole made in the jacket so that the calorimeter leads could be brought out and connected to the rest of the circuitry. The leads (eight core, screened cable) were protected in the thermostat bath by stout rubber tubing which surrounded them and was held in place on the brass tube by a 'Jubilee' clip. Two four-way, non-reversible connectors were used to connect the leads to the external circuitry.

### 5.6 STIRRING MECHANISM

The calorimeter jacket was supported in the thermostat by a stand equipped with suitable gearing to enable adequate stirring. A handle on the top of the assembly was lifted through 90° several times to promote stirring of the liquids. The gearing was such that the angle of rotation could not be exceeded and so there was no possibility of the liquids coming into contact with the ground glass joint.

### 5.7 THE THERMOSTAT

The thermostat consisted of a large galvanised tank, lagged with expanded polystyrene and covered with wood. The tank was fitted with a wooden lid covered with 'Formica'. The underside of the lid held a

frame to support the regulator, heaters, and stirrer, and a hole in the centre accommodated the calorimeter assembly.

The permanent heater consisted of a 'heater rod', and variac transformer. The intermittent heater consisted of a length of Pyrotenax resistance cable of resistance  $10\Omega$  wound on the frame and connected to a reduction transformer. The output of the transformer was controlled by a mercury-toluene regulator, of conventional design (57), and an electronic relay.

The bath was stirred by a Gunn, continuous rating pump stirrer.

The temperature of the thermostat was taken using a mercury in glass thermometer, calibrated by the National Physical Laboratory. The stability of the thermostat was investigated using a platinum resistance thermometer as in section (6.5).

#### 5.8 LOADING OF THE CALORIMETER

The calorimeter was thoroughly washed out with concentrated nitric acid, followed by deionised water and finally with Analar acetone. It was attached to a vacuum line and pumped on for thirty minutes by which time all of the acetone had evaporated. The calorimeter was then filled with mercury from a reservoir incorporated into the vacuum line. It was clamped, above a mercury tray, with its B7 socket almost horizontal and the end of the glass partition visible from above.

The two components were injected into the sides of the calorimeter, in turn, using hypodermic syringes fitted with bent 2" 26G needles.

Each component had to first be syringed out of its storage ampoule using an 8" needle so when this needle was replaced with the 2" one care was taken to ensure that, all the air had been expelled from the needle and syringe, no mercury had been introduced into the syringe, and that no liquid was leaking from the joint between the needle and the syringe.

The weight of each component taken was calculated by difference weighings. The smaller volume component was syringed first and its weight noted, then the volume of the second component,  $V_2$ , required was calculated from the expression

$$V_2 = \frac{W_1 M_2 X_2}{\rho_2^* M_1 X_1} \quad (5.8.1)$$

Where  $W_1$  is weight of component 1,  $M$  is molecular weight, and  $X$  is the mole fraction.

The expansion bulb, shown in figure (5.2.1), was gently inserted into the B7 socket of the calorimeter. Some mercury was forced into the bulb. The bulb was held in place by an elastic band attached to glass hooks on the sides of the stem and passed around the calorimeter.

The calorimeter was then placed in the polystyrene jacket.

A reference calorimeter was loaded, in a similar way, with one of the two liquids being mixed and also put into the polystyrene jacket. The calorimeters were then inserted into the brass jacket and the end plate bolted into place before the assembly was carefully lowered into the thermostat bath.

The calorimeters were allowed to reach thermal equilibrium by being left in the thermostat overnight.

#### 5.9 ENDOTHERMIC MEASUREMENTS - OPERATION OF APPARATUS

Measurements of endothermic energies of mixing involved only one calorimeter, (cal. 2), in current input, although the reference calorimeter (cal.1) was present as the fourth arm of the Wheatstone bridge.

When thermal equilibrium had been achieved switch  $S_E$  was set in the bridge position and the galvanometer series resistance was reduced to a suitable small value. The bridge balance control was adjusted, if necessary, until the recording galvanometer was zeroed and the recorder was started.

The potentiometer, in the heater circuit, was standardised and the previously set current in the dummy heater resistance circuit was checked. This was done by having switch  $S_D$  in the 1 ohm position and measuring the potential drop,  $V$ , across the standard resistance. This directly gave the current.

The recorder was allowed to draw a suitable base line for about thirty minutes. Switches  $S_B$  and  $S_C$  were checked to be set in the Cal. 2 position before switch  $S_A$  was thrown into the heater position, which also started the timer.

The recorder pen was seen to move to one side of the chart paper. The precise value of the current was measured by adjusting the potentiometer reading to give zero deflection of the spot galvanometer.

After half the provisional heating time had elapsed, that is at sixty seconds, the brass jacket was inverted ten times to promote mixing. The recorder pen was seen to move to the opposite side of the chart paper. The position of the pen was closely observed so that when it began to move back to the zero point switch  $S_A$  was opened, stopping the timer, and put back into the dummy position. By the procedure accurate compensation was obtained. The brass jacket was inverted a further ten times to promote a uniform temperature. Both the time and heater current were noted.

After thirty minutes the cooling curve had been traced out and steady conditions prevailed so a calibration for the stirring correction was done. This merely involved inverting the brass jacket twenty times.

When steady conditions were again achieved, after only about twenty minutes, switch  $S_A$  was thrown so as to pass a measured amount of heat into the mixing calorimeter. The current was accurately measured with the potentiometer, as before, and switch  $S_A$  opened after about thirty seconds so that the recorder pen remained on scale. The calorimeter was again stirred twenty times to promote a uniform temperature distribution. The time and heater current were noted.

When a suitable cooling curve had been traced the recorder was switched off and its pen removed.

The resistance of the calorimeter heater was then measured as described in section (5.3).

The method of calculation for the endothermic enthalpies of mixing is given in section (5.11) along with a typical recorder trace and experimental data.

#### 5.10 EXOTHERMIC MEASUREMENTS - OPERATION OF APPARATUS

Again a null technique was used but mixing was carried out in calorimeter 2 whilst heat was put into calorimeter 1.

When thermal equilibrium had been achieved the galvanometer series resistance was reduced to a suitable value, the recorder was started, and zeroed with the bridge balance control, and the value of the set heater current was checked.

After thirty minutes, when the recorder had drawn a suitable base line, switch  $S_A$  was put into the heater position and the timer and heating current were simultaneously switched on. Switches  $S_B$  and  $S_C$  were checked to be in the Cal. 1 position. The heater current was measured with the potentiometer by evaluating the potential drop across the 1 ohm resistance, switch  $S_D$  was set in the '1 ohm' position.

The recorder pen was deflected in one direction but after sixty seconds had elapsed the calorimeters were stirred ten times causing the pen to be deflected in the opposite direction. As soon as the pen started to move back towards the zero point switch  $S_A$  was put in the dummy position. In this way accurate compensation was achieved. The calorimeters were stirred a further ten times and the heater time and current were noted.

Thirty minutes later the calorimeters were stirred twenty times.

After a further twenty minutes the calibrations for calorimeters 1 and 2 were made in the following way.

Switches  $S_B$  and  $S_C$  were put in the Cals. 1 and 2 position and  $S_A$  in the 'heater' position, thus putting the same current through both calorimeter heaters. The accurate value of the heater current was measured, as before, and after sixty seconds the calorimeters were stirred ten times. The current was allowed to flow for approximately as long as in the mixing process. Switch  $S_A$  was set in the dummy position at the end of this time, and the calorimeters were again stirred ten times. The heater current and time were noted.

When steady conditions had existed for about ten minutes, usually thirty minutes after the previous measurement, the calibration for calorimeter 1 was done.

Switches  $S_B$  and  $S_C$  were set in the Cal. 1 position before  $S_A$  was put in the heater position. Heat was put into the calorimeters for about thirty seconds so that the recorder pen remained on scale. The heater current was measured during this time but all the stirring of the calorimeters, that is twenty times, had to be done at the end of the heating time. The current and time were noted.

When a suitable cooling curve had been traced the recorder pen was removed and the recorder switched off.

The resistance of calorimeter 2 was determined as described in section (5.3).

The calculation of the exothermic energies of mixing is given in section (5.12) along with a typical recorder trace and experimental data.

#### 5.11 CALCULATION OF THE ENDOTHERMIC MOLAR EXCESS ENTHALPY CHANGE, $H_{\text{endo}}^E$

A typical recorder trace and corresponding experimental data are shown in figures (5.11.1) and table (5.11.1).



$\Delta_2$  is seen to be equal to zero so no stirring correction has to be made in the calculation of the enthalpy change. However if a value existed the quantities  $\Delta_1$  and  $\Delta_3$  would have to be adjusted accordingly.

If  $\Delta_2$  were in the same direction as  $\Delta_1$  and  $\Delta_3$  then it would have to be subtracted and conversely it would have to be added if it were in the opposite direction.

The enthalpy change on mixing  $\Delta_H$ , is equal to the electrical energy,  $W_{el}$ , required for compensation in the mixing process with an adjustment made for any slight over or under compensation.

For table (5.11.1) the enthalpy change is over compensated for so the adjustment has to be subtracted.

$$\Delta H = W_{el} = i_1^2 R_2 t_1 - \Delta W_{el} \quad (5.11.1)$$

A deflection,  $\Delta_3$ , is caused by  $i_2^2 R_2 t_2$  Joules therefore a deflection  $\Delta_1$  would be caused by  $\frac{i_2^2 R_2 t_2 \Delta_1}{\Delta_3}$ . This is the amount

of heat by which the mixing has been over compensated therefore,

$$\Delta W_{el} = \frac{\Delta_1}{\Delta_3} i_2^2 R_2 t_2 \quad (5.11.2)$$

Substituting (5.11.2) in (5.11.1)

$$\Delta H = i_1^2 R_2 t_1 - \frac{\Delta_1}{\Delta_3} i_2^2 R_2 t_2 \quad (5.11.3)$$

$$H_{\text{endo}}^E = \frac{\Delta H}{n_1 + n_2} = \frac{(i_1^2 R_2 t_1 - \frac{\Delta_1}{\Delta_3} i_2^2 R_2 t_2)}{(n_1 + n_2)} \quad (5.11.4)$$

TABLE (5.11.1)

EXPERIMENTAL DATA CORRESPONDING TO FIGURE (5.11.1)

Date = 4.6.75      Temperature = 333.15K

System: Pentafluorobenzonitrile (1) + Cyclohexane (2)

$$\text{Mwt (1)} = 193.084 \text{ d (1)} = 1.563 \quad \text{Mwt (2)} = 84.162 \text{ d (2)} = 0.779$$
$$\text{wt. of syringe} + (1) = 14.9701\text{g} \quad \text{wt. of syringe} + (2) = 13.3186\text{g}$$

wt. of syringe = 14.4879g      wt. of syringe = 13.0508g

wt. of (1) = 0.4822g      wt. of (2) = 0.2678g

$$n_1 = 0.0024934 \quad n_2 = 0.0031820$$

Total number of moles = 0.0056793

$$x_1 = 0.4397$$
$$H^E \approx 2180 \text{ J mol}^{-1}$$

Expected value of heat = 12.38 J

Suitable current = 0.05769 A

1st.heater current,  $i_1$  = 0.05767 A

```
lst.heater time, t1           =    120.34  S
```

1st. deviation,  $\Delta_1$  = 0.2 cm. (over compensation)

2nd. deviation,  $\Delta_2$  = 0 cm.

2nd. heater current,  $i_2$  = 0.05767 A

2nd.heater time,  $t_2$  = 39.04 S

3rd. deviation,  $\Delta_3$  = 7.6 cm.

Resistance of Cal.2 + leads = 31.29 ohms.

Resistance of leads = 0.43 ohms.

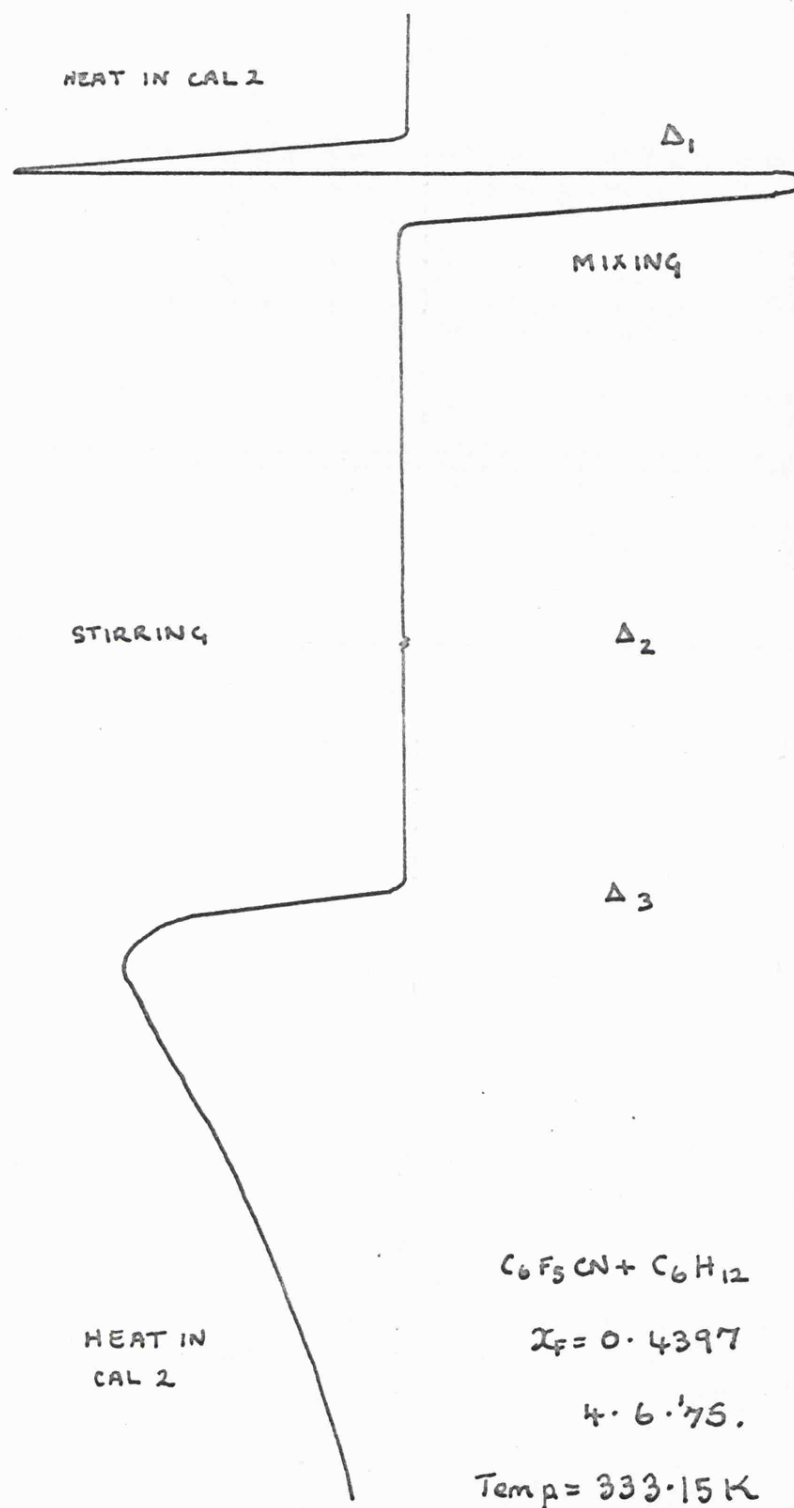
Resistance of Cal.2 = 30.86 ohms.

Therefore,  $\Delta H = 12.24 \text{ J}$

$$\text{and } H^E = 2,156.0 \text{ J mol}^{-1}$$

FIGURE (5.11.1)

A RECORDER TRACE FOR A TYPICAL ENDOTHERMIC RUN



## 5.12 CALCULATION OF THE EXOTHERMIC EXCESS ENTHALPY CHANGE, $H_{EXO}^E$

A typical recorder trace and experimental data are given in figure (5.12.1) and table (5.12.1).

The liquids are mixed in calorimeter 2 and heat is given out. To compensate for this electrical energy is put into the reference calorimeter, calorimeter 1.

Again, as in the case of endothermic enthalpy changes, a correction due to stirring must be applied to the deviations as described in section (5.11) if any deflections due to stirring exists.

The enthalpy change,  $\Delta H$ , can then be calculated as follows.

If  $C_2$  is the heat capacity of calorimeter 2 and  $C_1$  the heat capacity of calorimeter 1 then from the mixing process and its compensation,

$$\frac{C_1}{C_2} = \frac{i_1^2 R_1 t_1 + \frac{\Delta_1}{\Delta_4} (i_3^2 R_1 t_3)}{-\Delta H} \quad (5.12.1)$$

The electrical work has to be adjusted to account for under compensation. This is done by using the calibration for calorimeter 1.

However from the heat input into both calorimeters the following must also be true,

$$\frac{C_1}{C_2} = \frac{i_2^2 R_1 t_2 + \frac{\Delta_3}{\Delta_4} (i_3^2 R_1 t_3)}{i_2^2 R_2 t_2} \quad (5.12.2)$$

Table (5.12.1) EXPERIMENTAL DATA CORRESPONDING TO FIGURE (5.12.1)

Date = 17.12.74.      Temperature = 323.15K

System: Pentafluorobenzonitrile (1) + Toluene (2)

Mwt (1) = 193.084    d(1) = 1.563    Mwt (2) = 92.141    d(2) = 0.867

wt of syringe + (1) = 33.1325g    wt. of syringe + (2) = 31.9867g.

wt. of syringe                      = 32.1601g    wt. of syringe                      = 31.8764g.

wt. of (1)                            = 0.9724 g.    wt. of (2)                            = 0.1103g.

$n_1$                                       = 0.0050361       $n_2$                                       = 0.0011971

Total number of moles = 0.0062332

$X_1 = 0.8079$

$H^E \approx - 620 \text{ J mol}^{-1}$

Expected value of heat = 3.844 J.

Suitable current = 0.03793 A

1st. heater current,  $i_1$  = 0.03790 A

1st. heater time,  $t_1$  = 119.03 S

1st. deviation,  $\Delta_1$  = 2.4 cm (under compensation)

2nd. deviation,  $\Delta_2$  = 0 cm

2nd. heater current,  $i_2$  = 0.03161 A

2nd. heater time,  $t$ , = 117.75 S

3rd. deviation,  $\Delta_3$  = 5.5 cm

3rd. heater current,  $i_3$  = 0.03790 A

3rd. heater time,  $t_3$  = 36.58 S

4th. deviation,  $\Delta_4$  = 3.7 cm

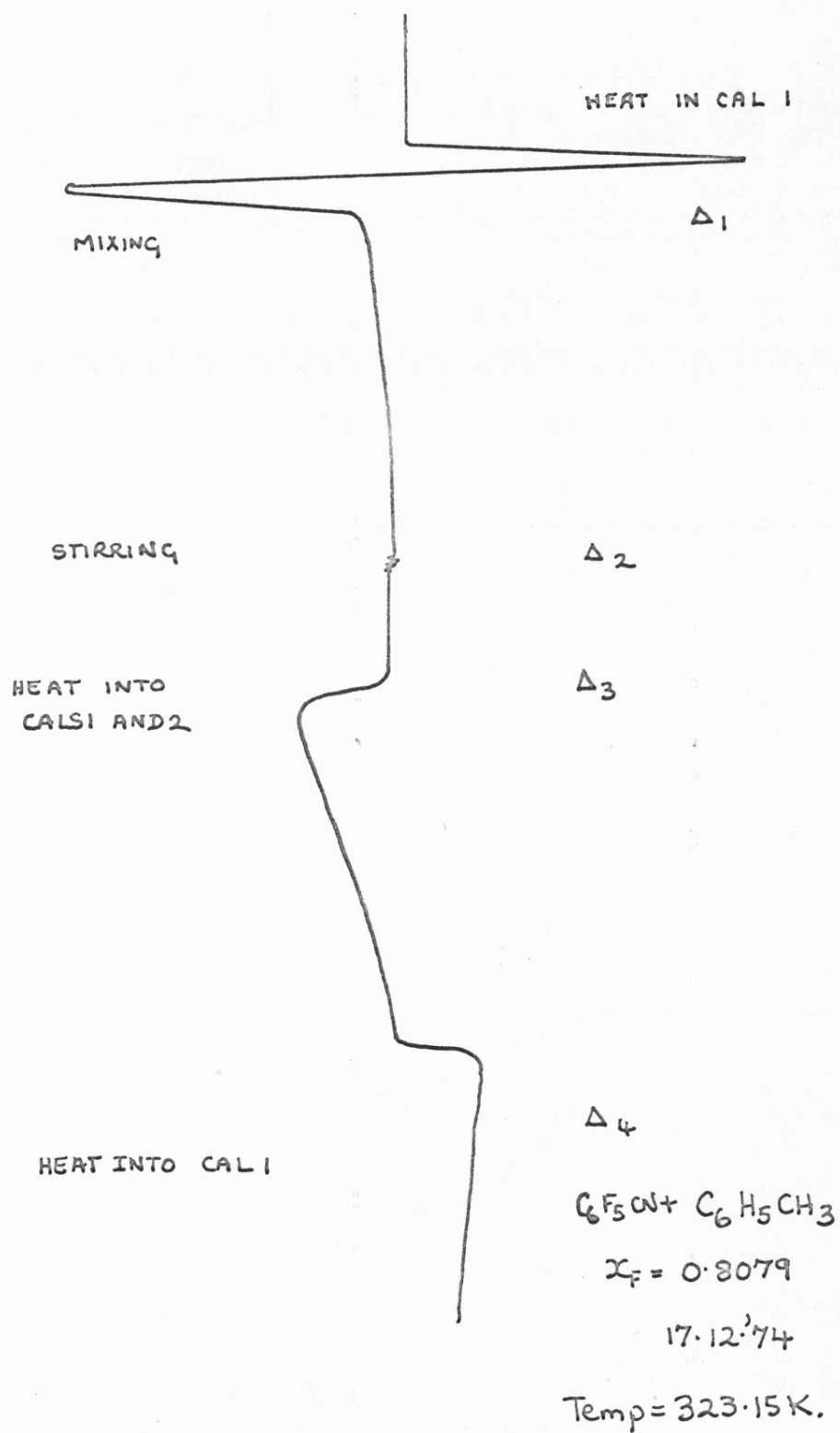
Resistance of Calorimeter 2 = 30.83 ohms

Therefore,  $\Delta H$  = - 3.79 J

and  $H^E$  = - 609.2 J mol<sup>-1</sup>

FIGURE (5.12.1)

A RECORDER TRACE OF A TYPICAL EXOTHERMIC RUN



Again using the calibration of calorimeter 1 to obtain accurate compensation.

Combining the above two equations gives (5.12.1) and (5.12.2),

$$\frac{i_1^2 R_1 t_1 + \frac{\Delta 1}{\Delta 4} (i_3^2 R_1 t_3)}{-\Delta H} = \frac{i_2^2 R_1 t_2 + \frac{\Delta 3}{\Delta 4} (i_3^2 R_1 t_3)}{i_2^2 R_2 t_2} \quad (5.12.3)$$

Therefore,

$$\Delta H = - \frac{i_2^2 R_2 t_2 (i_1^2 t_1 + \frac{\Delta 1}{\Delta 4} (i_3^2 t_3))}{i_2^2 t_2 + \frac{\Delta 3}{\Delta 4} (i_3^2 t_3)} \quad (5.12.4)$$

and the molar excess enthalpy is,

$$H_{ex}^E = \frac{\Delta H}{n_1 + n_2}$$

### 5.13 TEST MEASUREMENTS

The type of apparatus used here had been rigorously tested when first constructed (65,66).

Therefore only a few measurements were made on an exothermic system and an endothermic system so as to become familiar with the experimental techniques.

The endothermic system which was used was hexafluorobenzene + cyclohexane at 313.2 K. The excess enthalpies of mixing,  $H^E$ , are given in table (5.13.1) a) along with the corresponding mole fraction of hexafluorobenzene,  $X_F$ .

TABLE (5.13.1 a)

The excess Enthalpies of Mixing,  $H^E$ , for the system hexafluorobenzene + cyclohexane of 313.2K.

<u><math>X_F</math></u>	<u><math>H^E/J \text{ mol}^{-1}</math></u>
0.2148	1117.4
0.4125	1489.4
0.5755	1478.5
0.6951	1239.1

TABLE (5.13.1 b)

The excess Enthalpies of Mixing,  $H^E$ , for the system hexafluorobenzene + benzene at 313.2K.

<u><math>X_F</math></u>	<u><math>H^E/J \text{ mol}^{-1}</math></u>
0.3569	-287.1
0.4045	-349.9
0.4915	-440.2
0.6483	-459.4



FIGURE (5.13.1)

EXCESS ENTHALPIES OF MIXING FOR HEXAFLUOROBENZENE + CYCLOHEXANE

AT 313.2K

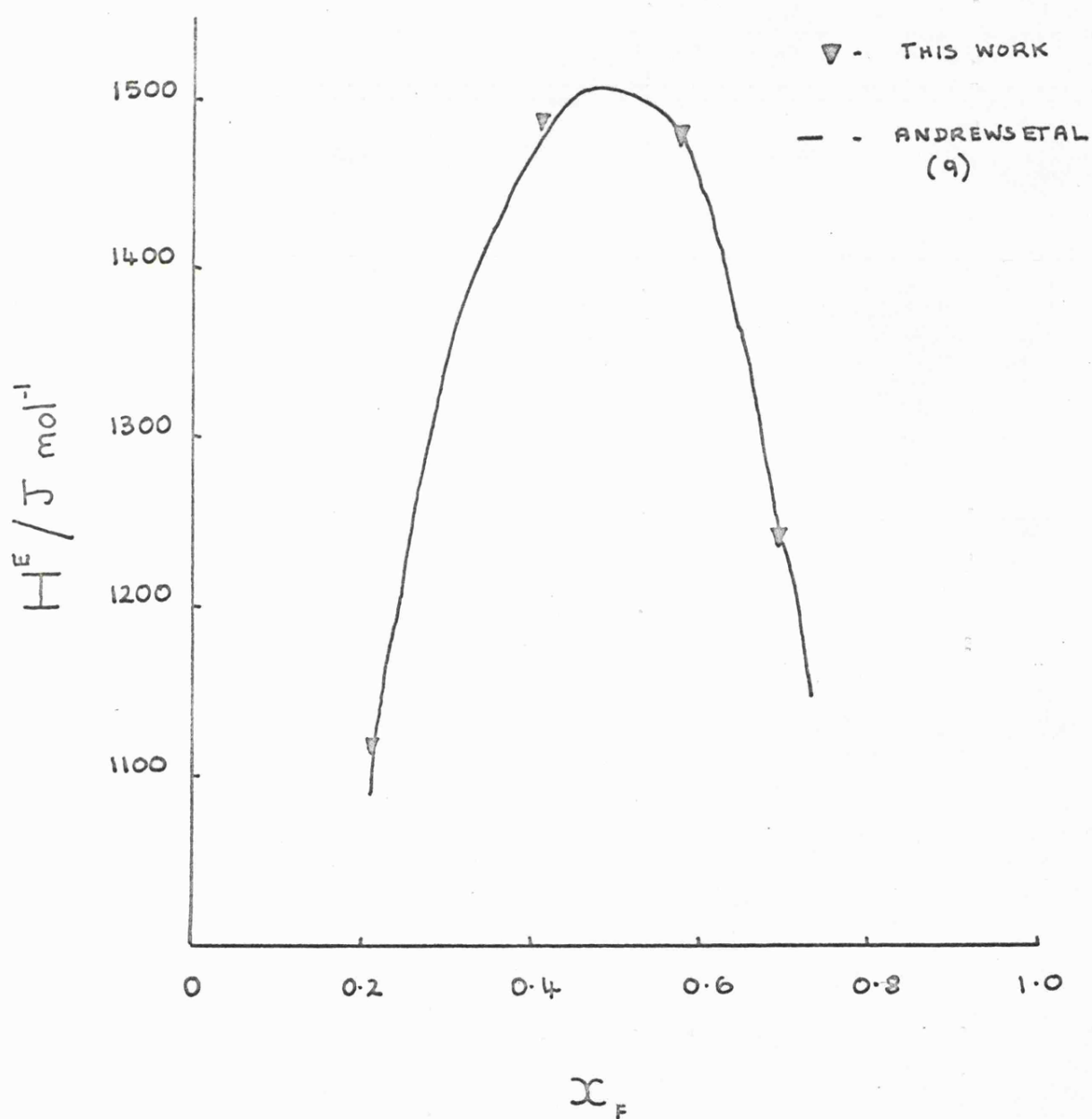
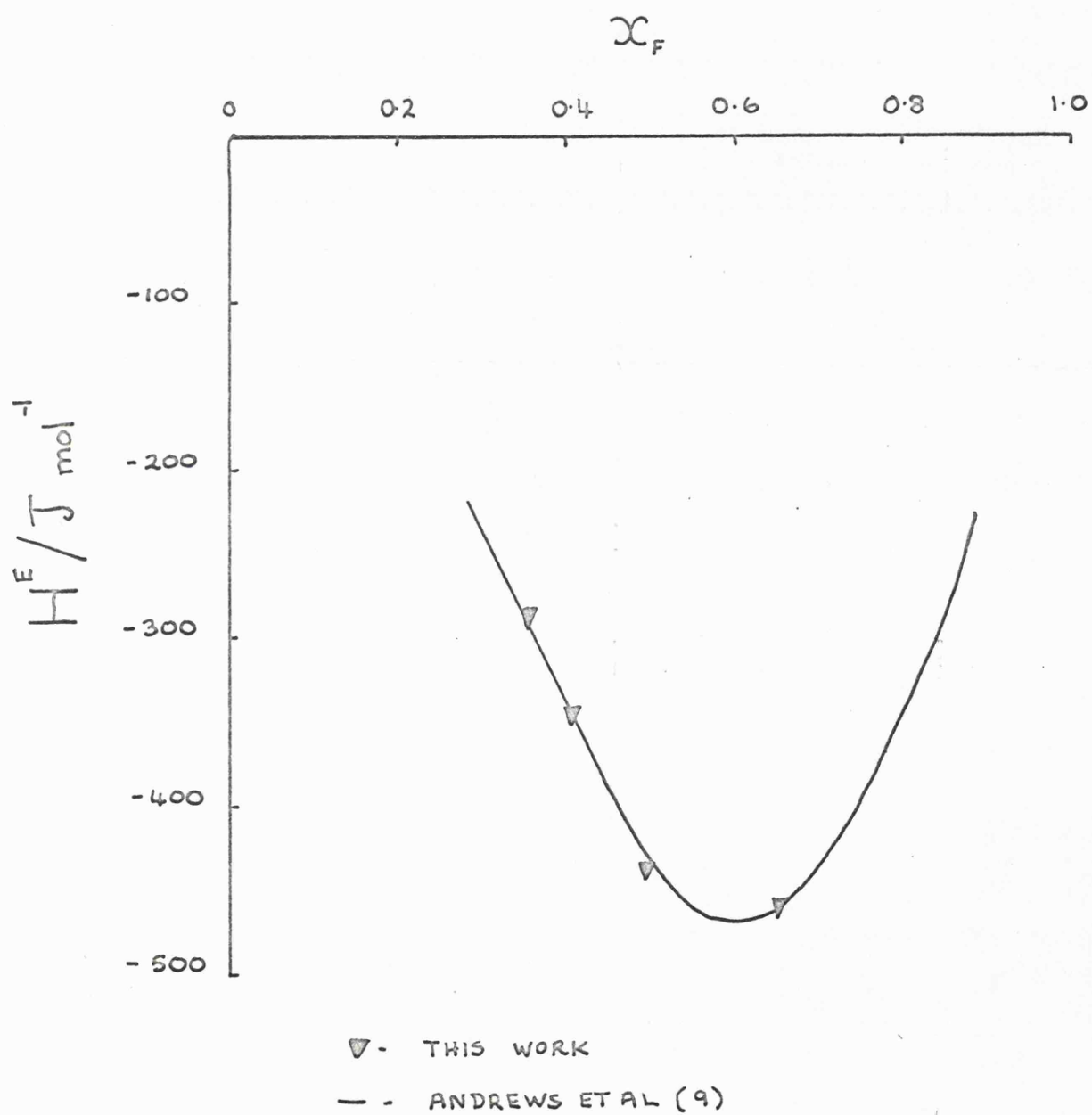


FIGURE (5.13.2)

EXCESS ENTHALPIES OF MIXING, AT 313.2K, FOR HEXAFLUOROBENZENE

+ BENZENE



The results are represented with those of Andrews, Pollock and Morcom ( 9 ) in figure (5.13.1). They are seen to be in excellent agreement.

The exothermic system which was used was hexafluorobenzene + benzene at 313.2K.

The excess enthalpies of mixing,  $H^E$ , are given in table (5.13.1 b) along with the corresponding mole fraction of hexofluorobenzene,  $X_F$ .

The results are represented with those of Duncan and Swinton ( 9 ) in figure (5.13.2). They are also seen to be in excellent agreement.

#### 5.14 MOLAR EXCESS ENTHALPY OF MIXING RESULTS

Measurements on the following systems were made, to complement the excess volume results given in chapter (6), and to give a clearer picture of how pentafluorocyanobenzene behaves in those systems as compared to the behaviour of other fluoro-carbons (9,25,13) in similar systems.

The systems studied were pentafluorocyanobenzene with benzene, toluene, p-xylene and cyclohexane at 323.15K. Some measurements were made at 343.15K for the first three systems so that their excess heat capacities,  $C_p^E$ , at equimolar compositions could be determined.

Pentafluorocyanobenzene and cyclohexane was studied at 333.15K and 308.15K in addition as it appeared to have an excess heat capacity of opposite sign to that expected.

The results are given in tables (5.14.1) to (5.14.4) and represented in figures (5.14.1) and (5.14.2).

The results were fitted to a polynomial of the form,

TABLE (5.14.1)

Excess Enthalpies of Mixing for Pentafluorocyanobenzene + Benzene at

323.15K

$X_F$	$H^E/J \text{ mol}^{-1}$
0.2982	-308.0
0.4646	-475.0
0.6313	-487.1
0.7662	-361.0
0.9016	-175.5

$$H_1 = -1957.0 \text{ J mol}^{-1}, H_2 = 756.8 \text{ J mol}^{-1} \quad H_3 = 1049.0 \text{ J mol}^{-1}$$

$$\text{R.M.S.} = 4.6 \text{ J mol}^{-1}$$

$$\text{S.D.} = 6.1 \text{ J mol}^{-1}$$

Excess Enthalpies of Mixing for Pentafluorocyanobenzene + Benzene at

343.15K

$X_F$	$H^E/J \text{ mol}^{-1}$
0.3837	-388.9
0.5385	-491.0
0.6395	-478.4

TABLE (5.14.2)

Excess Enthalpies of Mixing for Pentafluorocyanobenzene + Toluene at  
323.15K

$x_F$	$H^E/J \text{ mol}^{-1}$
0.0673	-169.9
0.1167	-353.6
0.2228	-623.0
0.3309	-826.8
0.4221	-945.0
0.5035	-993.1
0.5998	-978.2
0.7152	-854.4
0.8079	-609.2
0.8819	-389.2

$$H_1 = -3959.4 \text{ J mol}^{-1}, H_2 = 644.0 \text{ J mol}^{-1}, H_3 = -160.6$$

$$\text{J mol}^{-1}, H_4 = -666.8 \text{ J mol}^{-1}, H_5 = 1727.1 \text{ J mol}^{-1}$$

$$\text{RMS.} = 9.0 \text{ J mol}^{-1}$$

$$\text{S.D.} = 11.8 \text{ J mol}^{-1}$$

Excess Enthalpies of Mixing for Pentafluorocyanobenzene + Toluene at

343.15K

$x_F$	$H^E/J \text{ mol}^{-1}$
0.4215	-899.5
0.5021	-948.0
0.5845	-926.6

TABLE (5.14.3)

Excess Enthalpies of Mixing for Pentafluorocyanobenzene + P-xylene at  
323.15K

$X_F$	$H^E/J \text{ mol}^{-1}$
0.1457	-815.9
0.1942	-1014.5
0.3233	-1515.9
0.3973	-1694.0
0.4887	-1737.8
0.6064	-1631.1
0.6941	-1433.6
0.7969	- 997.1
0.8740	- 657.8

$$H_1 = -7006.2 \text{ J mol}^{-1}, \quad H_2 = -308.5 \text{ J mol}^{-1}$$

$$H_3 = 1562.5 \text{ J mol}^{-1}$$

$$\text{R.M.S.} = 13.5 \text{ J mol}^{-1}$$

$$\text{S.D.} = 15.9 \text{ J mol}^{-1}$$

Excess Enthalpies of Mixing for Pentafluorocyanobenzene + P-xylene at  
343.15K

$X_F$	$H^E/J \text{ mol}^{-1}$
0.3999	-1349.7
0.4489	-1454.9
0.5082	-1505.2
0.5605	-1456.8

FIGURE (5.14.1)

THE EXCESS ENTHALPIES FOR PENTAFLUOROCYANOBENZENE +

BENZENE, TOLUENE, P-XYLENE AT 323.15K

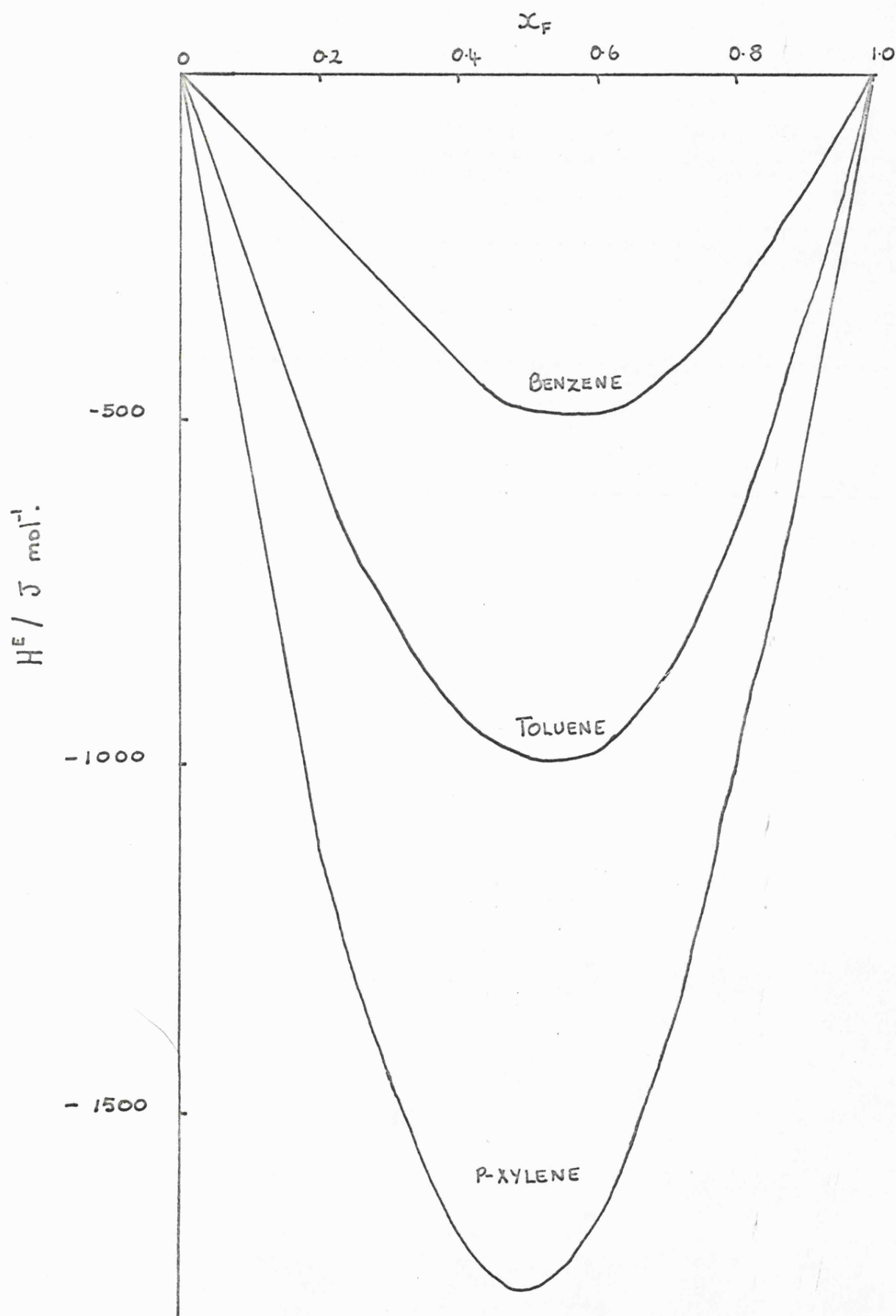


TABLE (5.14.4)

Excess Enthalpies of Mixing for Pentafluorocyanbenzene + Cyclohexane

at 323.15K

$X_F$	$H^E/J \text{ mol}^{-1}$
0.0408	551.4
0.1103	1122.1
0.1656	1456.8
0.2075	1684.3
0.3690	2092.2
0.4777	2140.9
0.5495	2112.3
0.7080	1681.7
0.8359	1196.9
0.8898	809.8

at 308.15K

$X_F$	$H^E/J \text{ mol}^{-1}$
0.2039	1605.9
0.3124	1880.0
0.4438	2059.5
0.4529	2072.0
0.5171	2072.7

at 333.15K

$X_F$	$H^E/J \text{ mol}^{-1}$
0.4397	2156.0
0.4853	2175.5
0.5079	2154.0
0.5507	2100.0



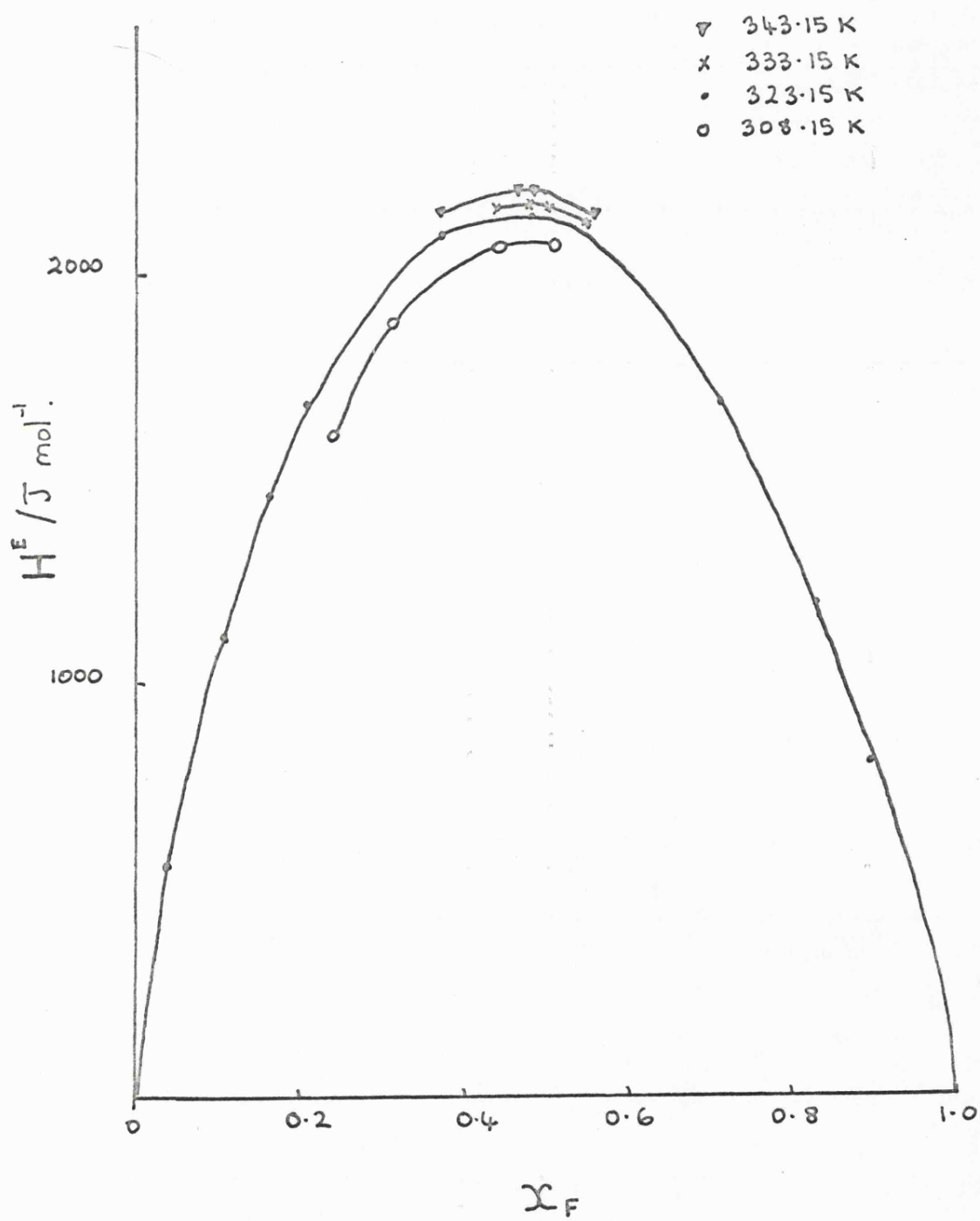
TABLE (5.14.4) Continued

Excess Enthalpies of Mixing for Pentafluorocyanobenzene + Cyclohexane  
at 343.15K

$x_{\text{H}}$	$H^{\text{E}}/\text{J mol}^{-1}$
0.3762	2144.9
0.4656	2186.1
0.4791	2183.9
0.5538	2111.6
0.5548	2111.7

FIGURE (5.14.2)

EXCESS ENTHALPIES FOR PENTAFLUOROCYANOBENZENE + CYCLOHEXANE



$$H^E = X_F (1 - X_F) \sum_{i=1}^{i=n} H_i (1 - 2X_F)^i \quad (5.14.1)$$

Where  $H_i$  is coefficient  $i$  ( $J \text{ mol}^{-1}$ ) and  $n$  is the number of coefficients required for a smooth curve.

The root mean square deviation ( $R.M.S./J \text{ mol}^{-1}$ ) is given by,

$$RMS = (\sum (S_H^E)^2 / m)^{1/2} \quad (5.14.2)$$

where  $m$  is the number of experimental points.

The standard deviation ( $S.D./J \text{ mol}^{-1}$ ) is given by,

$$S.D. = (\sum (S_H^E)^2 / m - (n))^{1/2} \quad (5.14.3)$$

Both of these quantities for each curve fit is quoted in the tables.

The excess heat capacities,  $C_p^E$ , at equimolar compositions for the systems studied are given in table (5.14.5).

The temperature dependence of the excess enthalpies for the system pentafluorocyanobenzene with cyclohexane is shown in figure (5.14.3).

FIGURE (5.14.3)

THE TEMPERATURE DEPENDENCE OF THE EXCESS ENTHALPIES  
FOR PENTAFLUOROCYANOBENZENE + CYCLOHEXANE

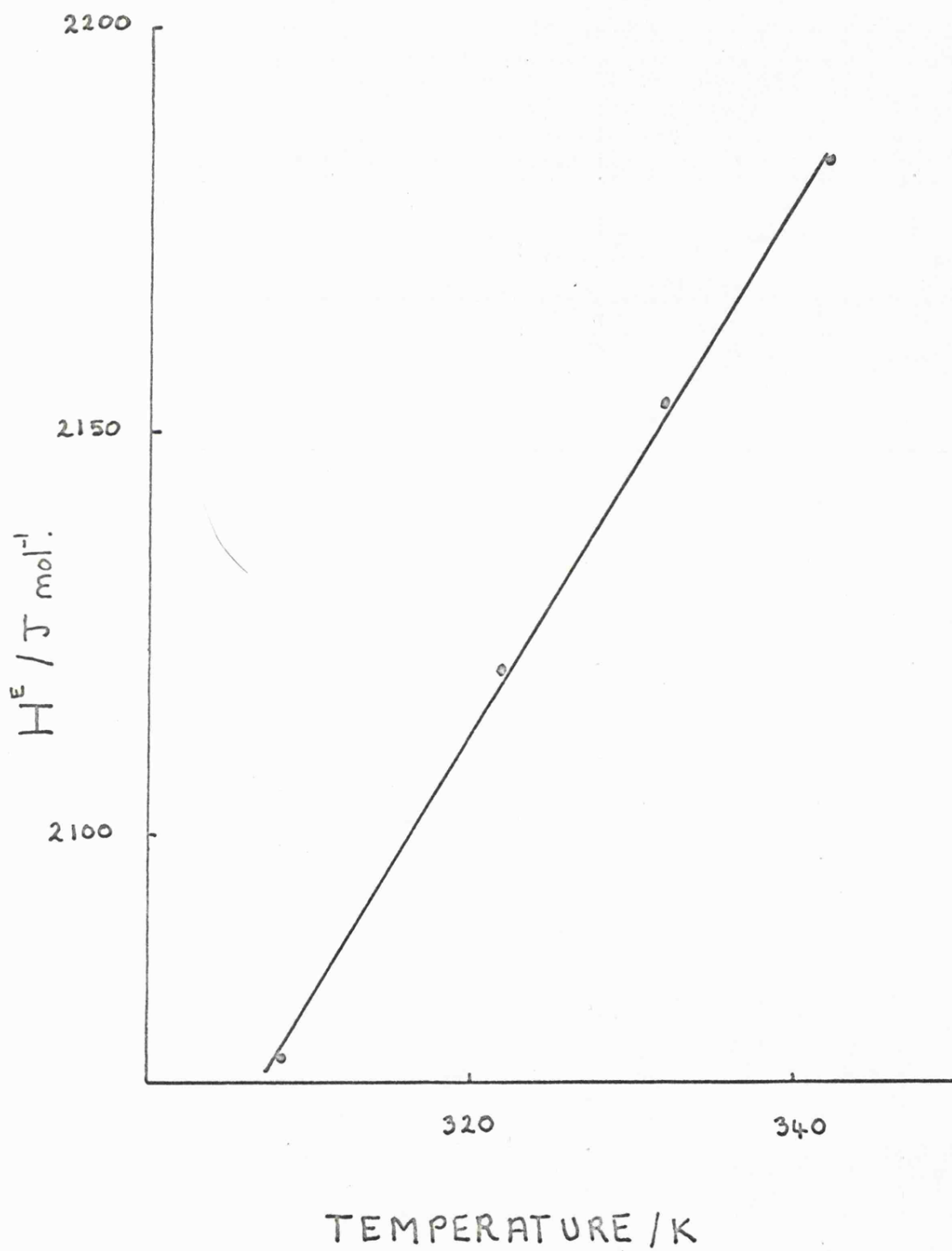


TABLE (5.14.5)

The Excess Heat Capacities  $C_P^E$  for Equimolar Mixtures at 323.15K

<u>SYSTEM</u>	$C_P^E / \text{J mol}^{-1} \text{K}^{-1}$
Pentafluorocyanobenzene + Benzene	0
Pentafluorocyanobenzene + Toluene	+2.3
Pentafluorocyanobenzene + p-Xylene	+11.6
Pentafluorocyanobenzene + Cyclohexane	+ 3.3

## CHAPTER SIX

### EXCESS VOLUMES OF MIXING

## EXCESS VOLUMES OF MIXING

### 6.1 INTRODUCTION

The excess volume,  $V^E$ , of a mixture is defined by

$$V^E = X_1 V_1 + X_2 V_2 - X_1 V_1^* - X_2 V_2^*$$

where  $X$  is mole fraction,  $V$  is partial molar volume of given component and  $V^*$  is the molar volume of the pure component.

Excess volumes of mixing can be determined either by precise density measurements and application of the following expression:-

$$V^E = \frac{X_1 M_1 + X_2 M_2}{\rho_{12}} - \left[ \frac{X_1 M_1}{\rho_1^*} + \frac{X_2 M_2}{\rho_2^*} \right]$$

$X$  - mole fraction,  $M$  - molecular weight,  $\rho_{12}$  - density of solution,  $\rho^*$  - density of pure component, or by direct measurement of the volume change.

The drawback to the first method is that the density measurements have to be made with a high degree of accuracy.

The second method, in which the volume change on mixing the two liquids in a dilatometer is observed, can be carried out using a dilution dilatometer of various designs (89-94), or a single composition dilatometer again of numerous designs (95-98).

## 6.2 THE PRESENT METHOD: APPARATUS

The apparatus used was a single composition dilatometer which had been developed at Leicester (65). The design is shown in figure (6.2.1) and consisted of a boat-shaped vessel fitted with a B10 socket and a capillary side arm. The side arm was made from a length of Veridia precision bore tube with a right angle bend, a B10 cone at the bottom, and a small glass cup attached to the top by araldite. A scratch was made quite near the top of the tube as a reference mark. Hooks were present on the capillary so that an elastic band could be attached to go around the centre of the vessel and ensure a tight joint.

## 6.3 EXPERIMENTAL TECHNIQUE

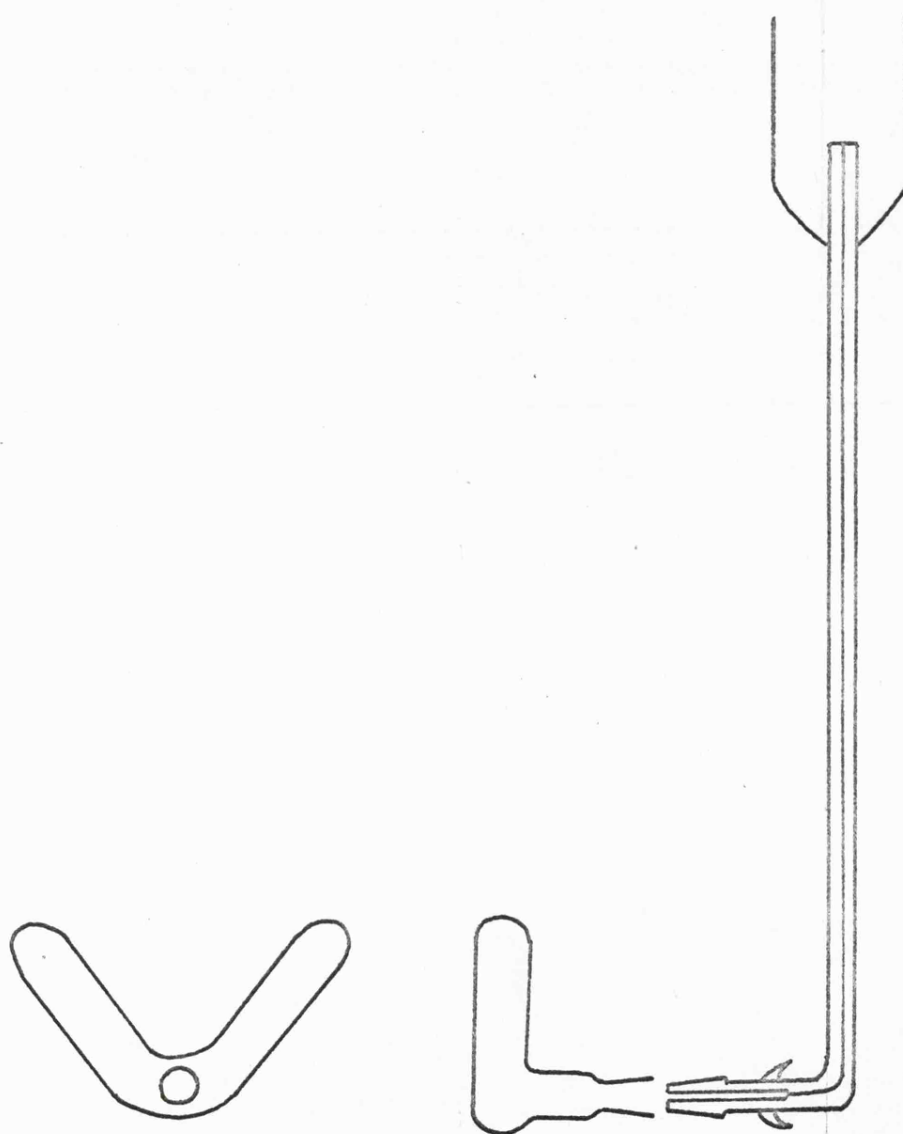
The dilatometer was cleaned using concentrated nitric acid and thoroughly washed with de-ionised water, and then with 'Analar' acetone. It was dried in an air oven, then evacuated and filled with mercury. When full it was removed and clamped with the B10 socket almost horizontal.

The two components, which had been degassed, were injected into the appropriate sides of the u-tube from Hamilton hypodermic syringes fitted with bent 3" long 26G needles. The weights of the components were known by difference weighings of the syringes. Suitable amounts were injected, depending upon the estimated excess volume, and the densities of the components. It was possible to use a vessel with one enlarged side arm if measurements at the extreme ends of the mole fraction range were being carried out.



FIGURE (6.2.1)

VOLUME OF MIXING APPARATUS



The required capillary was selected (diameter 0.0003M, or 0.0005M) and its cone lightly greased with Apiezon Type L grease before being pushed hard into the socket, taking care to exclude all air. The elastic band was then attached to the hooks to hold the joint tightly in place.

The dilatometer was then immersed in the thermostat and allowed to reach thermal equilibrium, which took about half an hour. It was then taken out and the vessel warmed with a hot air blower, so expelling some mercury from the side arm until the meniscus was at the required level.

The dilatometer was replaced in the thermostat and checked to be vertical in all planes by observation through the cathetometer telescope. After the dilatometer had reached thermal equilibrium the height of the meniscus, relative to the reference mark on the tube, was measured through a glass windows in the side of the thermostat using a Precision Tool and Instrument Co. Ltd., cathetometer. A further measurement was taken to check that the reading was constant to within  $\pm 0.002\text{cm}$ .

The components were then mixed by removing the assembly from the thermostat and rotating it through  $90^\circ$ , such that no liquid came in contact with the joint, and rocking the vessel from side to side twenty times. The process was completed quickly so that the thread of mercury remained in the capillary. The new meniscus height, after re-establishment of thermal equilibrium was reached, was again measured as described above.

The volume change on mixing,  $\Delta V$ , was then calculated from the equation.

$$\Delta V = \pi \frac{d^2}{4} \Delta l = A \times \Delta l$$

where  $\Delta l$  is the measured change in thread height on mixing,  $d$  is the diameter of the tube, and  $A$  is its cross sectional area.

Then if  $n_1$  moles of component 1 and  $n_2$  moles of component 2 are mixed.

$$\frac{V^E}{n_1+n_2} = \Delta V \quad \text{and} \quad X_1 = \frac{n_1}{n_1+n_2}$$

#### 6.4 CALIBRATION OF CAPILLARY TUBES

The cross sectional area was required to a high degree of accuracy and was determined by weighing the capillary containing a known length of mercury. The weighings were made on a balance reading to  $\pm 0.0001g$  and the thread was measured with a travelling microscope. The length of thread was taken as the average of four readings. The results are shown in table (6.4.1).

#### 6.5 WATER THERMOSTAT

The thermostat consisted of a large galvanised tank, lagged with expanded polystyrene and covered with wood except on one side where a window was present.

The water was heated by permanent and intermittent heaters. The permanent heater was made from Pyrotenax resistant cable coiled around a metal frame and controlled by a variac transformer. The intermittent heater was also made of coiled resistance cable but controlled by a variac transformer, contact thermometer, and electronic relay system. The water was stirred with a powerful pump stirrer from Messrs. D.A.Gunn (Engineering) Ltd.

TABLE (6.4.1)  
CALIBRATION OF CAPILLARY TUBES

A) NOMINAL DIAMETER,  $d = 5 \times 10^{-4}$  m, CROSS SECTIONAL AREA,  $A = 1.964 \times 10^{-7} \text{ m}^2$

wt of Mercury/kg	Density of Mercury /kg m <sup>-3</sup>	Average Length of thread/m	Cross Sectional Area/m <sup>2</sup>	True Diameter/m
0.0002871	13538.9	0.010565	$2.006 \times 10^{-7}$	$5.052 \times 10^{-4}$
0.0002391	13543.8	0.008800	$2.006 \times 10^{-7}$	

B) NOMINAL DIAMETER,  $d = 3 \times 10^{-4}$  m, CROSS SECTIONAL AREA,  $A = 7.071 \times 10^{-8} \text{ m}^2$

wt of Mercury/kg	Density of Mercury /kg m <sup>-3</sup>	Average Length of thread/m	Cross Sectional Area/m <sup>2</sup>	True Diameter/m
0.0001088	13543.8	0.011005	$7.304 \times 10^{-8}$	$3.048 \times 10^{-4}$
0.0000939	13538.9	0.00495	$7.304 \times 10^{-8}$	

The temperature of the thermostat was observed using a mercury in glass thermometer calibrated by the National Physical Laboratory. The stability of the thermostat was determined using a platinum resistance thermometer (Type 1-51878A Messrs. H. Pinsley and Co. Ltd.) and a Precision Comparison Bridge (Model VLF 51A - Rosemount Engineering Company Limited). The temperature was found to be steady to within  $\pm 0.001\text{K}$  for long periods.

## 6.6 RESULTS

The results of the experimental measurements of the excess volumes ( $\text{m}^3 \text{mol}^{-1}$ ) for the systems studied, are given in tables (6.6.1) to (6.6.8). The mole fraction values quoted are always those of the fluorocarbon.

The results were fitted to an excess function polynomial of the form

$$V^E = x_F (1 - x_F) \sum_{i=1}^{i=n} V_i (1 - 2x_F)^i$$

The coefficients  $V_i$  ( $\text{m}^3 \text{mol}^{-1}$ ) and smoothed values of  $V^E$  ( $\text{m}^3 \text{mol}^{-1}$ ) are given in the tables along with the root mean square deviations (R.M.S.  $\text{m}^3 \text{mol}^{-1}$ ) and standard deviations (S.D.  $\text{m}^3 \text{mol}^{-1}$ ) for the best curve fit.

All the measurements were carried out at 323.15K except for pentafluorocyanobenzene with N,N-dimethylp-toluidine where a solid complex was formed at about 325 K. In this case the excess volumes were measured at 328.15K.

TABLE (6.6.1)

$V^E$  for the system hexafluorobenzene (F) + N,N-dimethylaniline (DMA)  
at 323.15K

$x_F$	$10^6 \times V^E_{Exp} / m^3 \text{ mol}^{-1}$	$10^6 \times V^E_{fitted} / m^3 \text{ mol}^{-1}$
0.1229	-0.1285	-0.1280
0.2679	-0.3014	-0.3020
0.3291	-0.3687	-0.3677
0.4107	-0.4349	-0.4366
0.5231	-0.4824	-0.4821
0.6089	-0.4680	-0.4699
0.6678	-0.4437	-0.4366
0.7308	-0.3810	-0.3797
0.7937	-0.2848	-0.3038
0.8054	-0.2972	-0.2880
0.8937	-0.1626	-0.1573

$$V_1 = -1.913 \times 10^{-6} \quad V_2 = +0.468 \times 10^{-6}$$

$$V_3 = 0.828 \times 10^{-6} \quad V_4 = -0.229 \times 10^{-6}$$

$$\text{R.M.S.} = 6.41 \times 10^{-9} \text{ m}^3 \text{ mol}^{-1}$$

$$\text{S.D.} = 7.71 \times 10^{-9} \text{ m}^3 \text{ mol}^{-1}$$

TABLE (6.6.2)

$V^E$  for the system hexafluorobenzene (F) + isooxonylcyclohexane (IPCH)  
at 323.15K

<u><math>X_F</math></u>	<u><math>10^6 \times V^E_{\text{exp}}/\text{m}^3 \text{ mol}^{-1}</math></u>	<u><math>10^6 \times V^E_{\text{fitted}}/\text{m}^3 \text{ mol}^{-1}</math></u>
0.2163	1.3317	1.3339
0.3103	1.7390	1.7221
0.3867	1.9304	1.9426
0.4955	2.0971	2.0989
0.6370	2.0091	2.0034
0.6880	1.8631	1.8805
0.8040	1.4311	1.4150

$$V_1 = 8.405 \times 10^{-6}$$

$$V_2 = -0.945 \times 10^{-6}$$

$$\text{R.M.S.} = 1.073 \times 10^{-8} \text{ m}^3 \text{ mol}^{-1}$$

$$\text{S.D.} = 1.216 \times 10^{-8} \text{ m}^3 \text{ mol}^{-1}$$

TABLE (6.6.3)

$V^E$  for the system hexafluorobenzene (F) + N,N-dimethylp-toluidine (DMT)  
at 323.15K

$X_F$	$10^6 \times V^E_{Exp}/m^3 \text{ mol}^{-1}$	$10^6 \times V^E_{fitted}/m^3 \text{ mol}^{-1}$
0.1322	-0.2587	-0.2591
0.2066	-0.3990	-0.3979
0.3441	-0.6211	-0.6239
0.4112	-0.7083	-0.7055
0.5229	-0.7702	-0.7701
0.6367	-0.7155	-0.7192
0.7056	-0.6337	-0.6293
0.8065	-0.4332	-0.4351
0.9132	-0.1922	-0.1917

$$V_1 = 3.062 \times 10^{-6} \quad V_2 = 0.615 \times 10^{-6}, \quad V_3 = 1.399 \times 10^{-6}$$

$$V_4 = -0.920 \times 10^{-6} \quad V_5 = -0.398 \times 10^{-6}, \quad V_6 = 0.355 \times 10^{-6}$$

$$\text{R.M.S.} = 2.216 \times 10^{-9} \quad m^3 \text{ mol}^{-1}$$

$$\text{S.D.} = 3.287 \times 10^{-9} \quad m^3 \text{ mol}^{-1}$$



FIGURE (6.6.1)

$V_s^E$  FOR HEXAFLUOROBENZENE WITH IPCH., DMA AND DMT

AT 323.15K

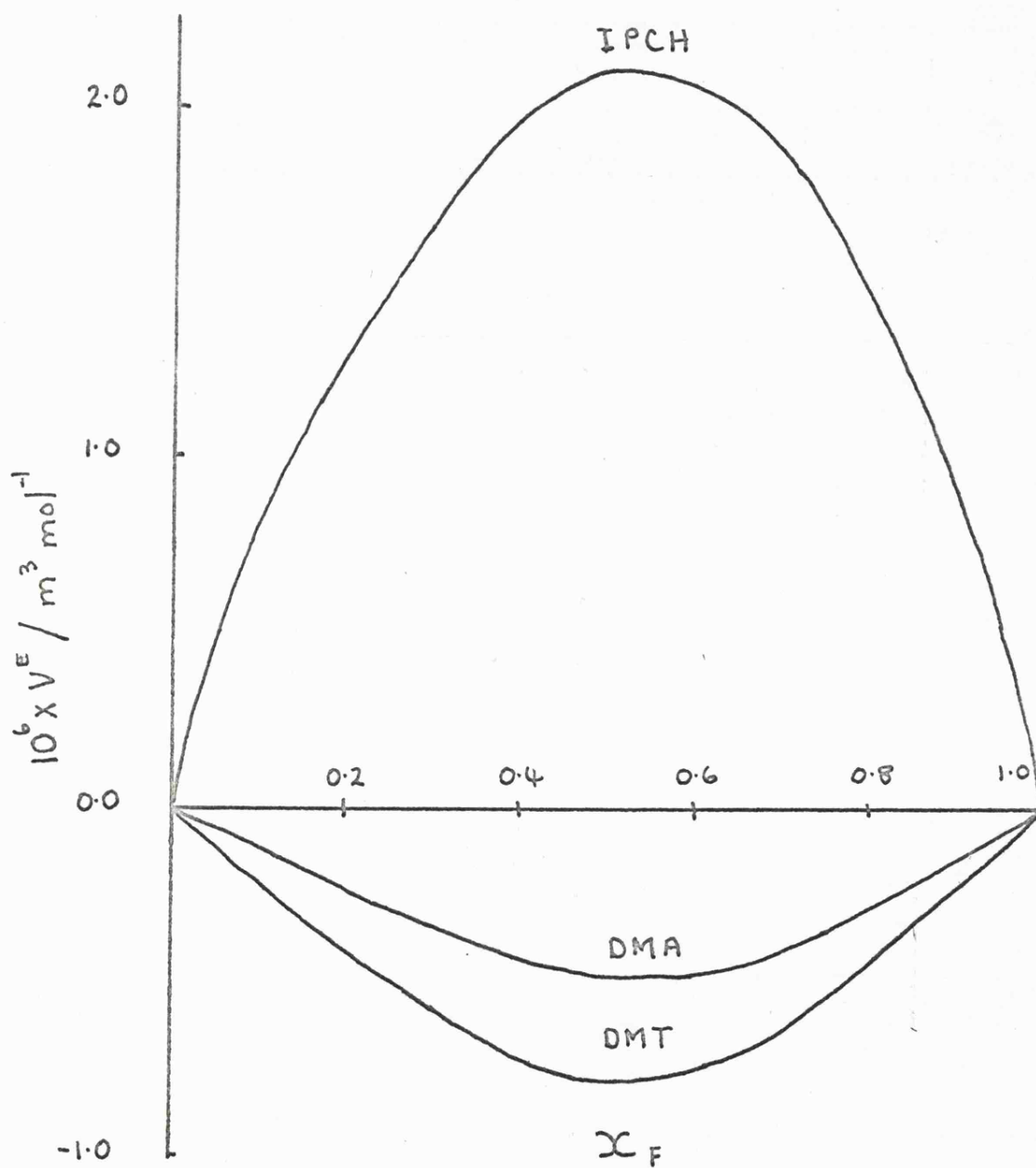


TABLE (6.6.4)

$V^E$  for pentafluorocyanobenzene (F) + N,N-dimethylaniline (DMA)  
at 323.15K

$x_F$	$10^6 \times V^E / m^3 \text{ mol}^{-1}$
0.1610	-0.1222
0.2453	-0.1890
0.3388	-0.2645
0.4203	-0.3065
0.5289	-0.3127
0.6329	-0.2465
0.7136	-0.1567
0.8085	-0.0754
0.9074	-0.0202

It was not possible to curve fit the data with a low enough number of coefficients to make the process meaningful.

TABLE (6.6.5)

$V^E$  for pentafluorocyanobenzene (F) + N,N-dimethylp-toluidine (DMT)  
at 323.15K

<u><math>x_F</math></u>	<u><math>10^6 \times V^E / m^3 \text{ mol}^{-1}</math></u>
0.2100	-0.4544
0.3261	-0.6817
0.4316	-0.8259
0.5447	-0.8232
0.6760	-0.6091
0.7502	-0.4487
0.8983	-0.1465

It was not possible to curve fit the data with a low enough number of coefficients to make the process meaningful.

FIGURE (6.6.2)

$V_s^E$  FOR PENTAFLUOROCYANOBENZENE WITH DMA. AT

323.15K AND WITH DMT. AT 328.15K

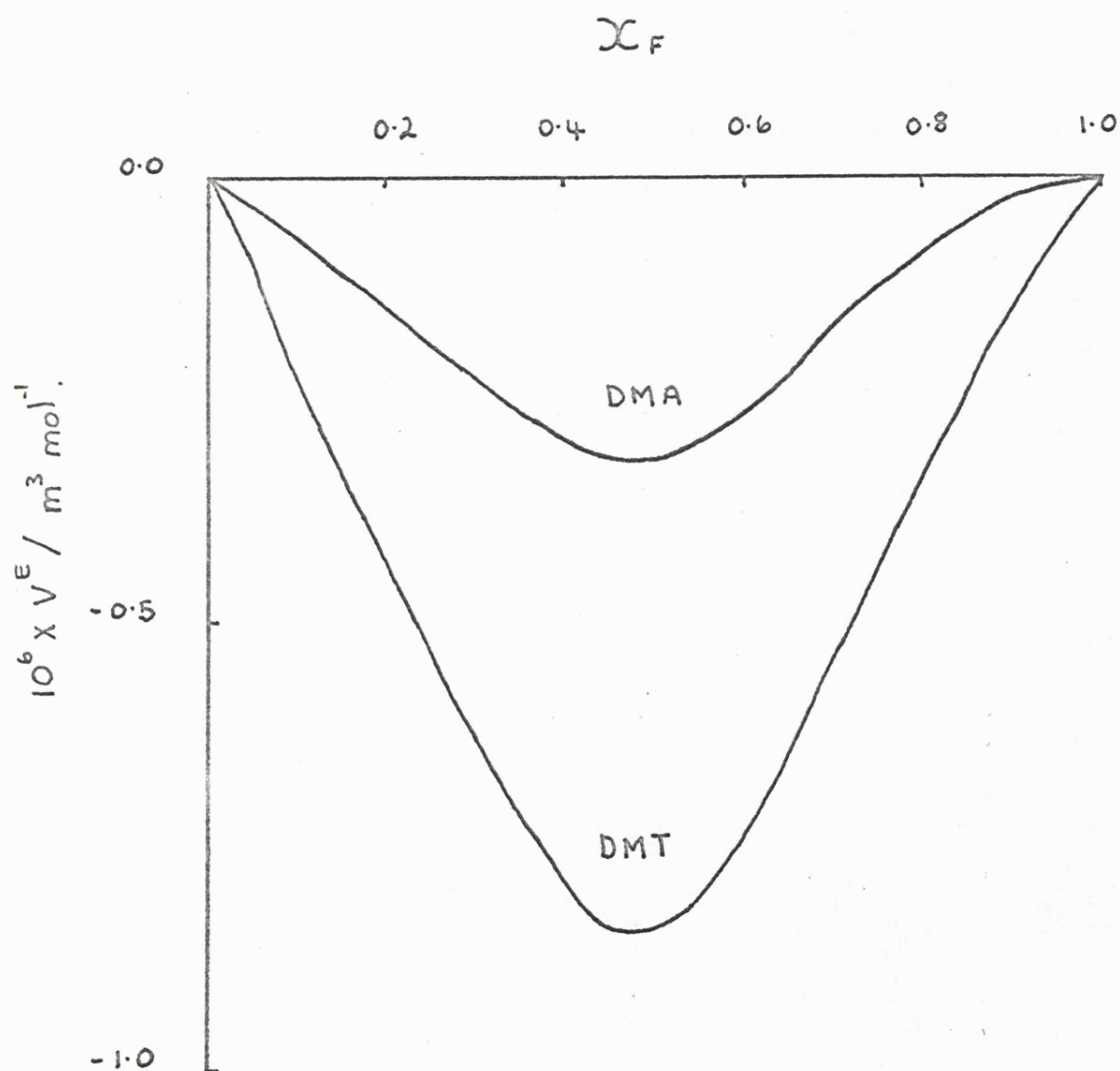


TABLE (6.6.6)

$V^E$  for pentafluorocyanobenzene (F) + benzene at 323.15K

$X_F$	$10^6 \times V^E_{\text{exp}}/\text{m}^3 \text{ mol}^{-1}$	$10^6 \times V^E_{\text{fitted}}/\text{m}^3 \text{ mol}^{-1}$
0.0770	0.3378	0.3312
0.1926	0.5960	0.6019
0.3258	0.6819	0.6798
0.4300	0.6340	0.6342
0.6774	0.3802	0.3789
0.8001	0.2376	0.2389

$$V_1 = 2.296 \times 10^{-6} \quad V_2 = 1.942 \times 10^{-6}, \quad V_3 = 1.007 \times 10^{-6}$$

$$\text{R.M.S.} = 3.293 \times 10^{-9} \text{ m}^3 \text{ mol}^{-1}$$

$$\text{S.D.} = 4.165 \times 10^{-9} \text{ m}^3 \text{ mol}^{-1}$$

TABLE (6.6.7)

$V^E$  for pentafluorocyanobenzene (F) + toluene at 323.15K

<u><math>X_F</math></u>	<u><math>10^6 \times V^E_{Exp}/m^3 \text{ mol}^{-1}</math></u>
0.0854	0.1915
0.1491	0.2794
0.2918	0.3427
0.3864	0.3255
0.4653	0.2849
0.5607	0.2372
0.7366	0.1383

It was not possible to curve fit the data with a low enough number of coefficients to make the process meaningful.

TABLE (6.6.8)

$V^E$  for pentafluorocyanobenzene (F) + p-xylene at 323.15K

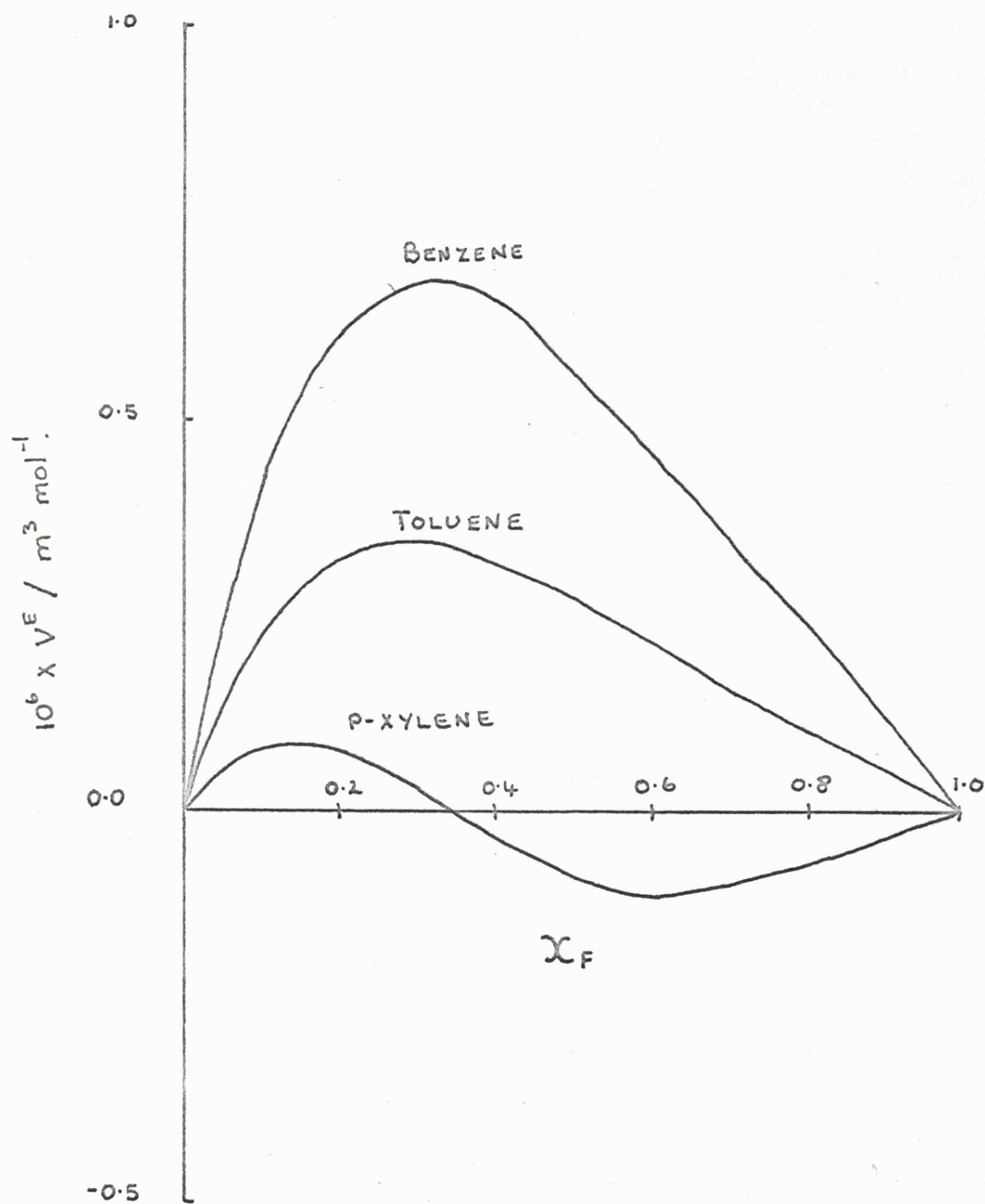
<u><math>x_F</math></u>	<u><math>10^6 \times V^E \text{ Exp. / m}^3 \text{ mol}^{-1}</math></u>
0.0877	0.0696
0.1485	0.0824
0.2296	0.0619
0.3222	0.0087
0.3768	-0.0258
0.5062	-0.0930
0.6000	-0.1085
0.6833	-0.1016
0.8026	-0.0741

It was not possible to curve fit the data with a low enough number of coefficients to make the process meaningful.

FIGURE (6.6.3)

$\bar{V}_s^E$  FOR PENTAFLUOROCYANOBENZENE + BENZENE, TOLUENE

AND P-XYLENE AT 323.15K





The results for the systems containing hexafluorobenzene are given in figure (6.6.1). The pentafluorocyanobenzene results are represented in figures (6.6.2) and (6.6.3). The former figure gives the results for the aromatic amines and the latter the results with benzene, toluene and p-xylene.

The temperature dependence for an equimolar composition of the system pentafluorocyanobenzene and benzene is found to be  $-0.003 \times 10^{-6} \text{ m}^3 \text{ mol}^{-1}$  when the only literature data available (15) is used in conjunction with the present data at 323.15K. This indicates that the excess volume is nearly independent of temperature.

## CHAPTER SEVEN

### PHASE DIAGRAMS

## PHASE DIAGRAMS

### 7.1 INTRODUCTION

The phase rule, which is usually written in the form,

$$C + 2 = F + P$$

where C is number of components, P the number of phases and F the number of degrees of freedom, applies to all macroscopic systems in a state of equilibrium and which are influenced only by changes in pressure, temperature and composition. It is assumed that under ordinary conditions the equilibrium is not affected by gravitational, electrical or magnetic forces.

If a two component system is treated as being at some fixed pressure, for convenience atmospheric pressure, then the remaining significant degrees of freedom are temperature and composition. Diagrams can therefore be made showing the phase behaviour in terms of these variables.

## LIQUID - LIQUID EQUILIBRIA

### 7.2 TECHNIQUE

The two components were injected into a small pyrex ampoule of 1cm<sup>3</sup> capacity, their weights being determined in the usual manner (6.3) and the ampoule was then attached to a vacuum line by a B10 cone. The sample was only quickly pumped on, to remove air, and it was then frozen down in liquid nitrogen and sealed.

The effect of pressure on the critical solution temperature has been shown to be undetectable with this technique by R.W. Smith (99), as would be expected (100).

The ampoule was totally immersed in a large beaker of water which was warmed slowly on a hot plate and stirred by a magnetic bead.

The temperature of the bath was measured with an N.P.L. certificated mercury in glass thermometer to  $\pm 0.1\text{K}$ . The point of miscibility was detected visually so the liquid meniscus had to be well defined. This was achieved by illuminating the meniscus from behind and then it was observed as a sharp red line. The ampoule was shaken frequently and the point of miscibility was taken as being the point at which the meniscus disappeared. This procedure was repeated at least twice for each sample and the average taken as the result. The results had a reproducibility better than  $\pm 0.5\text{ K}$ .

### 7.3 RESULTS

Table (7.3.1) shows the mutual solubilities of pentafluorocyanobenzene and isopropylcyclohexane together with the mole fraction,  $X_F$ , of pentafluorocyanobenzene. The results are represented in figure (7.3.1).

A few preliminary measurements have been made on pentafluorocyanobenzene and cyclohexane and these are given in table (7.3.2). These measurements were carried out while making calorimetric measurements on this system, because it was thought that phase separation might be occurring in the calorimeter. There was insufficient time to determine the complete mutual solubility curve.

Both systems have upper critical solution temperatures but the peaks occur in different mole fraction regions.

### SOLID - LIQUID EQUILIBRIA

### 7.4 APPARATUS

The apparatus used was a scaled down version of the N.P.L. freezing apparatus described by Herington and Handley (101), with a few modifications. It was developed in Leicester by R.W.Smith (102).

TABLE (7.3.1)

MUTUAL SOLUBILITIES OF PENTAFLUOROCYANOBENZENE AND ISOPROPYLCYCLOHEXANE

MIXTURES

<u><math>x_F</math></u>	<u>Temperature/K</u>
0.214	292.6
0.282	293.5
0.400	295.5
0.411	295.7
0.439	296.0
0.500	296.8
0.553	297.7
0.604	298.7
0.635	299.3
0.741	300.4
0.776	299.8
0.890	296.8

FIGURE (7.3.1)

MUTUAL SOLUBILITIES FOR PENTAFLUOROCYANOBENZENE AND ISOPROPYL-  
CYCLOHEXANE MIXTURES

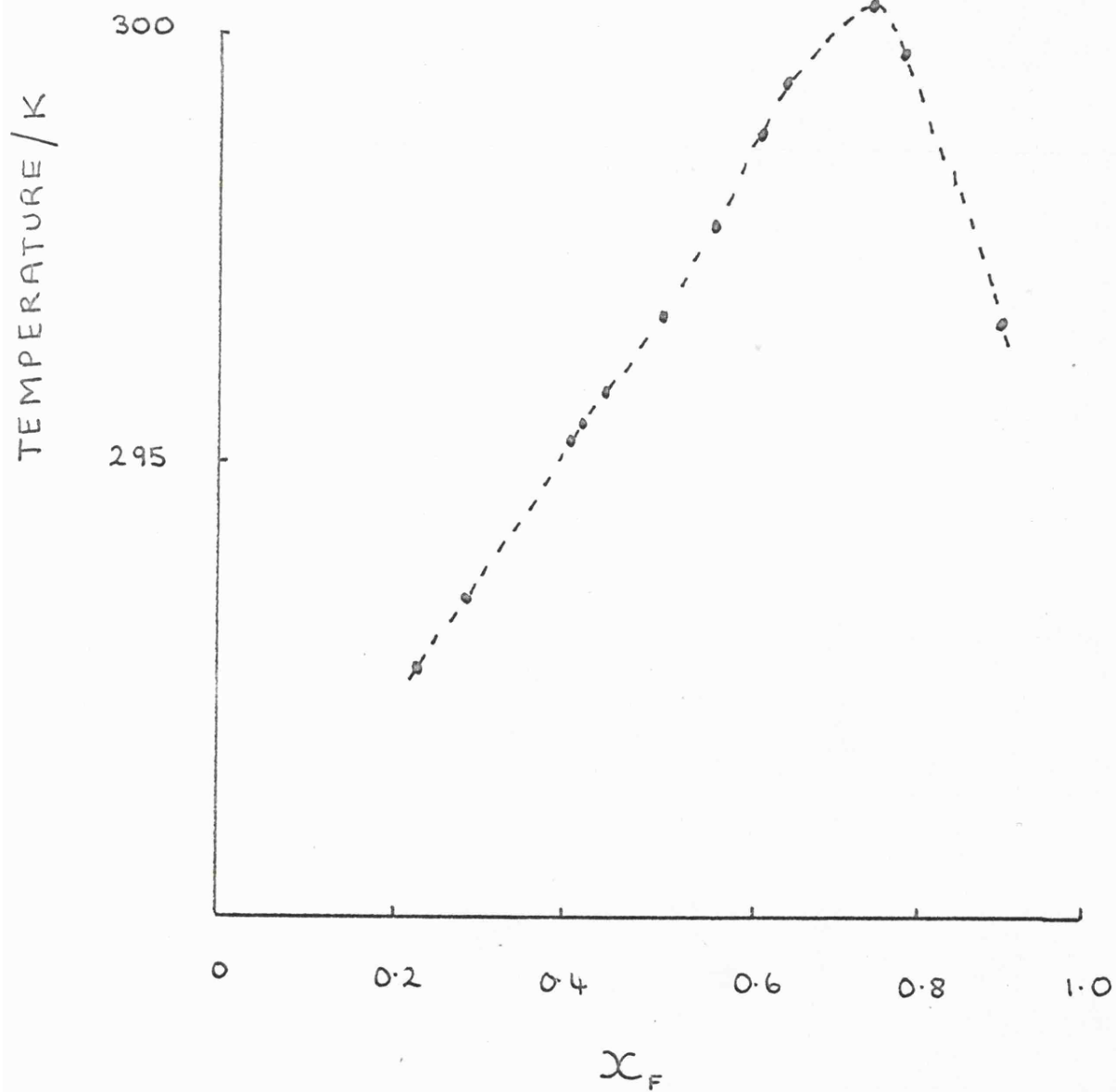


TABLE (7.3.2)

PRELIMINARY MEASUREMENTS ON THE MUTUAL SOLUBILITIES OF PENTAFLUOROCYANO-  
BENZENE AND CYCLOHEXANE MIXTURES

<u><math>X_F</math></u>	<u>Temperature/K</u>
0.207	298.2
0.440	299.6
0.502	299.4
0.554	298.7

The cell, which is shown in figure (7.4.1), consisted of a pyrex U-tube, with a squared off end, and slight indentations in the glass wall to facilitate mixing. One end of the U-tube incorporated a Quickfit screw thread joint which held the thermocouple pocket, while the other end was sealed by means of a Suba seal serum cap. The two limbs of the U-tube were joined at the top by a length of capillary tube incorporating a straight through stop cock between the limbs and B10 cones at either end. The stop cock bore was packed with glass wool and left open so that equilisation of the pressure difference across the cell occurred over a period of minutes.

A length of pyrex tube was sealed into the bottom section of the cell between the limbs so that it could accommodate a cooled piece of thin metal rod and enable the introduction of a cold spot in order to induce crystallisation in a super cooled sample.

The liquid in the cell was stirred by continuously applying pressure pulses of dry nitrogen to one side of the cell using a pulsing meter of the type described by Preston and Worthington (103). Plastic tubing was used to connect the pulsing meter to both the nitrogen supply and the cell, as shown in figure (8.4.2). The pulse was 'relayed' through a 20 cm high U-tube containing mercury, to ensure that the cell was a closed system.

On the opposite side of the cell to the U-tube a vessel, of volume  $15 \text{ cm}^3$ , provided the optimum stirring within the cell. This vessel and the U-tube both had taps which allowed the equipment to be flushed out with dry nitrogen before introduction of the sample.

The cell was supported by a polystyrene lid in the top of a small silvered dewar. This was then surrounded by another silvered dewar



FIGURE (7.4.1)

FREEZING POINT CELL

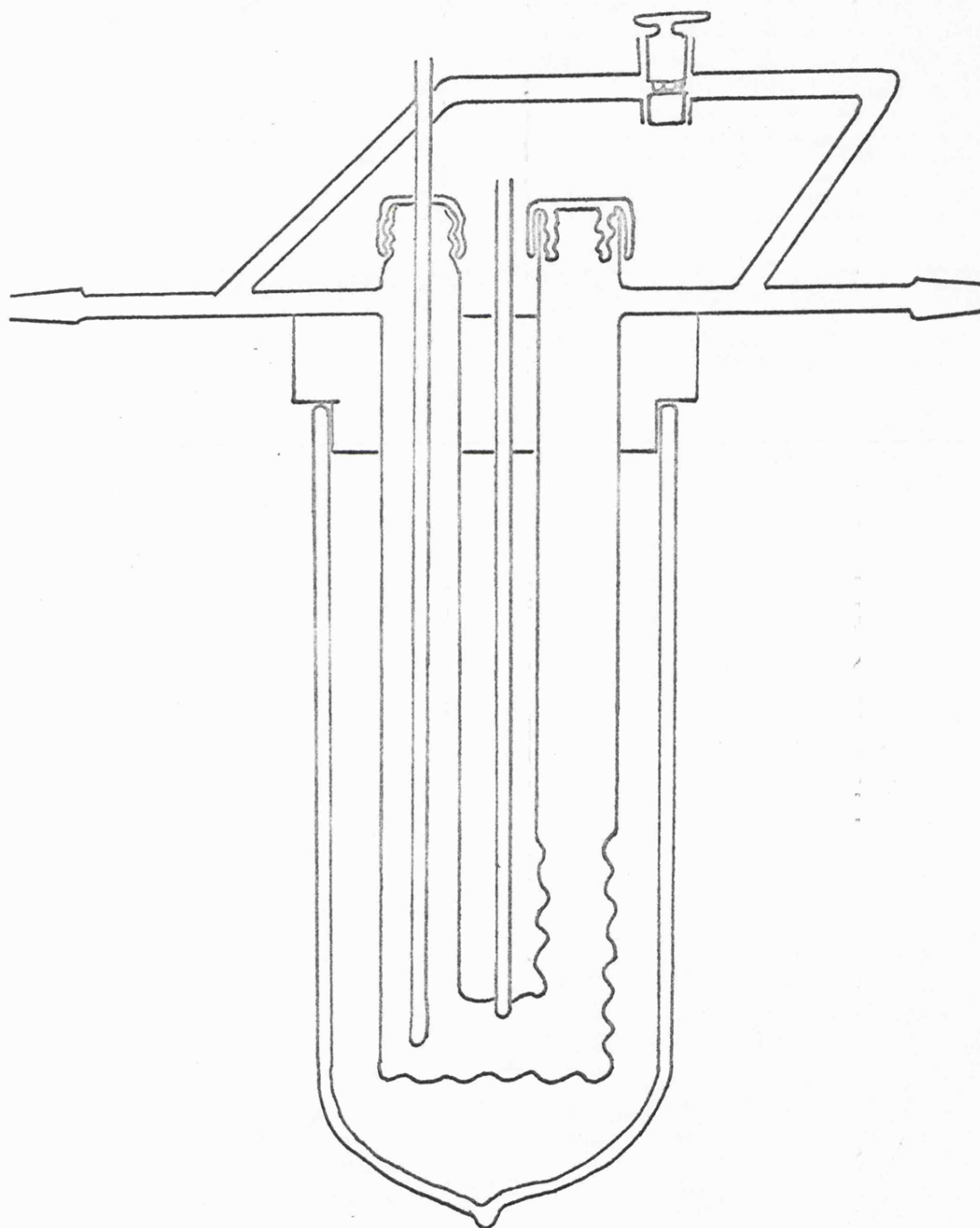
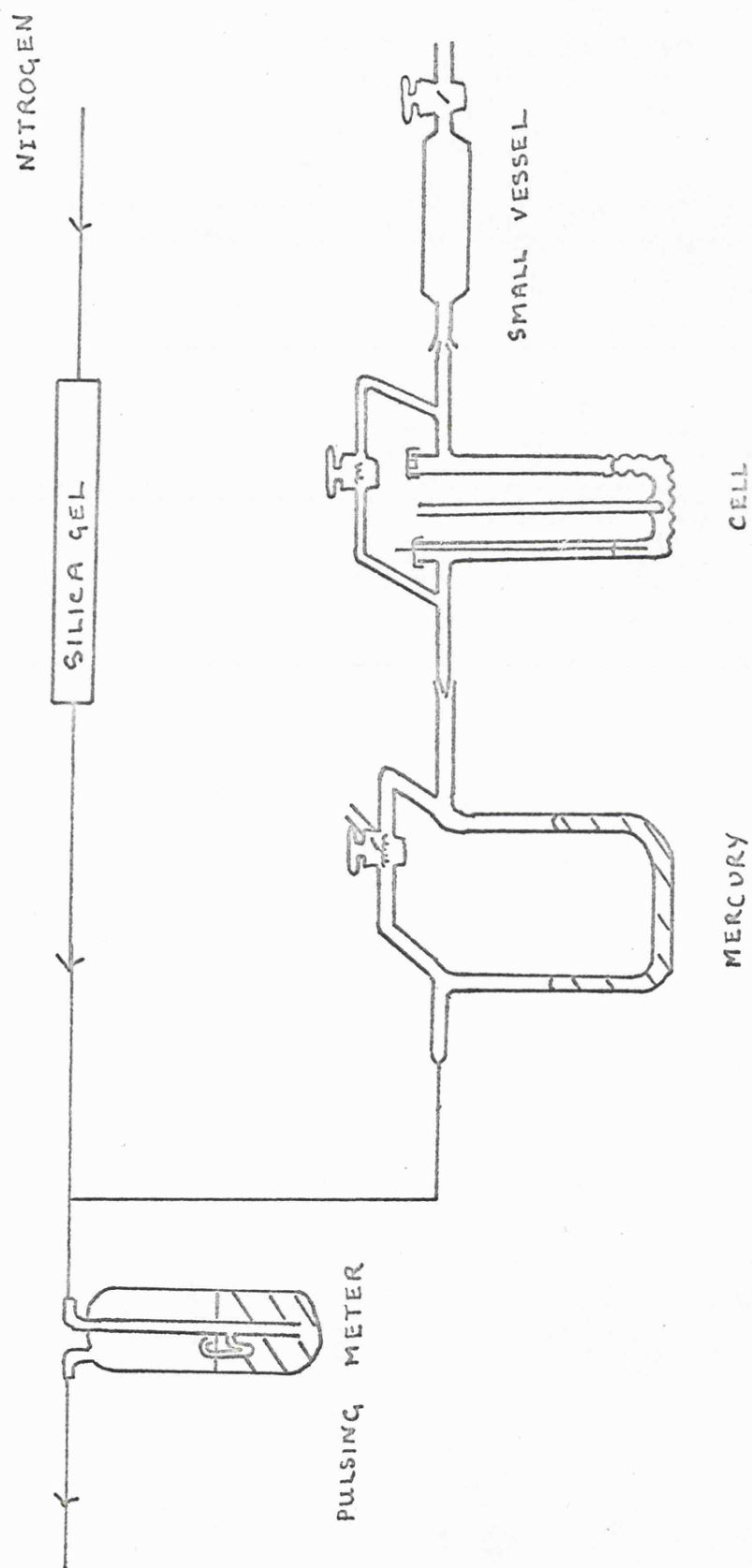


FIGURE (7.4.2)

DIAGRAMATIC REPRESENTATION OF THE FREEZING POINT APPARATUS



which was placed in liquid nitrogen as the coolant medium.

This gave a linear cooling rate for temperatures above 273.15K but was too slow a rate of cooling for temperatures below this. The required rate of cooling was achieved by using only one silver dewar around the cell and immersing this in the liquid nitrogen.

#### 7.5 CALIBRATION OF THERMOCOUPLE

A three junction thermocouple was made from a length of 30 s.w.g. copper-constantan thermocouple wire (Type 1A Saxonia Electrical Wire Co. Ltd.), using the technique described by Hart and Elkin (104).

The reference junction used for the thermocouple consisted of a dewar containing a mixture of water and crushed ice.

The sensor junction of the thermocouple was then placed in a series of baths, the temperatures of which were measured using a platinum resistance thermometer. The EMF generated by the thermocouple was measured using a Solartron IM 1604 digital voltmeter which was coupled to a Solartron data transfer unit 3230 and printer type 3244. An average of three readings were taken for each result.

The thermocouple used by previous workers was re-calibrated using the technique and fixed temperature baths described by Smith (99).

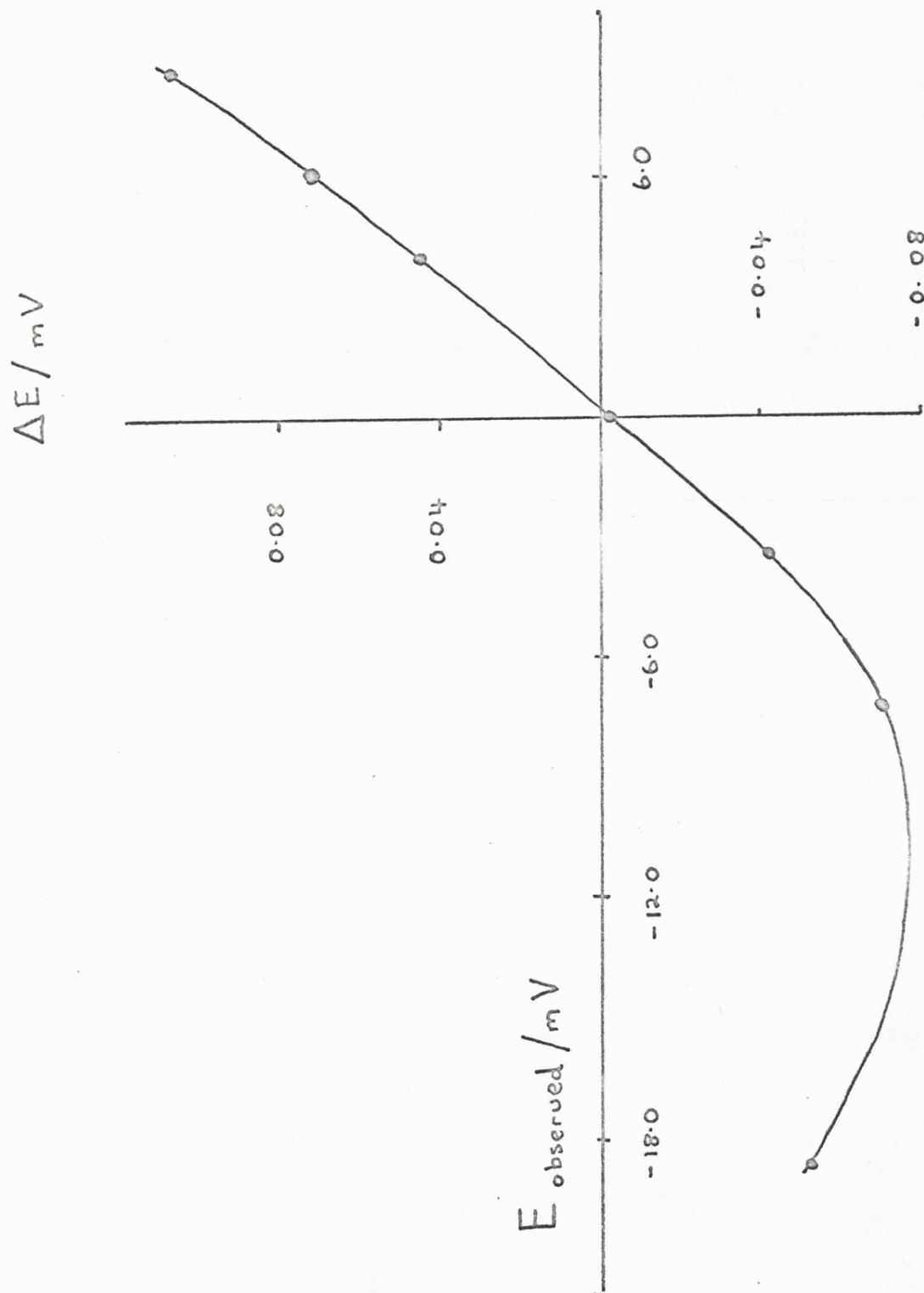
The calibration values obtained which are shown in table (7.5.1), were used to plot a curve of the deviation of the emf generated by the thermocouple from that of a standard thermocouple whose response had been precisely determined over a wide temperature range (105). The deviation,  $\Delta E$ , was plotted against the observed emf. as shown in figure (7.5.1). This allowed an observed emf to be corrected to a standard emf and then by use of the standard thermocouple tables (105) the temperature could be obtained.

TABLE (7.5.1) CALIBRATION VALUES FOR THE THERMOCOUPLE AT VARIOUS TEMPERATURES

Bath	Temperature/K	Observed emf/mV	$\Delta E/\mu V$
Water Thermostat	343.24	+8.625	+0.108
Water Thermostat	323.18	+6.034	+0.073
Sodium sulphate decahydrate Transition Temp.	305.53	+3.832	+0.044
Ice Point	273.16	+0.003	-0.002
Pure Mercury	234.29	-4.229	-0.049
Solid Carbon Dioxide	193.74	-8.169	-0.072
Liquid Nitrogen	77.56	-16.358	-0.052

FIGURE (7.5.1)

CALIBRATION CURVE FOR THE THERMOCOUPLE



## 7.6 OPERATION OF APPARATUS

The cell was washed with warm chromic acid, then distilled water followed by analar acetone. It was dried in an air oven for two hours,

The thermocouple pocket and serum cap were inserted into the side arms of the cell and all the ground glass joints were lightly greased with silicone grease before assembling the apparatus as shown in figure (7.4.2).

The cell was flushed out with dry nitrogen and the sample introduced into the cell, by way of the serum cap, using a hypodermic syringe with a long needle. The weight of each component was known by difference weighing of the syringe. The minimum total volume of the sample was  $6 \text{ cm}^3$ . This volume adequately covered the thermocouple junctions when the sample was being stirred. The nitrogen supply had to be altered each time until the pulsing meter operated at about 100 pulses per minute.

The required cooling rate was obtained as described in (section 7.4) and the typical length of a cooling run was about two hours. Readings of the emf values were taken at intervals of one minute up to the region of an arrest point where they were noted every twenty seconds. The emf values were plotted against time, as shown in figure (7.6.1) and the freezing point determined.

## 7.7 TEST MEASUREMENTS

The measurements made on the system hexafluorobenzene and cyclohexane are given in table (7.7.1) and shown in figure (7.7.1) along with the measurements of Duncan and Swinton (8). The two sets of data are seen to be in excellent agreement.

FIGURE (7.6.1)

A COOLING CURVE FOR PURE CYCLOHEXANE

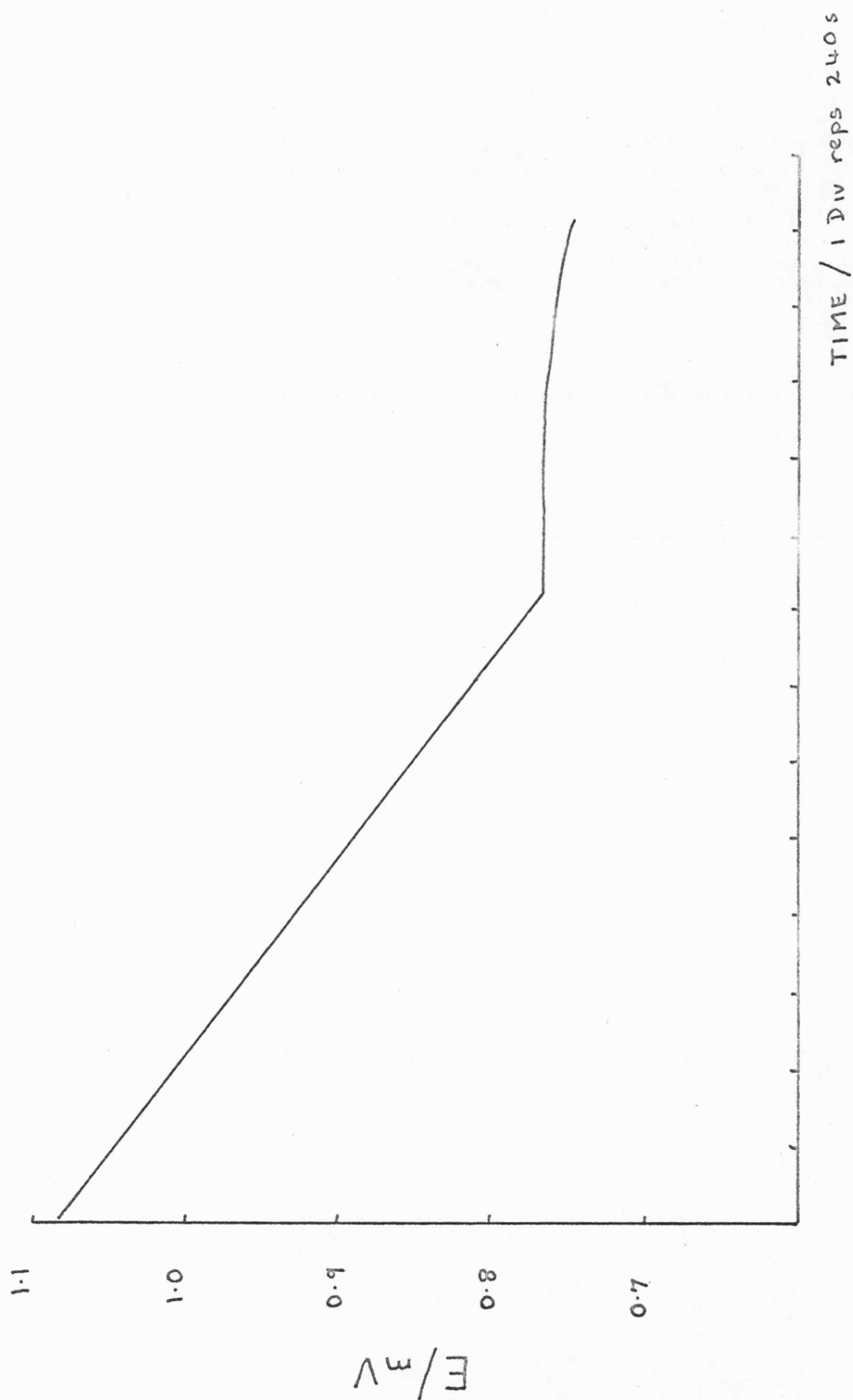


TABLE (7.7.1)

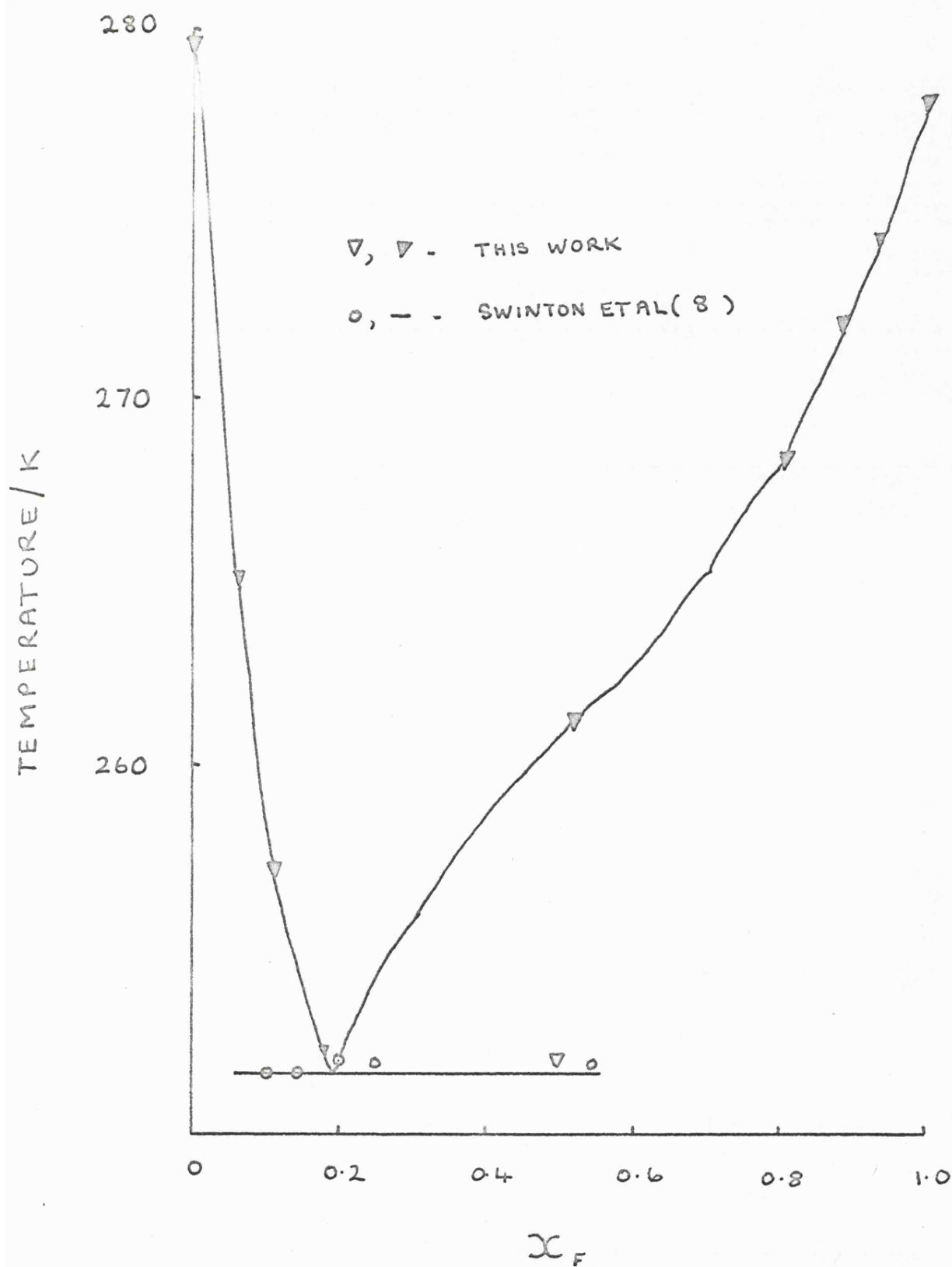
FREEZING POINTS OF HEXAFLUOROBENZENE (F) AND CYCLOHEXANE MIXTURES

<u><math>X_F</math></u>	<u>Freezing Point/K</u>	<u>Eutectic Temperature/K</u>
0.0000	279.70	
0.0612	265.74	
0.1128	257.18	
0.1883	252.19	252.19
0.5183	261.21	252.19
0.8037	268.20	
0.8835	272.14	
0.9336	274.21	
1.0000	278.05	



FIGURE (7.7.1)

SOLID-LIQUID PHASE DIAGRAM FOR HEXAFLUOROBENZENE AND CYCLOHEXANE



## 7.8 RESULTS

The measurements made on the system hexafluorobenzene and N,N-dimethylp-toluidine are given in table (7.8.1) and shown in figure (7.8.1) These measurements completent the earlier measurements made by Hall (34).

TABLE (7.8.1)

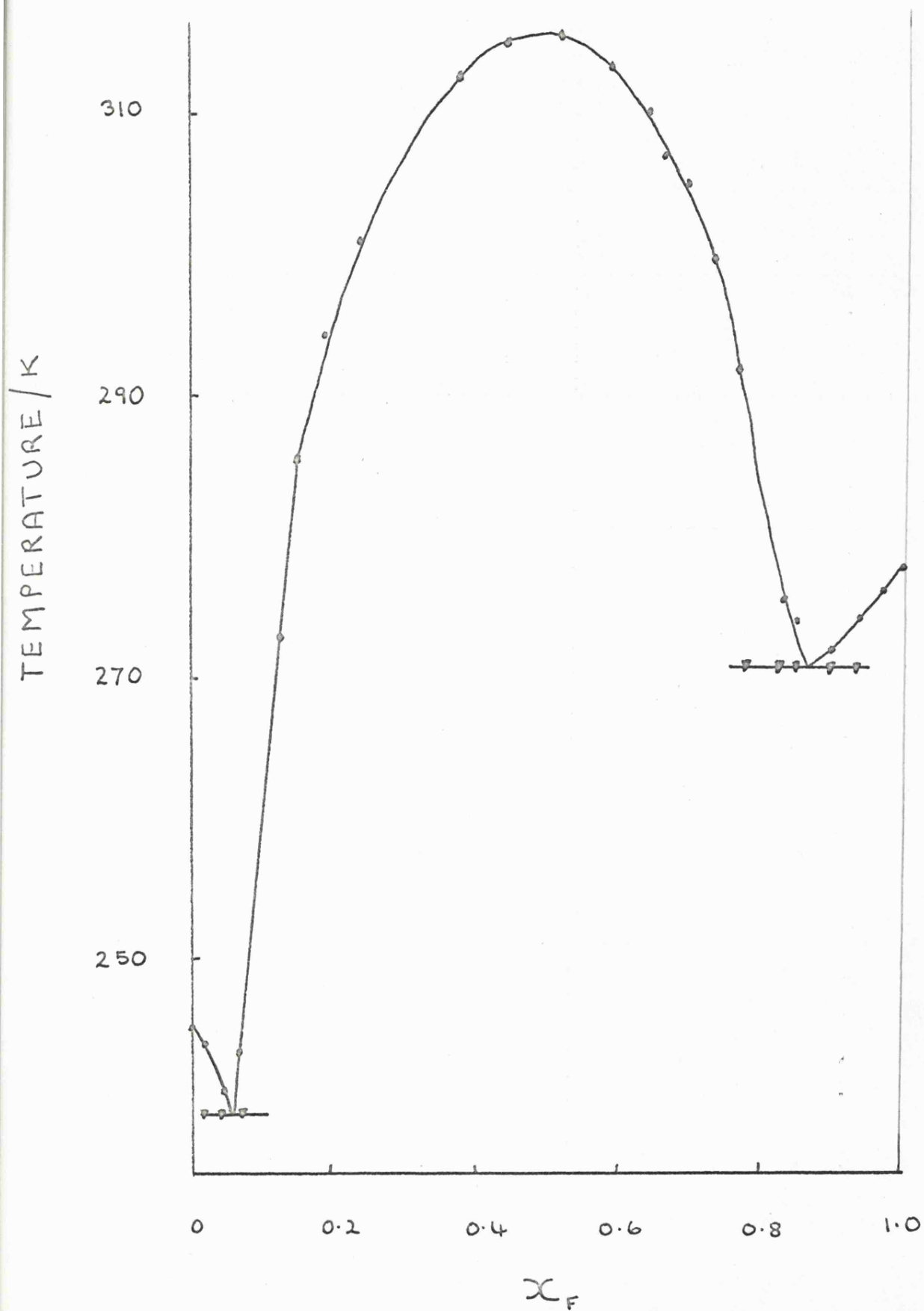
FREEZING POINTS OF HEXAFLUOROBENZENE (F) + N,N-DIMETHYLP-TOLUIDINE

MIXTURES

<u>X<sub>F</sub></u>	<u>Freezing Point/K</u>	<u>Eutectic Temperature/K</u>
0.0000	245.58	
0.0224	243.79	239.17
0.0406	241.10	239.17
0.0564	243.46	239.17
0.1258	273.90	
0.1552	286.58	
0.1986	295.70	
0.2551	302.23	
0.3651	312.27	
0.4422	315.18	
0.5172	315.59	
0.5822	313.99	
0.6384	309.40	
0.6678	307.50	
0.6975	304.76	
0.7266	301.07	
0.7603	293.49	270.76
0.8284	276.78	271.25
0.8521	274.88	270.76
0.8750	271.11	
0.8999	271.64	270.99
0.9481	274.44	270.94
0.9788	276.18	
1.0000	278.05	

FIGURE (7.8.1)

SOLID-LIQUID PHASE DIAGRAM FOR HEXAFLUOROBENZENE + N,N-DIMETHYL-  
P-TOLUIDINE



CHAPTER EIGHT

DISCUSSION OF RESULTS

## DISCUSSION

### 8.1 HEXAFLUOROBENZENE SYSTEMS

#### 8.1.1 Introduction

Armitage et al (34) determined the excess enthalpies of hexafluorobenzene + *N,N*-dimethylaniline, and *N,N*-dimethyl *p*-toluidine (plus several other amines) at 298.15K, 323.15K, and 343.15K. The values were large and exothermic

(*N,N*-dimethylaniline system,  $X_F = 0.5$  at 323.15K  $H^E = -1760 \text{ J mol}^{-1}$ ; *N,N*-dimethyl-*p*-toluidine system,  $X_F = 0.5$  at 323.15K  $H^E = -2616 \text{ J mol}^{-1}$  ).

The amine with the greater electron donating power gave the most exothermic result, which suggests that donor - acceptor complexing is possibly taking place.

As described in chapter 1, we may regard the excess property  $X^E$ , as being made up of two contributions, a physical, non-interacting contribution  $X_p^E$ , and a chemical, complexing contribution  $X_c^E$ .

In order to estimate the physical contribution  $X_p^E$ , a model, non-interacting system was chosen, namely hexafluorobenzene + isopropylcyclohexane. Isopropylcyclohexane was selected as being as close as possible, in shape, to *N,N*-dimethylaniline but with there being no possibility of any specific interaction occurring with hexafluorobenzene.

The actual chemical contribution to the excess enthalpies  $H_c^E$  ( $X_F=0.5$ ) for both amine systems, was obtained by subtracting  $H_p^E$  ( $X_F=0.5$ ), for isopropylcyclohexane + hexafluorobenzene ( $H_p^E = 1280 \text{ J mol}^{-1}$ ).

$H_c^E$  ( $X_F=0.5$ ) for the *N,N*-dimethylaniline system was  $-3040$   $J\ mol^{-1}$ , and for the *N,N*-dimethyl *p*-toluidine system was  $-3896$   $J\ mol^{-1}$ .

Armitage et al (17) then derived a value for  $H_c^E$ , for both systems, from the spectrophotometric data that they had obtained.  $H_c^E$  for the *N,N*-dimethylaniline system at 323.15K was  $-2810\ J\ mol^{-1}$  and for the *N,N*-dimethyl *p*-toluidine system was  $-3856\ J\ mol^{-1}$ .

Unexpectedly isopropylcyclohexane + hexafluorobenzene was a reasonable model for hexafluorobenzene + *N,N*-dimethyl *p*-toluidine, although the isopropylcyclohexane did not have the same skeletal shape as the amine.

The agreement was even more remarkable in view of the various assumptions made. In particular it was assumed that the equilibrium constant  $K_x$ , determined from spectroscopic measurements using dilute solutions in an inert solvent, could be used to calculate the extent of complex formation in the binary system when no solvent was present.

In view of this it was felt that a completely independent estimate of  $K_x$ , in the absence of solvent, was desirable. Such an estimate may be obtained from the excess Gibbs function measurements.

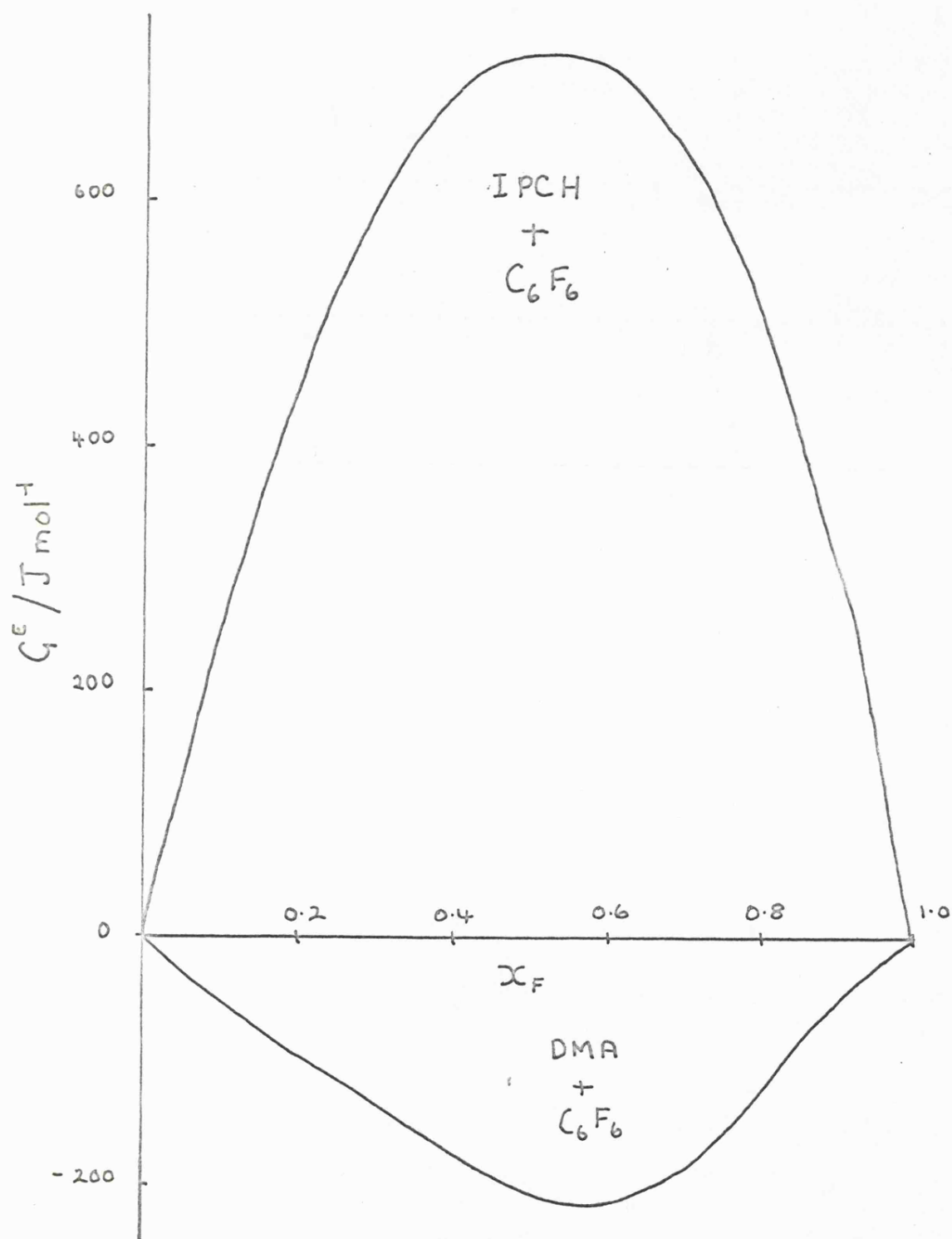
#### 8.1.2 Excess Gibbs Functions

The excess Gibbs functions for *N,N*-dimethylaniline + hexafluorobenzene at 322.52K, and the excess Gibbs functions for isopropylcyclohexane + hexafluorobenzene at 323.15K, are shown in figure (8.1.2a).

FIGURE (8.1.2a)

EXCESS GIBBS FUNCTIONS FOR HEXAFLUOROBENZENE + N,N-DIMETHYLANILINE

AT 322.52K AND ISOPROPYLCYCLOHEXANE AT 323.15K





The excess Gibbs functions for hexafluorobenzene + N,N-dimethylaniline are seen to be negative, (at  $X_F=0.5$ ,  $G^E=-207 \text{ J mol}^{-1}$ ). This is consistent with the excess volume and enthalpy data, and indicates complexing in the liquid state.

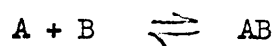
The excess Gibbs functions for the non-interacting analogue of N,N-dimethylaniline + hexafluorobenzene, isopropylcyclohexane + hexafluorobenzene, are large and positive, (at  $X_F=0.5$ ,  $G^E=724 \text{ J mol}^{-1}$ ). This equimolar value for the excess Gibbs function is close to that for hexafluorobenzene + cyclohexane, ( $X_F=0.5$ ,  $G^E=755 \text{ Jmol}^{-1}$ ) determined by Gaw and Swinton (10).

The excess Gibbs function for the chemical (or complexing) contribution  $G_c^E$ , to the N,N-dimethylaniline + hexafluorobenzene system, can be obtained by taking into account the non-interacting contribution  $G_p^E$ , as measured by isopropylcyclohexane + hexafluorobenzene.

At  $X_F=0.5$   $G_c^E$  is then  $-931 \text{ J mol}^{-1}$ .

Saroléa - Mathot (47) has developed a theory of associated solutions which can be made use of to obtain  $G_c^E$  in terms of the equilibrium constant for complex formation  $K_x$ , and the stoichiometric mole fractions of components,  $X_A$  and  $X_B$  in the following manner:-

If there are  $N_A$  moles of A and  $N_B$  moles of B, initially, and for convenience  $N_A + N_B = 1$  mole then if complexing takes place,



at equilibrium there are  $N_{A1}$  moles of uncomplexed A

$N_{B1}$  moles of uncomplexed B

$N_{AB}$  moles of complex, AB

( in 1 mole of mixture)

$$\text{and } N_A = N_{Ai} + N_{AB} \quad 8.1$$

$$N_B = N_{Bi} + N_{AB} \quad 8.2$$

The association constant K, is defined by

$$K = \frac{N_{AB} (N_{Ai} + N_{Bi} + N_{AB})}{N_{Ai} N_{Bi}} \quad 8.3$$

from Sarolea - Mathot (47)

Substituting 8.1 and 8.2 in 8.3

$$K = \frac{N_{AB} (N_A + N_B - N_{AB})}{(N_A - N_{AB}) (N_B - N_{AB})} \quad 8.4$$

Therefore

$$K(N_A N_B - N_{AB} N_B - N_{AB} N_A + N_{AB}^2) = N_{AB} N_A + N_{AB} N_B - N_{AB}^2 \quad 8.5$$

and writing equation 8.5 as a quadratic in  $N_{AB}$

$$N_{AB}^2 (1+K) - N_{AB} ((N_A + N_B)(1+K)) + K N_A N_B = 0 \quad 8.6$$

Solution of this quadratic gives

$$N_{AB} = \frac{(N_A + N_B)(1+K) \pm \sqrt{(N_A + N_B)^2 (1+K)^2 - 4(1+K) K N_A N_B}}{2(1+K)} \quad 8.7$$

In terms of mole fraction then,

$$X_{AB} = \frac{N_{AB}}{N_A + N_B} = \frac{(1+K) \pm \sqrt{(1+K)^2 - 4(1+K) K X_A X_B}}{2(1+K)} \quad 8.8$$

and by removing  $(1+K)$  from the denominator

$$X_{AB} = \frac{1 \pm \sqrt{1 - (4K X_A X_B)/(1+K)}}{2} \quad 8.9$$

$$X_A + X_B = 1, \text{ therefore } (X_A + X_B)^2 = 1$$

and

$$X_A^2 + X_B^2 + 2X_A X_B = 1 \quad 8.10$$

Substituting 8.10 in 8.9 gives

$$\chi_{AB} = \frac{1 \pm \sqrt{\chi_A^2 + \chi_B^2 + 2\chi_A\chi_B - 4K\chi_A\chi_B/(1+K)}}{2} \quad 8.11$$

and this reduces to

$$\chi_{AB} = \frac{1 \pm \sqrt{\chi_A^2 + \chi_B^2 + 2\chi_A\chi_B(1-K)/(1+K)}}{2} \quad 8.12$$

When  $K=0$ ,  $\chi_{AB}$  must be zero and this is only true if the negative root is adopted,

$$\chi_{AB} = \frac{1 - \sqrt{\chi_A^2 + \chi_B^2 + 2\chi_A\chi_B(1-K)/(1+K)}}{2} \quad 8.12$$

The excess Gibbs function for this system arises out of complex formation and so it can be termed  $G_c^E$ .

$$G_c^E = RT (\chi_A \ln f_A + \chi_B \ln f_B) \quad 8.13$$

It has been shown by Prigogine, Mathot and Desmyter (107) that for associated solutions, the activity coefficients are given by,

$$f_A = \frac{1}{\chi_{A1}^*} \frac{\chi_{A1}}{\chi_A} \quad ; \quad f_B = \frac{1}{\chi_{B1}^*} \frac{\chi_{B1}}{\chi_B} \quad 8.14$$

where  $\chi_A, \chi_B$  are the mole fractions of A and B,  $\chi_{A1}$  and  $\chi_{B1}$  are the effective mole fractions, when taking into account the presence of complexes AB, and  $\chi_{A1}^*, \chi_{B1}^*$  are the values of  $\chi_{A1}, \chi_{B1}$  in the pure liquids A and B.

$$\text{Here } \chi_{A1}^* = \chi_{B1}^* = 1$$

so 8.14 becomes

$$f_A = \frac{\chi_{A1}}{\chi_A} \quad ; \quad f_B = \frac{\chi_{B1}}{\chi_B} \quad 8.15$$

$X_{A1}$  is given by

$$X_{A1} = \frac{N_A - N_{AB}}{N_A + N_B - N_{AB}} \quad 8.16$$

Dividing through by  $N_A + N_B$  on the right hand side,

$$X_{A1} = \frac{X_A - X_{AB}}{1 - X_{AB}} \quad 8.17$$

Similarly for  $X_{B1}$ ,

$$X_{B1} = \frac{X_B - X_{AB}}{1 - X_{AB}} \quad 8.18$$

Substituting 8.17 and 8.18 into equations 8.15,

$$f_A = \frac{X_A - X_{AB}}{X_A(1 - X_{AB})} ; f_B = \frac{X_B - X_{AB}}{X_B(1 - X_{AB})} \quad 8.19$$

If in equation 8.13 the expressions for  $f_A$  and  $f_B$  are substituted,

$$G_c^E = RT \left[ X_A \ln \left( \frac{X_A - X_{AB}}{X_A(1 - X_{AB})} \right) + X_B \ln \left( \frac{X_B - X_{AB}}{X_B(1 - X_{AB})} \right) \right]$$

8.20

This equation, together with equation 8.12,

$$X_{AB} = \frac{1 - \sqrt{X_A^2 + X_B^2 + 2X_A X_B(1 - K_x)}}{2} / (1 + K_x)$$

(where  $K = K_x$ ) can be used in conjunction with the experimental value of  $G_c^E$ , to obtain a value for the equilibrium constant of complexing  $K_x$ .

For N,N-dimethylaniline + hexafluorobenzene, the equilibrium constant  $K_x$ , which is obtained, is 2.3 (at 323K). The spectroscopic value for  $K_x$  is 3.1. The agreement, though moderate, is encouraging in view of the assumptions that have to be made in evaluating the equilibrium constants both from spectroscopy and vapour pressure measurements.

### 8.1.3 Solid - Liquid Phase Diagrams

The solid-liquid phase diagram for hexafluorobenzene + N,N-dimethyl-p-toluidine is given in figure (8.1.3a), and shows a well defined maximum at  $X_F$  0.5, indicating the existence of a 1:1 solid complex with a melting point of 315.6K.

This result is again consistent with the idea of 1:1 complexing occurring insolution.

The solid-liquid phase diagrams for both hexafluorobenzene + N,N-dimethylaniline and pentafluorocyanobenzene + N,N-dimethylaniline have been studied by Hall et al (34) and show the existence of congruently melting 1:1 solid complexes as shown in figure (8.1.3b).

### 8.1.4 Excess Volumes of Mixing

The excess volumes of mixing at 323.15K for hexafluorobenzene + N,N-dimethylaniline, N,N-dimethyl p-toluidine and isopropylcyclohexane are shown in figure (8.1.4a).

The aromatic amine systems both have negative volumes of mixing, with the N,N-diemthyl p-toluidine system being slightly more negative.

FIGURE (8.1.3a)

THE SOLID-LIQUID PHASE DIAGRAM FOR HEXAFLUOROBENZENE + N,N-DIMETHYL-P-TOLUIDINE

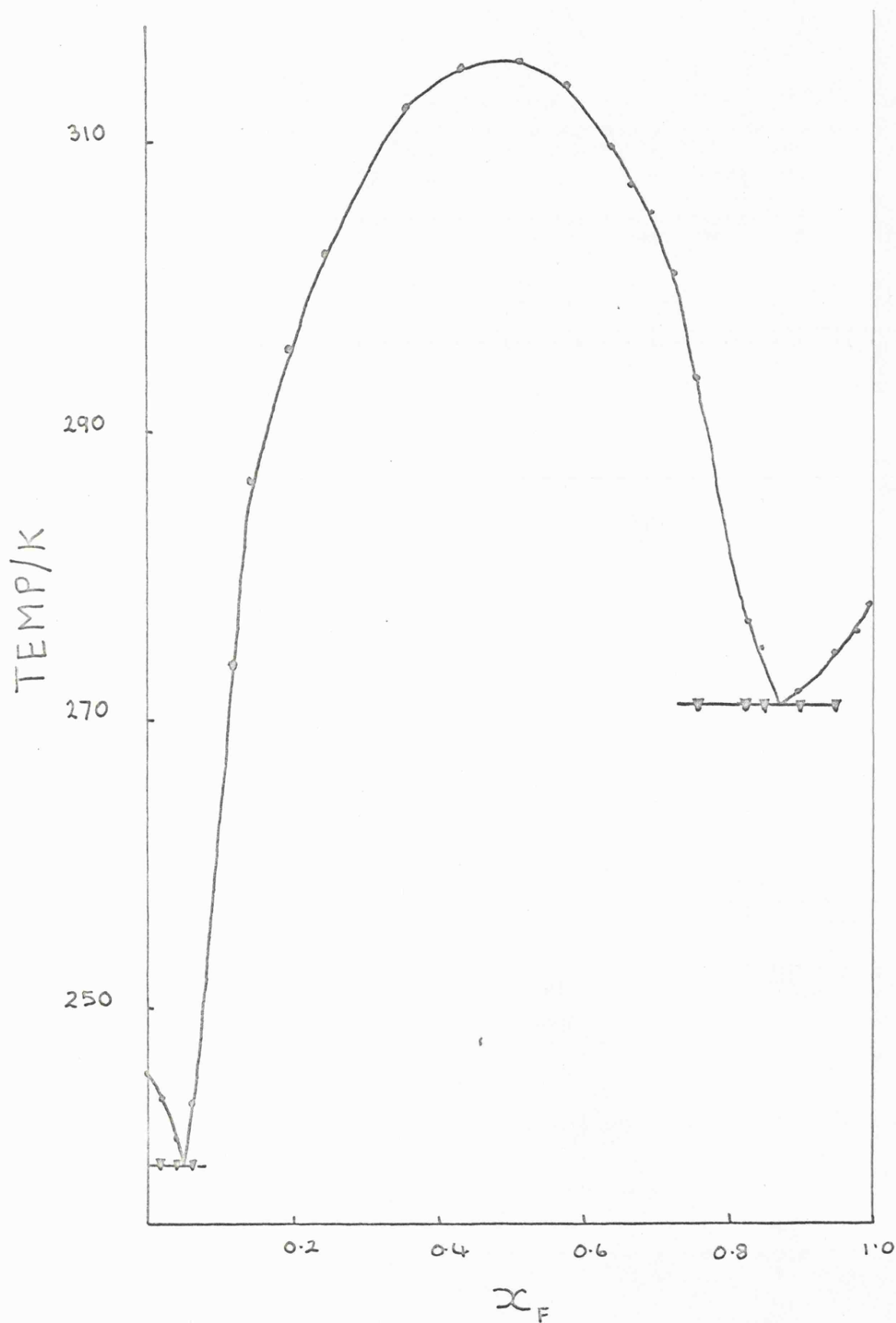


FIGURE (8.1.3b)

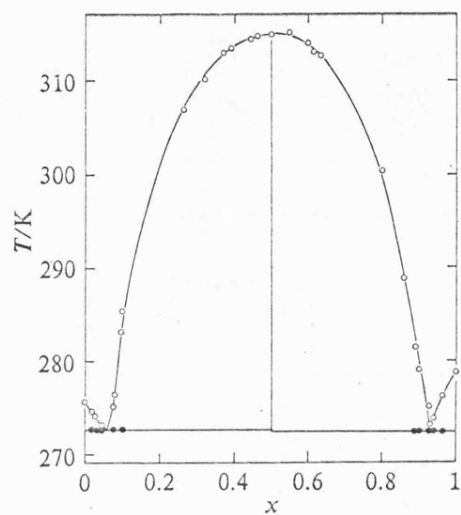


FIGURE 1. Phase diagram for  $x\text{C}_6\text{F}_6 + (1-x)\text{C}_6\text{H}_5\text{N}(\text{CH}_3)_2$ .

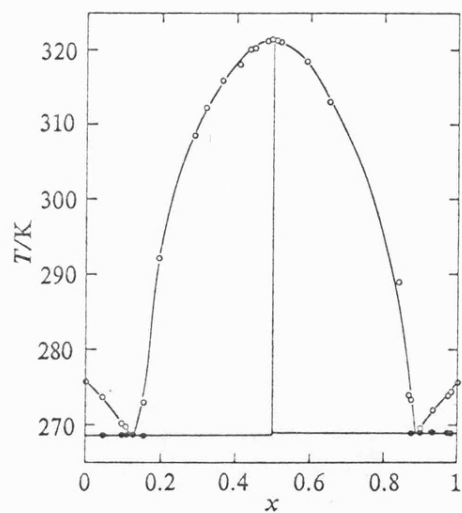
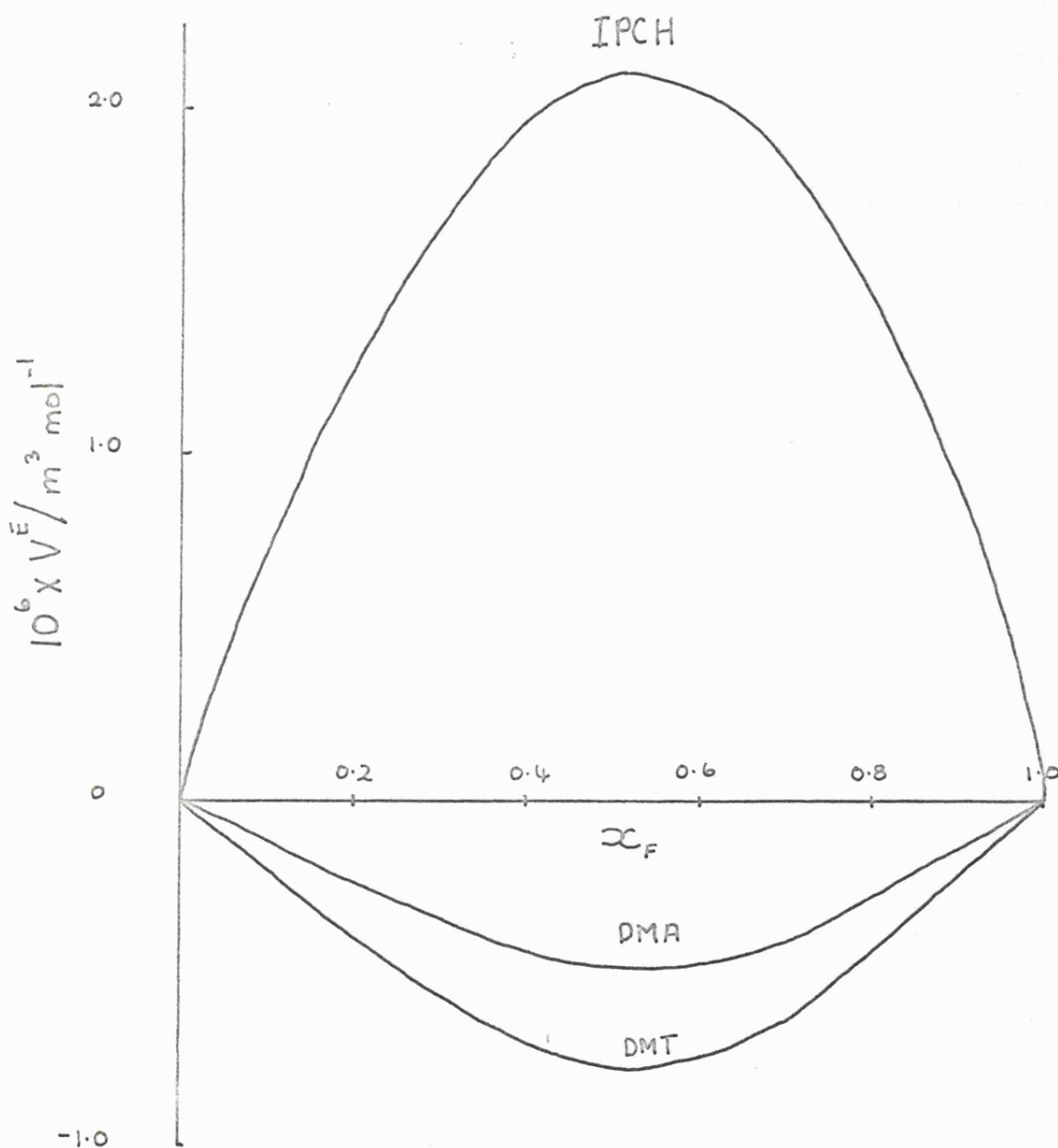


FIGURE 3. Phase diagram for  $x\text{C}_6\text{F}_5\text{CN} + (1-x)\text{C}_6\text{H}_5\text{N}(\text{CH}_3)_2$ .

FIGURE (8.1.1a)

$V_s^E$  FOR HEXAFLUOROBENZENE + ISOPROPYLCYCLOHEXANE (IPCH), +  
N,N-DIMETHYLANILINE (DMA) AND N,N-DIMETHYL-P-TOLUIDINE (DMT)  
AT 323.15K





The sign and magnitude of the excess volumes of mixing are often regarded as giving an indication of the strength of the unlike interaction in a binary mixture. A large negative excess volume is taken as indication of possible complex formation.

By adopting the same model as used previously the chemical (complexing) contribution  $V_c^E$ , can be obtained for both amine systems if  $V_p^E$  is measured by isopropylcyclohexane + hexafluorobenzene in both cases. For the N,N-dimethylaniline system  $V_c^E = -2.564 \times 10^{-6} \text{ m}^3 \text{ mol}^{-1}$  and  $X_F = 0.5$ , and for the N,N-dimethyl p-toluidine system  $V_c^E = -2.944 \times 10^{-6} \text{ m}^3 \text{ mol}^{-1}$  and  $X_F = 0.5$ . These quantities are considerably more negative than the excess volumes for the systems and are stronger evidence for possible complexing.

However it must be remembered that molecular packing in the pure components, as well as in the mixture, make a major contribution to the volumes of mixing so their interpretation is speculative.

#### 8.1.5 Summary

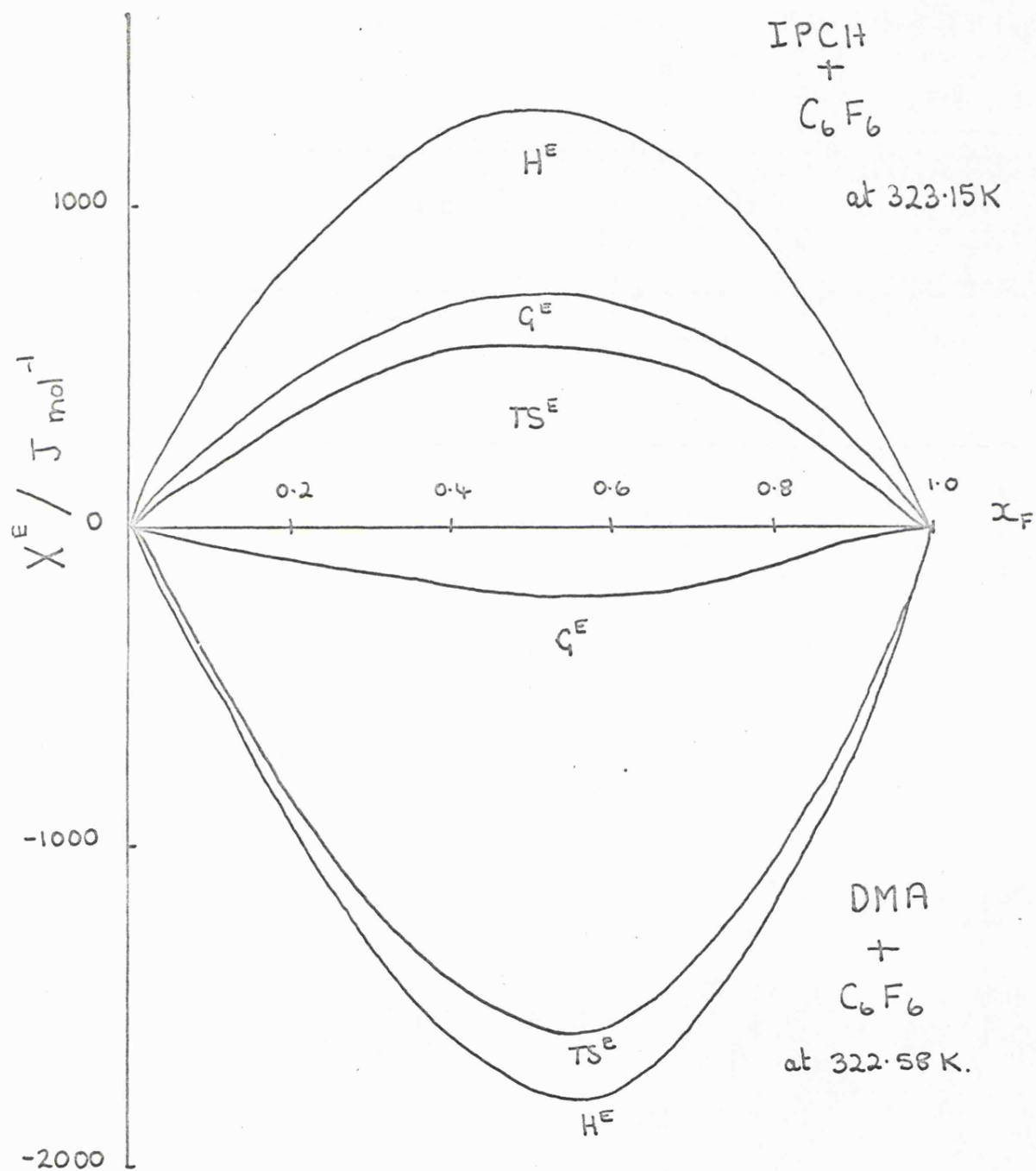
The excess thermodynamic functions at 323.15K for hexafluorobenzene + N,N-dimethylaniline, and isopropylcyclohexane are given in figure (8.1.5a).

All of the excess functions for hexafluorobenzene + N,N-dimethylaniline, together with the other thermodynamic (35) and spectroscopic (17, 32, 33) evidence available for other amine systems, indicates that strong complexing occurs in these systems.

The actual nature of the specific interaction is thought to be of the charge - transfer type.

FIGURE (3.1.5a)

THERMODYNAMIC EXCESS FUNCTIONS



For charge transfer to occur, there must be a favourable overlap between the highest filled orbital of the donor molecule and the lowest unfilled orbital of the acceptor, Morcom and Armitage (35) have carried out a Hückel molecular orbital calculation on both hexafluorobenzene and N,N-dimethylaniline. Figure (8.1.5b) gives the highestfilled  $\pi$  orbital for N,N-dimethylaniline (II) and the two lowest unfilled orbitals of hexafluorobenzene, (III, IV).

A considerable degree of overlap is possible between configurations (II) and (III) if the donor and acceptor molecules are 'off set' (V). Such a configuration could account for the charge-transfer bands observed by Beaumont and Davis (33), and therefore it would appear that charge transfer complexing is occurring in these systems.

## 8.2 PENTAFLUOROCYANOBENZENE + HYDROCARBON SYSTEMS

### 8.2.1 Excess Volumes of Mixing

The excess volumes of mixing results at 323.15K for pentafluorocyanobenzene with benzene, toluene and p-xylene are shown in figure (8.2.1a). The curves are all skewed but to various degrees and the p-xylene curve is S shaped.

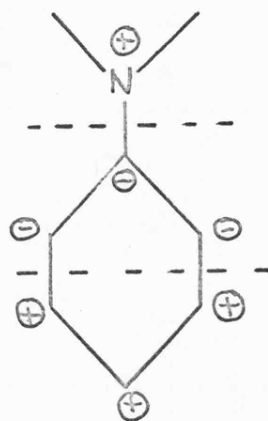
The results of Swinton and Duncan (7) for the parallel hexafluorobenzene systems at 313.15K have similarly shaped curves, as shown in figure (8.2.1b), although the p-xylene curve does not change sign. The values for  $V^E$  at  $X_F = 0.5$  are also quite close but more positive than those for the pentafluorocyanobenzene systems.

Stubley (12) has also obtained results for pentafluorobenzene with benzene, toluene and p-xylene at 298.15K. As expected these results are the most positive of all the three groups of results and are given in figure (8.2.1b).

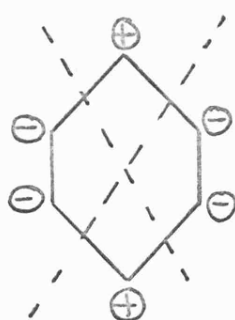
FIGURE (8.1.5b)



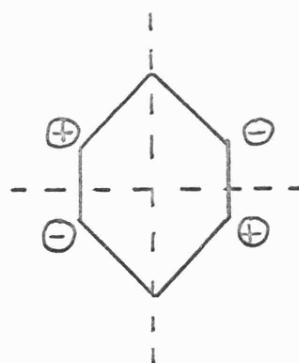
I amine skeleton



II highest filled donor orbital



III unfilled acceptor orbital



IV unfilled acceptor orbital



V Possible configuration of complex

FIGURE (8.2.1a)

$V^E$  FOR PENTAFLUOROTOLUENE + BENZENE, TOLUENE AND P-XYLENE

AT 323.15K

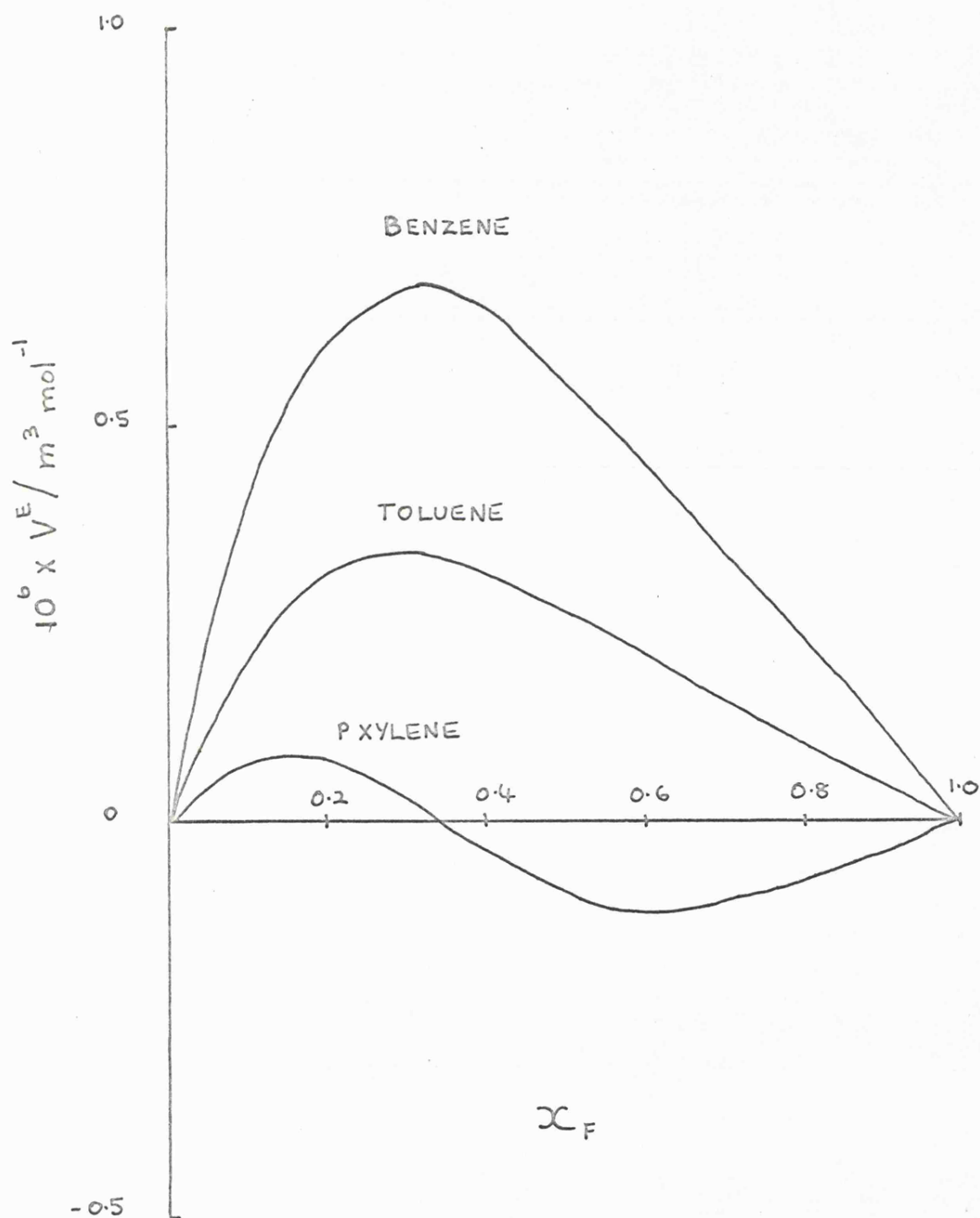
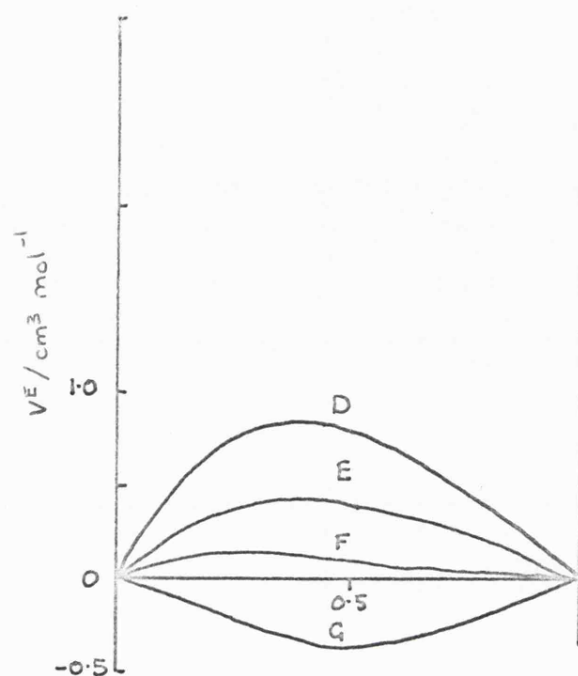


FIGURE (8.2.1b)



Excess volumes of mixing  $V^E$  at  $40^\circ\text{C}$  for hexafluorobenzene + D, Benzene; E, Toluene; F, P-xylene; G, mesitylene.

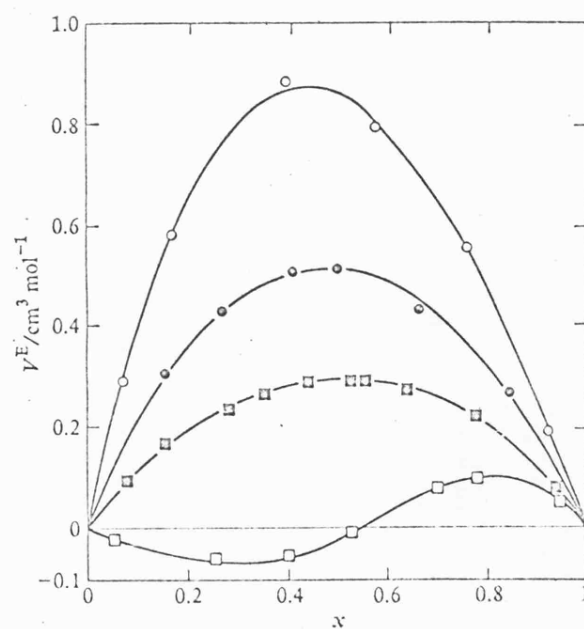


FIGURE 2. Excess volumes  $V^E$  at 298.15 K plotted against mole fraction  $x$  of pentafluorobenzene.  $\circ$ , pentafluorobenzene + benzene;  $\circ$ , + toluene;  $\square$ , + *p*-xylene;  $\square$ , + mesitylene.

Figure (8.2.1c) shows the results for all the three groups of systems at  $X_F = 0.5$  plotted against the number,  $n$ , of methyl groups substituted in the aromatic nucleus. The excess volumes decrease with increasing substitution of the aromatic ring. The aromatic hydrocarbons have increasingly lower ionisation potentials in the series from benzene to p-xylene. There is also an enhancement of interaction between fluorocarbon and hydrocarbon in the series although this is not necessarily due to the decreasing ionisation potentials.

$V_c^E$  at  $X_F = 0.5$ , the complexing contribution to the excess volume, is obtained by using the fluorocarbon + cyclohexane system as the model for the fluorocarbon + benzene mixtures. Then the  $V_c^E$  values are as follows:- hexafluorobenzene + benzene  $V_c^E = -1.77 \times 10^6 \text{ m}^3 \text{ mol}^{-1}$ , pentafluorobenzene + benzene  $V_c^E = -1.27 \times 10^6 \text{ m}^3 \text{ mol}^{-1}$  and pentafluorocyanobenzene + benzene  $V_c^E = -1.54 \times 10^6 \text{ m}^3 \text{ mol}^{-1}$  all at 323.15K. The complexing contribution to the pentafluorocyanobenzene + benzene system is apparently less than for the hexafluorobenzene + benzene. This is an unexpected result if complexing is due to charge transfer complexing because pentafluorocyanobenzene would be expected to have the strongest complexing interaction with benzene. The shape and polarisability interpretations of the thermodynamic functions seem more probable although as mentioned previously, interpretation of excess volumes is speculative.

Powell and Swinton (11) have found that when studying the series hexafluorobenzene with alicyclic hydrocarbons (with increasing methyl substitution), and perfluoromethylcyclohexane with alicyclic hydrocarbons (again with increasing methyl substitution) at  $X_F = 0.5$  and 313.2K the

FIGURE (8.2.1c)

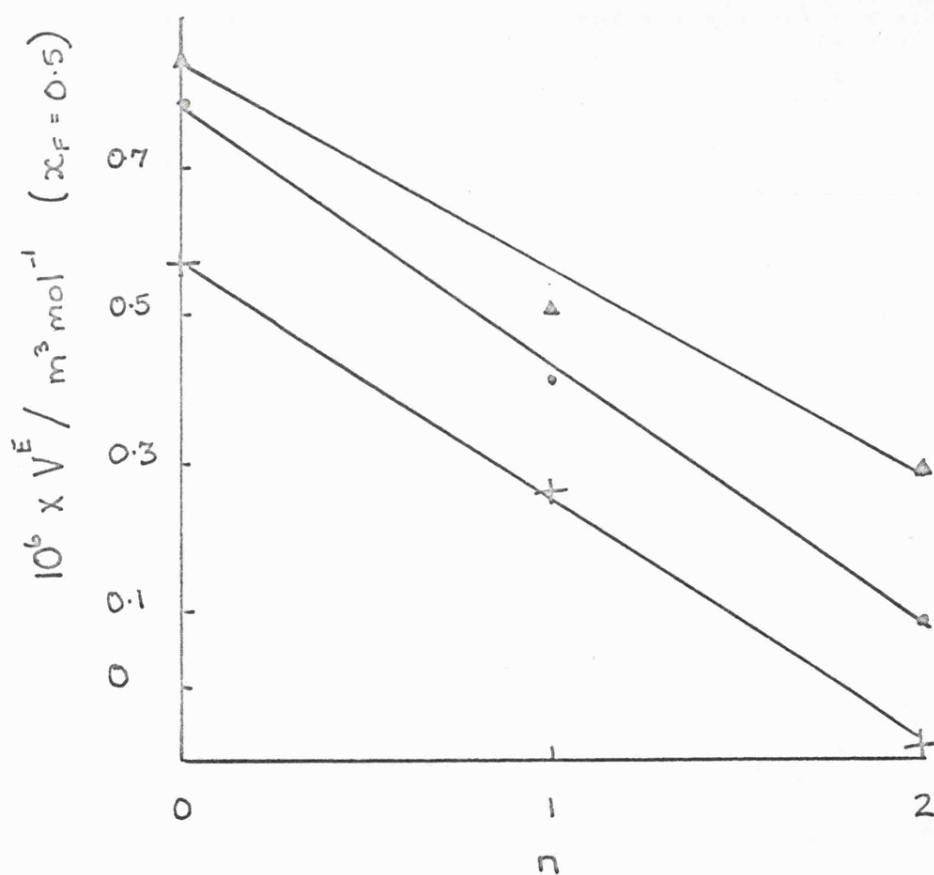
EXCESS VOLUMES OF FLUOROCARBON + AROMATIC HYDROCARBON

SYSTEMS VERSUS DEGREE OF METHYL SUBSTITUTION

△  $C_6F_5H$  Stubbley (12) at 298.15K

•  $C_6F_6$  Swinton (7) at 313.15K

+  $C_6F_5CN$  Present work



Degree of methyl substitution in  
Aromatic hydrocarbon.



plots of  $V^E$  versus degree of methyl substitution were parallel to, but more positive than, the corresponding hexafluorobenzene plot, as shown in figure (8.2.1d).

Therefore it is unreasonable to attribute the decrease in  $V^E$ , in the hexafluorobenzene, pentafluorocyanobenzene systems, to increased methyl substitution and consequent  $\pi - \pi$  interaction if complexing of this nature is impossible in the system where there is no  $\pi$  bonding structure.

### 8.2.2 Excess Enthalpies of Mixing

The excess enthalpies of mixing at 323.15K for pentafluorocyanobenzene + benzene, toluene and p-xylene are shown in figure (8.2.2a). All of the excess enthalpies are exothermic, which indicates the existence of complexing. When the values at  $X_F=0.5$  are compared with the results of Andrews et al (9) for the hexafluorobenzene systems there is little difference between the two sets of systems. These results are shown in table (8.2.2a) along with the corresponding pentafluorobenzene values at  $X_F=0.5$  obtained by Stubley (13) and Scott (25) and the excess heat capacities at  $X_F=0.5$ .

The excess enthalpies of the benzene + fluorocarbon systems appear to be largely independent of temperature change, except for a small positive excess heat capacity for the hexafluorobenzene system. Most of the other systems also have a positive excess heat capacity. This is consistent with the existence of some interactions in the liquid state which decreases with increase in temperature of the mixture.

The toluene + pentafluorobenzene system behaves unexpectedly in that it has a negative excess heat capacity. This is more common in a non-interacting system for example hexafluorobenzene + cyclohexane.

FIGURE (8.2.1d)

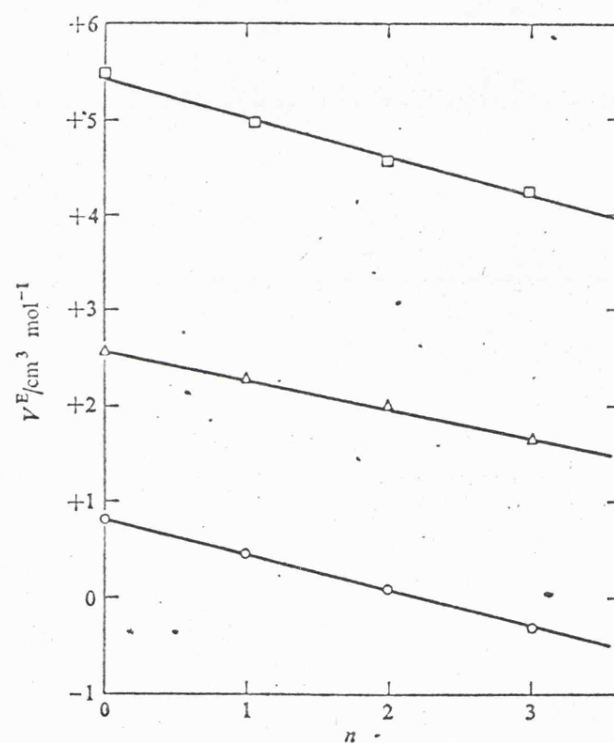


FIGURE 2. Excess volume of mixing  $V^E$  for equimolar fluorocarbon+hydrocarbon mixtures at 313.2 K as a function of the degree of substitution  $n$  of the hydrocarbon.  $\circ$ , Series A: hexafluorobenzene+aromatic hydrocarbons;  $\Delta$ , Series B: hexafluorobenzene+alicyclic hydrocarbons;  $\square$ , Series C: perfluoromethylcyclohexane+alicyclic hydrocarbons.

FIGURE (d.2.2a)

THE EXCESS ENTHALPIES OF MIXING FOR PENTAFLUOROCYANOBENZENE + BENZENE,  
TOLUENE AND P-XYLENE AT 323.15K

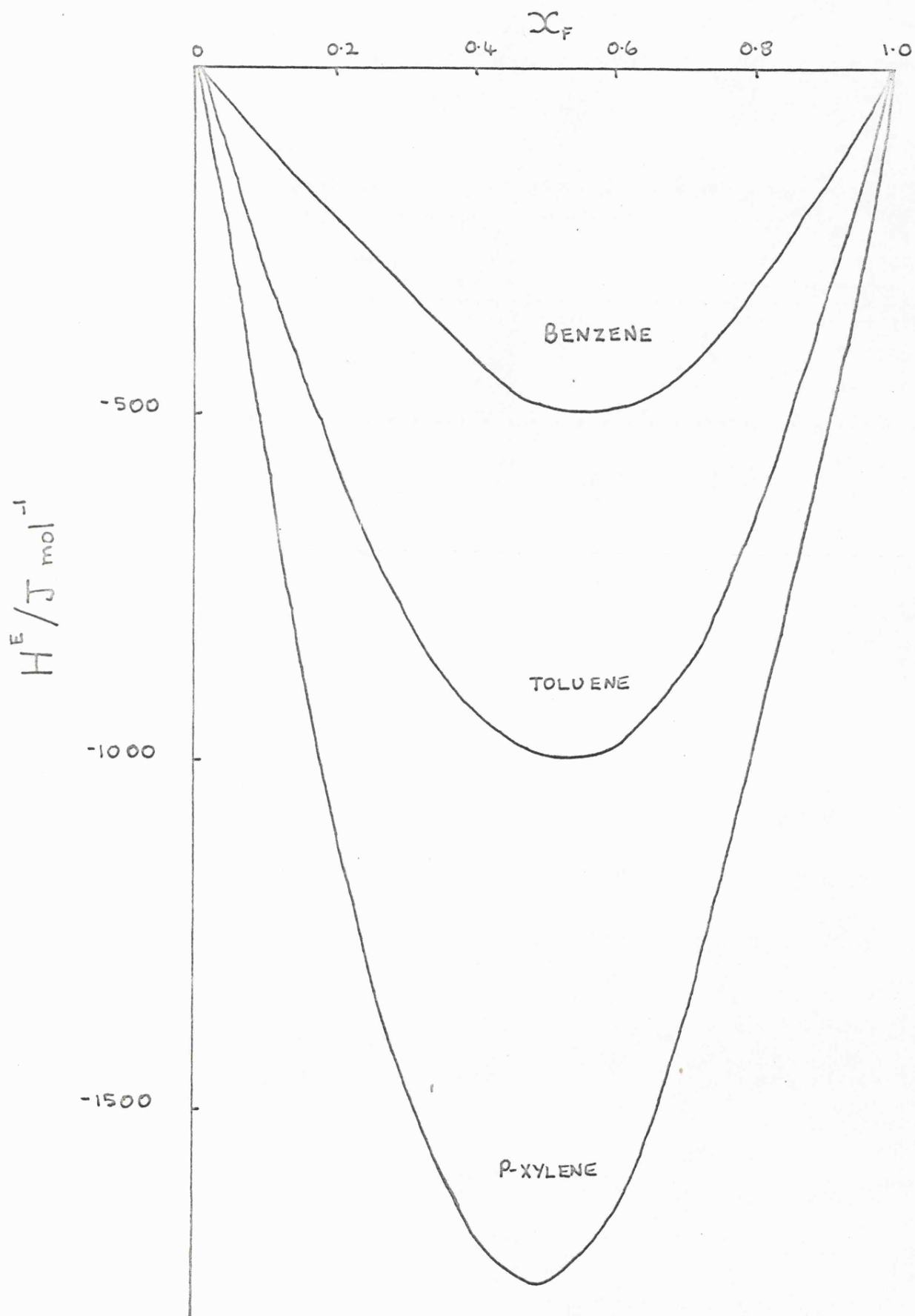


TABLE (8.2.2a)

HEATS OF MIXING ( $\text{J mol}^{-1}$ ) AT 323.15K AND  $X_F = 0.5$

	<u>Benzene</u>	<u>Toluene</u>	<u>p-Xylene</u> (at 328K)
$\text{C}_6\text{F}_5\text{H}$	60	-370	-761
$\text{C}_6\text{F}_6$	-415	-979	-1543
$\text{C}_6\text{F}_5\text{CN}$	-490	-993	-1735

EXCESS HEAT CAPACITIES  $C_P^E$  ( $\text{J mol}^{-1} \text{K}^{-1}$ ) AT  $X_F=0.5$  AND 323.15K

	<u>Benzene</u>	<u>Toluene</u>	<u>p-Xylene</u>
$\text{C}_6\text{F}_5\text{H}$	0	-1.5	-
$\text{C}_6\text{F}_6$	1.8	16.7	12.3
$\text{C}_6\text{F}_5\text{CN}$	0	2.3	11.6

The heats of mixing results for the pentafluorocyanobenzene and hexafluorobenzene systems do not differ as much as expected. However, as with the amine systems, the excess enthalpies can be regarded as being made up of two contributions,  $H_p^E$  and  $H_c^E$ .

Taking the non-interacting model to be fluorocarbon + cyclohexane in the fluorocarbon + benzene systems then  $H_c^E$  at  $X_F = 0.5$  and 323,15K are,

Pentafluorobenzene + benzene	$H_c^E = -1483 \text{ J mol}^{-1}$
Hexafluorobenzene + benzene	$H_c^E = -1905 \text{ J mol}^{-1}$
Pentafluorocyanobenzene + benzene	$H_c^E = -2615 \text{ J mol}^{-1}$

It is now apparent that there is considerable difference between the interactions in the three systems, as measured by the exothermic chemical contributions.

$H_c^E$  is least negative for pentafluorobenzene + benzene and becomes progressively more negative through hexafluorobenzene + benzene to pentafluorocyanobenzene + benzene.

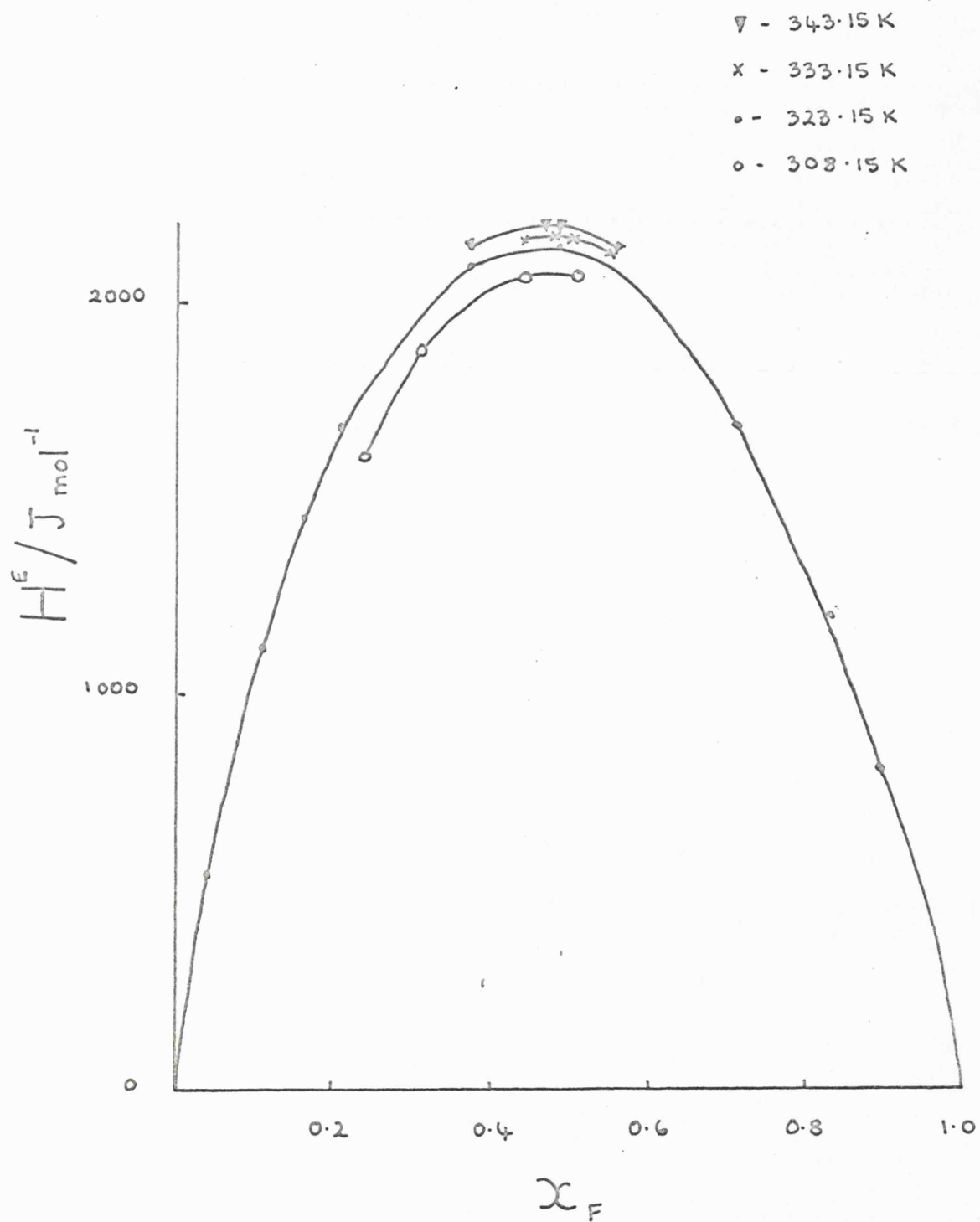
The excess volume results for these systems gave chemical contributions that did not differ greatly, however, as stated earlier, excess volume results can not be easily interpreted. Excess enthalpies of mixing give a clearer indication of the actual energy changes that are occurring on mixing two components.

The  $H_c^E$  results become more exothermic as the fluorocarbon increases in acceptor ability.

The excess enthalpies for pentafluorocyanobenzene + cyclohexane at 323.15K and three other temperatures are given in figure (8.2.2b).

FIGURE (6.2.2b)

EXCESS ENTHALPIES FOR PENTAFLUOROBENZENE + CYCLOHEXANE



The excess enthalpies are very large and endothermic, which is consistent with previous results for fluorocarbon + alicyclic hydrocarbon systems, however when the heats of mixing were obtained at 333.15K they indicated that the system had a positive excess heat capacity (at  $X_F = 0.5$  and 323.15K) of  $3.3 \text{ J mol}^{-1} \text{ K}^{-1}$ . This is unusual for a non-interacting system, increase in temperature in a non-interacting system usually brings about a decrease in the excess enthalpies.

The temperature was increased to 343.15K and this positive excess heat capacity still persisted.

A temperature was chosen below 323.15K but above the upper critical solution temperature of the system ( $X_F = 0.45$ , U.C.S.T. = 299.6 K) and again a positive excess heat capacity was obtained.

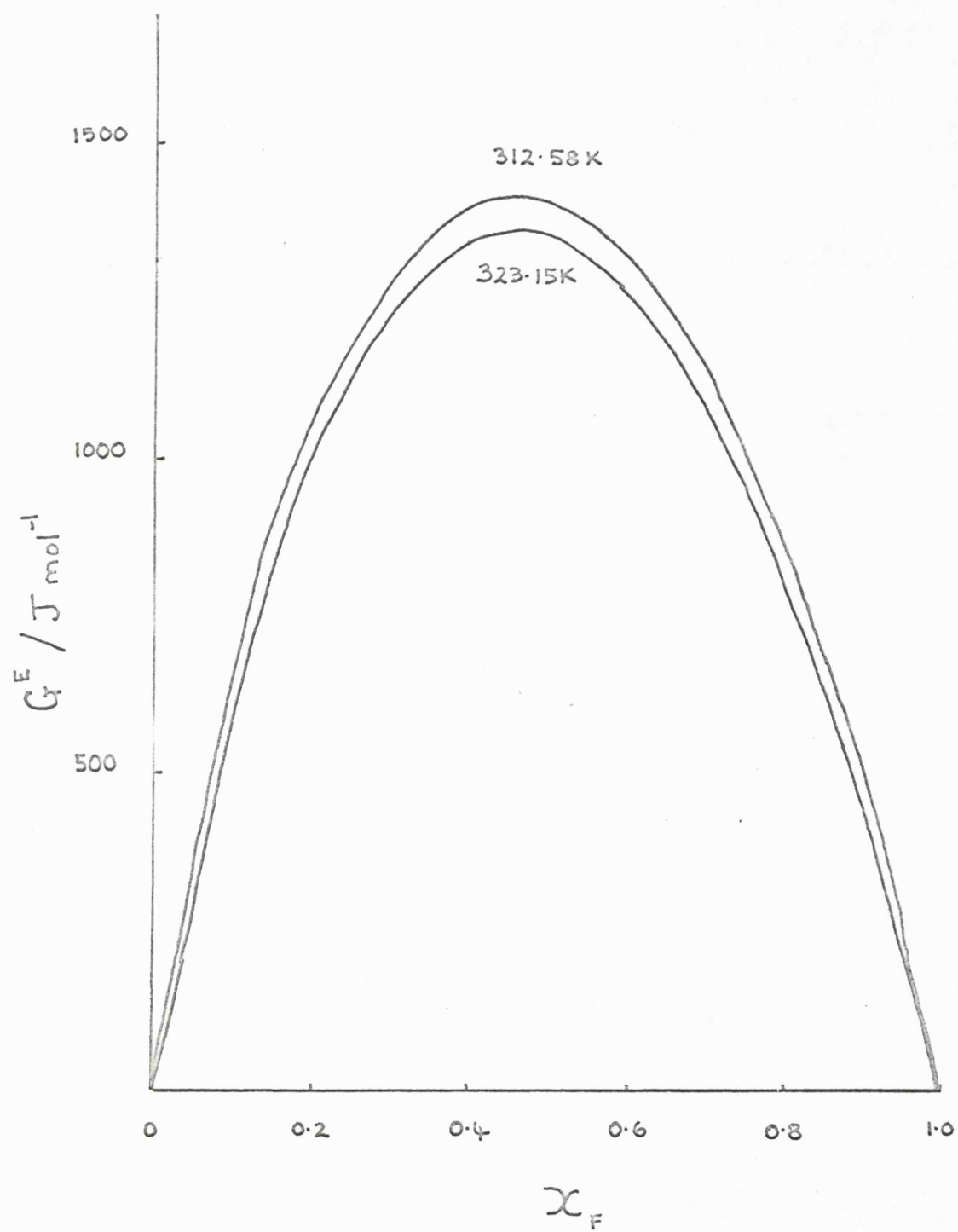
### 8.2.3 Excess Gibbs Functions

The excess Gibbs functions at 323.15K and 312.58K for pentafluorocyanobenzene + cyclohexane are shown in figure (8.2.3a).

The excess Gibbs function at  $X_F = 0.5$  and 323.15K is almost twice as large as the result for the corresponding hexafluorobenzene + cyclohexane system determined by Gaw and Swinton (10) ( $X_F = 0.5$   $G^E = 755 \text{ J mol}^{-1}$ ). This large positive result is typical of fluorocarbon + alicyclic hydrocarbon systems and indicates that the unlike interaction is small and that the system is close to immiscibility. In fact the upper critical solution temperature is 300K. Since the excess Gibbs functions are at two temperatures it is possible to calculate the excess enthalpies.

FIGURE (8.2.3a)

$G^E$  FOR PENTYL CYCLOHEXANEBENZENE + CYCLOHEXANE AT 323.15K AND 312.58K





However the temperature interval is small, because at lower temperatures the system phase separates, and so the calculation is very imprecise. Assuming the excess Gibbs functions at  $X_F = 0.5$  are reliable to  $\pm 20 \text{ J mol}^{-1}$ , then the excess enthalpy at 323.15K is calculated to be  $3.0 \pm 1.2 \text{ k J mol}^{-1}$ , which is of the same order as the experimentally determined excess enthalpy of  $2.12 \text{ k J mol}^{-1}$ .

### 8.3 PENTAFLUOROCYANOBENZENE + AROMATIC AMINE SYSTEMS

#### 8.3.1 Excess Volumes of Mixing

The excess volumes of mixing results for N,N-dimethylaniline + pentafluorocyanobenzene at 323.15K and N,N-dimethyl p-toluidine + pentafluorocyanobenzene at 328.15K are given in figure (8.3.1a). Both sets of results are negative which indicates that strong interactions must be occurring.

The N,N-dimethyl p-toluidine system has more negative excess volumes which is consistent with the existence of donor - acceptor complexing and stronger electron donor interacting more strongly with the pentafluorocyanobenzene. These measurements complement the studies initiated by Hall and Morcom (16), in which excess enthalpies and spectroscopic measurements have been made on pentafluorocyanobenzene + N,N-dimethylaniline and charge - transfer complexing is thought to be occurring.

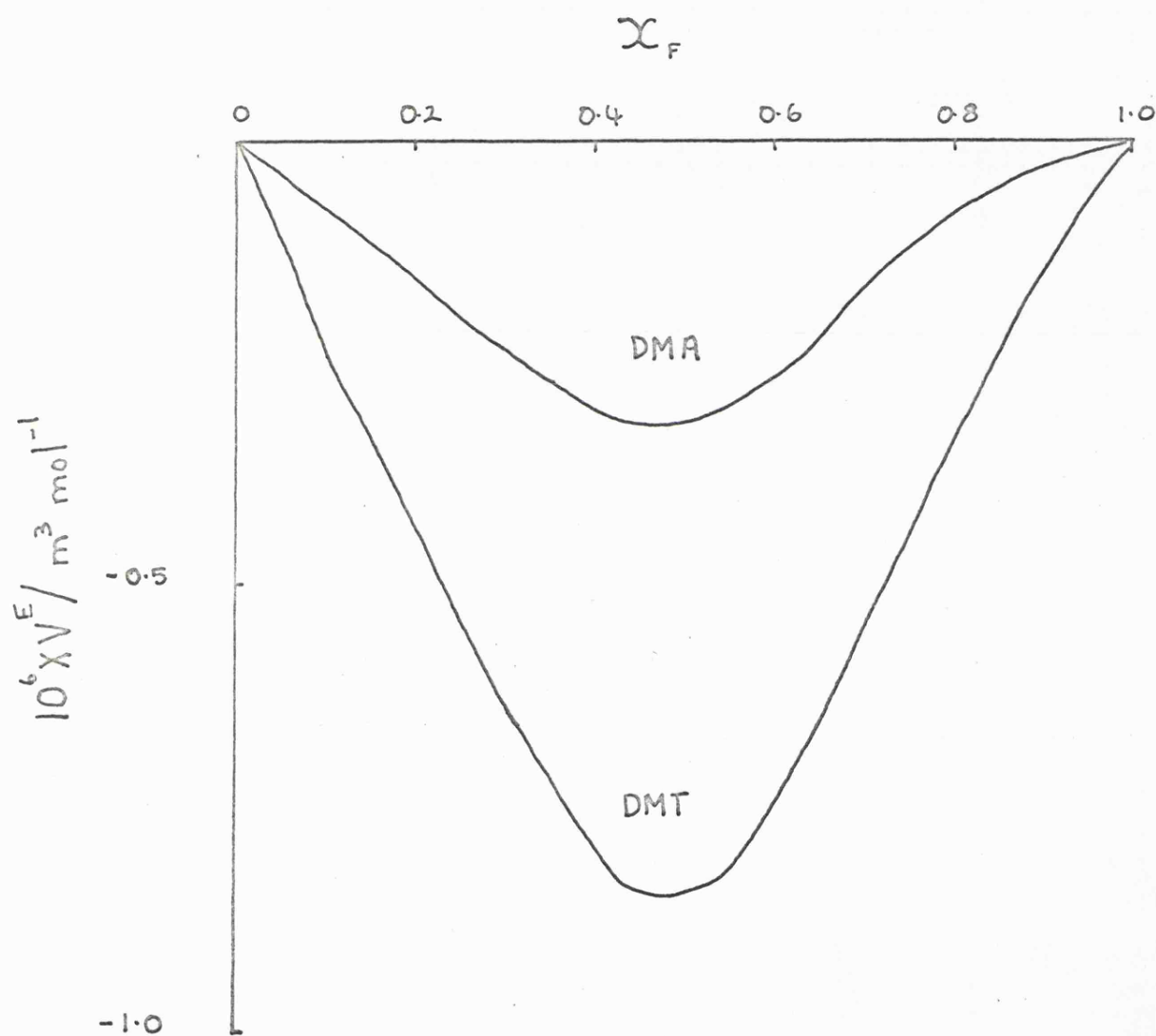
### 8.4 SUGGESTIONS FOR FURTHER STUDY

The central theme of the work was to have been the determination of excess Gibbs functions for a range of pentafluorocyanobenzene systems, including substituted aromatic hydrocarbons and aromatic amines.

FIGURE (8.3.1a)

$V_s^E$  FOR PENTAFLUOROCYANOBENZENE + N,N-DIETHYLANILINE AT 323.15K

AND + N,N-DIETHYL-P-TOLUIDINE AT 328.15K



Unfortunately due to greater difficulties than were anticipated with the vapour pressure measurements only the pentafluorocyanobenzene + cyclohexane system was studied.

Therefore the main aim for future studies lies in the vapour pressure measurements of the above mentioned systems, with particular interest being focused on the N,N-dimethylaniline + pentafluorocyanobenzene system with a view to determining an equilibrium constant of complexing  $K_x$ , which will be independent of solvent, and comparing this with the spectroscopically derived  $K_x$ .

The comparison between the results for the parallel hexafluorobenzene systems with those obtained for the pentafluorocyanobenzene systems should also be of interest.

## APPENDIX

### COMPUTER PROGRAMMES

A.1 PROGRAMME FOR THE EVALUATION OF VAPOUR PRESSURE

&CIST;

```

1  EVALUATION OF VAPOUR PRESSURE;
2  "BEGIN"
3  "INTEGER" I,J,N;
4  "REAL" RT,TT,H5D,MN2,MVAP,U,L,ALPHA,A,B,C,D,R,G,DENS,P5;
5  "REAL" "ARRAY" H,P4[1:4];
6  "REAL" "PROCEDURE" PHG(T);
7  "REAL" T;
8  PHG:=13595.1/(1+T*(A+T*(B+T*(C+T*D))));
9  "REAL" "PROCEDURE" EXPCOR(H,T);
10 "REAL" H,T;
11 "BEGIN"
12 H:=H*(1+ALPHA*(T-20));
13 EXPCOR:=H;
14 "END" OF PROCEDURE EXPCOR;
15 "READ" H;
16 "BEGIN"
17 ALPHA:=1.9e-5
18 ;
19 R:=8.3143;
20 G:=9.81288;
21 MN2:=0.028;
22 MVAP:=0.08416;
23 A:=1.81456e-4;
24 B:=9.205e-9;
25 C:=6.608e-12;
26 D:=6.732e-14;
27 SAMELINE;
28 "FOR" I:=1 "STEP" 1 "UNTIL" N "DO"
29 "BEGIN"
30 "READ" RT,TT;
31 H5D:=0.543;
32 DENS:=PHG(TT);
33 "PRINT" 'L' 'S25' EVALUATION OF VAPOUR PRESSURE 'L4' 'S20';
34 'G=' FREEPOINT(6),G,'M/SEC+2 'L3','S18' ROOM TEMP=';ALIGNED(2,
35 'L' 'S12' THERMOSTAT TEMP=';ALIGNED(2,3),TT,'S10' H5=';ALIGNED(
36 ,H5D;
37 'M','L2' S5' CUT-OFF 'S35' MERCURY DENSITY=';ALIGNED(5,1),DENS,
38 'KG/M+3 'L';OBSERVED HEIGHT 'S4';
39 "FOR" J:=1 "STEP" 1 "UNTIL" 4 "DO"
40 "BEGIN"
41 "READ" U,L;
42 HCJJ:=U-L;
43 "PRINT" '=';ALIGNED(2,5),HCJJ,'M'S3';
44 "END" J;

```

```

45 "PRINT" 'L\CORRECTED HEIGHT'S3';
46 "FOR" J:=1 "STEP" 1 "UNTIL" 4 "DO"
47 "PRINT" '=\,ALIGNED(2,5),EXPCOR(H[J],RT), M'S3';
48 H5D:=H5D-L;
49 "PRINT" 'L\PRESSURE(CUT-OFF)'S2';
50 "FOR" J:=1 "STEP" 1 "UNTIL" 4 "DO"
51 "BEGIN" P4[J]:=H[J]*DENS*G;
52 "PRINT" '=\,ALIGNED(6,1),P4[J], PA'S2';
53 "END" J;
54 RT:=RT+273.15;
55 TT:=TT+273.15;
56 P5:=H5D*MVAP*P4[1]*G/(R*TT);
57 "PRINT" 'L3'S13'M(N2) =\,ALIGNED(1,3),MN2, KG/MOL'S10'M(VAP)
58 MVAP,KG/MOL'L2',PRESSURE OF VAPOUR'S3'=\,P5,PA'L2'VAPOUR PRE
59 'S4';
60 "FOR" J:=1 "STEP" 1 "UNTIL" 4 "DO"
61 "BEGIN"
62 P4[J]:=P4[J]-P5;
63 "PRINT" '=\,ALIGNED(6,1),P4[J],PA'S2';
64 "END" J;
65 "END" I;
66 "END";
67 "END" OF EVALUATION OF VAPOUR PRESSURES;
388 MC
534 CODE
922 TOTAL

```

&RUN;  
EVALUATI  
DRO

# EVALUATION OF VAPOUR PRESSURE

```

1 "TITLE"
2 "NAME" P4:
3 "NAME" "CORRECTED HEIGHT" (L):
4 "NAME" "PRESSURE(CUT-OFF)" (P4):
5 "NAME" L:
6 "NAME" "CORRECTED HEIGHT" (H5D):
7 "NAME" "VAPOUR PRESSURE" (P5):
8 "NAME" "VAPOUR PRESSURE" (P4):
9 "NAME" "VAPOUR PRESSURE" (P4):
10 "NAME" "VAPOUR PRESSURE" (P4):
11 "NAME" "VAPOUR PRESSURE" (P4):
12 "NAME" "VAPOUR PRESSURE" (P4):

```



A.2 PROGRAMME FOR THE CALCULATION OF THE EXCESS GIBBS FUNCTIONS

```
&JOB;CH001587FREE;JMR24;
```

```
&ALGOL;
LIBRARY
ALGOL
```

```
&LIST;
```

```

1  FREE ENERGY CALCULATIONS USING FULL EQUATIONS;
2  "BEGIN"
3  "INTEGER" J;
4  "BOOLEAN" WRITE;
5  "INTEGER" I,N,VEDIM;
6  "INTEGER" CYCLE;
7  "REAL" P10,B11,V10,P20,B22,V20,B12,P12,D12,R1,T,KVE;
8  SAMELINE;
9  "READ" N,VEDIM;
10 "BEGIN"
11 "REAL" X;
12 "REAL" "ARRAY" N1,N2,V[1:N];
13 "REAL" "ARRAY" X1,P,Y1[1:N],VE[0:VEDIM-1];
14 "PROCEDURE" CFVP(N1,N2,Y1,P,VVAP,X1);
15 "REAL" N1,N2,Y1,P,VVAP,X1;
16 "BEGIN"
17 "REAL" TNOM,V,M1,M2,7,Y2,RTV,A;
18 Y2:=1-Y1;
19 Z:=(B11*Y1*Y1+2*B12*Y1*Y2+B22*Y2*Y2)/VVAP;
20 RTV:=R1*T/VVAP;
21 TNOM:=(-RTV+SQRT(RTV*RTV-4*P*RTV*Z))/(2*RTV*Z);
22 A:=P/(RTV*(1+Z*TNOM));
23 M1:=Y1*A;
24 M2:=Y2*A;
25 X1:=(N1-M1)/(N1+N2-M1-M2);
26 "END" OF CORRECTION FOR VAPOUR PHASE;
27 "PROCEDURE"RPMV(V,K,N,X1,V1,V2);
28 "INTEGER" N;
29 "REAL" K,X1,V1,V2;
30 "REAL" "ARRAY" V;
31 "BEGIN"
32 "INTEGER" I;
33 "REAL"VE,DIFF,X2,Z,CALC;
34 VE:=DIFF:=0;
35 X2:=1-X1;
36 Z:=X1-X2;
37 "FOR" I:=0 "STEP" 1 "UNTIL" N-1 "DO"
38 "BEGIN"
39 CALC:=X1*X2*V[I]*Z*(I-1)/(1-K*Z);
40 VE:=VE+CALC*Z;
41 DIFF:=DIFF+2*CALC*(I-Z+2/(2*X1*X2)-K*Z/(1-K*Z));
42 "END" I;
43 V1:=VE+X2*DIFF;
44 V2:=VE-X1*DIFF;
```

```

45 "END" OF PROCEDURE RPMV;
46 "REAL" "PROCEDURE" SUM(A,K,N);
47 "VALUE" K,N;
48 "INTEGER" K,N;
49 "REAL" "ARRAY" A;
50 "BEGIN" "INTEGER" I;
51 "REAL" S;
52 S:=0;
53 "FOR" I:=1 "STEP" 1 "UNTIL" N "DO" S:=S+A[I-K];
54 SUM:=S;
55 "END" OF PROCEDURE SUM;
56 "REAL" "PROCEDURE" SUMPROD(A,K,B,L,N);
57 "VALUE" K,I,N;
58 "INTEGER" K,L,N;
59 "REAL" "ARRAY" A,B;
60 "BEGIN" "INTEGER" I;
61 "REAL" SP;
62 SP:=0;
63 "FOR" I:=1 "STEP" 1 "UNTIL" N "DO" SP:=SP+A[I,K]*B[I,L];
64 SUMPROD:=SP;
65 "END" OF PROCEDURE SUMPROD;
66 "REAL" "PROCEDURE" PRODUCT(A,K,N);
67 "VALUE" K,N;
68 "INTEGER" K,N;
69 "REAL" "ARRAY" A;
70 "BEGIN" "INTEGER" I;
71 "REAL" P;
72 P:=1;
73 "FOR" I:=1 "STEP" 1 "UNTIL" N "DO" P:=P*A[I-K];
74 PRODUCT:=P;
75 "END" OF PROCEDURE PRODUCT;
ITEM INSERTED
76 "LIBRARY" UNSYMDFT;
ITEM INSERTED
133 "LIBRARY" UNSYMSOL;
134 "PROCEDURE" BARKER(X1,P,N,PARAMETERS,SKewed,Y1,WRITE);
135 "INTEGER" N,PARAMETERS;
136 "REAL" "ARRAY" X1,P,Y1;
137 "BOOLEAN" WRITE;
138 "BOOLEAN" SKewed;
139 "BEGIN"
140 "INTEGER" I,J,COUNT,MINUS,PLUS,DIM;
141 "BOOLEAN" STORE;
142 STORE:=WRITE;
143 WRITE:="FALSE";
144 COUNT:=0;
145 MINUS:=PARAMETERS-1;
146 "IF" SKewed
147 "THEN" DIM:=PARAMETERS
148 "ELSE" DIM:=MINUS;
149 PLUS:=DIM+1;
150 06:
151 "IF" WRITE "THEN"
152 "PRINT" 'F',DIGITS(2),'S51'NO. OF EXPERIMENTAL POINTS='N','L'
153 'S50'NO. OF PARAMETERS EVALUATED=',PARAMETERS,'L';
154 "BEGIN"
155 "REAL" "ARRAY" R[1:N,1:1],G,G1,G2,EG1,EG2,FX1,FX2,FK1,FK2,
156 GECALCO:MINUS],DPDGC[1:N,0:DIM],A[1:PLUS,1:PLUS],B[1:PLUS],
157 C[1:PLUS,1:1];
158 "REAL" VBPP10,VBPP20,F1,F2,P1D,P2D,X2,Y2,X,GE,RMS,RNSLAST,K,BBPP10

```



```

70 B3PP20,V1VPP,V2VPP,Z,V1,V2;
80 "REAL" PST;
90 "REAL" CCR1,COR2;
92 "SWITCH" TAG:=L;
93 PST:=101325.0;
94 "IF" (PARAMETERS=1) "THEN" "BEGIN"
95 GC0:=4*LN(2*P12/(P10+P20));
96 K:=0;
97 "END";
98 PMS:=0;
99 "FOR" I:=1 "STEP" 1 "UNTIL" N "DO"
100 "BEGIN"
101 "IF" ((I"LE" MINUS) "AND" PARAMETERS=1) "THEN"
102 GC1:=0;
103 "IF" WRITE "THEN"
104 "PRINT" FREEPOINT(4),'S50',X1[I],'S16',ALIGNED(6,1),P[I],'L';
105 "END" I;
106 Q7:
107 "FOR" COUNT:=COUNT+1 "DO"
108 "BEGIN"
109 "IF" WRITE "THEN"
110 "PRINT" 'I2','S56' TEMPERATURE=,ALIGNED(3,2),T,'K' 'L' 'S27',
111 'PURE1' S67 'PURE2' 'L' 'S5' 'P' 'S23' 'B' 'S23' 'V' 'S23' 'P' 'S23' 'B' 'S23' 'V' 'L' 'S',
112 ALIGNED(6,1),P10,FREEPOINT(7),PREFIX('S15'),B11,V10,ALIGNED(6,1),
113 P20,FREEPOINT(7),B22,V20,SAMELINE,'L2' 'S53' INTERACTION COEFFICIENTS',
114 'L' 'S32' 'B' 'S65' 'P' 'L' 'S28',B12,'S56',ALIGNED(6,1),P12;
115 "IF" ("NOT" WRITE) "THEN" "GO TO" Q;
116 "PRINT" 'F',DIGITS(2),'S57' ITERATION NO: ,COUNT,'L';
117 "FOR" J:=0 "STEP" 1 "UNTIL" MINUS "DO"
118 "PRINT" 'S56' GC,DIGITS(1),J,]=,ALIGNED(1,6),GC[J],'L';
119 "PRINT" 'S59' K=,ALIGNED(1,6),K,'L';
120 "PRINT" 'S5' X1'S16' P(EXP)'S13' P(CALC)'S14' RESID'S16' Y1'S18' GE'L';
121 Q:
122 "FOR" I:=1 "STEP" 1 "UNTIL" N "DO"
123 "BEGIN"
124 X2:=1-X1[I];
125 Z:=X1[I]-X2;
126 "FOR" J:=0 "STEP" 1 "UNTIL" MINUS "DO"
127 "BEGIN"
128 FX1[J]:=(X2+2)*(Z+(J-1))*((2*J+1)*X1[I]-X2+K*Z*(1-2*J*X1[I]))/((1-
129 K*Z)+2);
130 FX2[J]:=(X1[I]+2)*(Z+(J-1))*(X1[I]-(2*J+1)*X2+K*Z*(2*J*X2-1))/((1-
131 K*Z)+2);
132 FK1[J]:=(X2+2)*(Z+J)*G[J]*(2*((2*J+1)*X1[I]-X2)+(1-2*J*X1[I])*(1+K*Z))/
133 ((1-K*Z)+3);
134 FK2[J]:=(X1[I]+2)*(Z+J)*G[J]*(2*(X1[I]-(2*J+1)*X2)+(2*J*X2-1)*(1+K*Z))/
135 ((1-K*Z)+3);
136 G1[J]:=FX1[J]*G[J];
137 G2[J]:=FX2[J]*G[J];
138 EG1[J]:=EXP(G1[J]);
139 EG2[J]:=EXP(G2[J]);
140 GECALC[J]:=X1[I]*X2*G[J]*(Z+J)/(1-K*Z);
141 "END" J;
142 VBPP10:=(V10-B11)*(P[I]-P10)/(R1*T);
143 VBPP20:=(V20-B22)*(P[I]-P20)/(R1*T);
144 BBPP10:=B11*B11*(P[I]-P10)*(P[I]+P10)/(2*(R1*T)+2);
145 BBPP20:=B22*B22*(P[I]-P20)*(P[I]+P20)/(2*(R1*T)+2);
146 RPMV(VE,KVE,VEDIM,X1[I],V1,V2);
147 V1VPP:=V1*(P[I]-PST)/(R1*T);
148 V2VPP:=V2*(P[I]-PST)/(R1*T);

```

```

239 COR1:=EXP(VBRP10+BRPP10+V1VPP);
240 COR2:=EXP(VJPP20+BRPP20+V2VPP);
241 F1:=PRODUCT(FG1,1,PARAMETERS);
242 F2:=PRODUCT(FG2,1,PARAMETERS);
243 Y2:=COR2*F2*P20*Y2/PCI1; Y1CI1:=1-Y2;
244 P1D:=X1CI1*P10*COR1*EXP(-PCI1*D12*Y2+2/(R1*T));
245 P2D:=X2*P20*COR2*EXP(-PCI1*D12*Y1CI1+2/(R1*T));
246 RC1,1:=PCI1-(F1*P1D+F2*P2D);
247 GE:=R1*T*SUM(GECALC,1,PARAMETERS);
248 "IF" WRITE "THEN"
249 "PRINT" 'S2',FREEPOINT(4),X1CI1,ALIGNED(6,1),'S13',PCI1,'S10',
250 (PCI1-RC1,1),ALIGNED(5,4),'S11',RC1,1,FREEPOINT(4),'S10',Y1CI1,
251 ALIGNED(4,2),'S14',GE,'L';
252 "FOR" J:=0 "STEP" 1 "UNTIL" MINUS "DO"
253 DPDGCI,J:=F1*P1D*FX1[J]+F2*P2D*FX2[J];
254 "IF" SKEWED
255 "THEN"
256 DPDGCI,DIM:=F1*P1D*SUM(FK1,1,PARAMETERS)+F2*P2D*SUM(FK2,1,PARAMETERS
257 "END" I;
258 RMSLAST:=RMS;
259 RMS:=SQRT(SUMPROD(R,1,R,1,N)/N);
260 "IF" WRITE "THEN"
261 "PRINT" 'S52',R.M.S. DEVIATION=,SCALED(5),RMS,'L4';
262 RMS:=SQRT(RMS*RMS*N/(N-PLUS));
263 "IF" WRITE "THEN"
264 "PRINT" 'S50',STANDARD DEVIATION=,SCALED(5),RMS,'L4';
265 'S32',X1,'S63',GE,'L';
266 "FOR" X:=0 "STEP" 0.1 "UNTIL" 1 "DO"
267 "BEGIN"
268 X2:=1-X;
269 Z:=X-X2;
270 "FOR" J:=0 "STEP" 1 "UNTIL" MINUS "DO"
271 GECALC[J]:=X*X2*G[J]*Z+J/(1-K*Z);
272 GE:=R1*T*SUM(GECALC,1,PARAMETERS);
273 "IF" WRITE "THEN"
274 "PRINT" 'S29',FREEPOINT(4),X,'S59',ALIGNED(4,2),GE,'L';
275 "END" X;
276 "IF" (ABS(RMS-RMSLAST)<RMS*1.0E-5)
277 "THEN"
278 "GO TO" L;
279 "FOR" J:=1 "STEP" 1 "UNTIL" PLUS "DO"
280 "BEGIN"
281 CCJ,1:=SUMPROD(R,1,DPDG,J-1,N);
282 "FOR" I:=1 "STEP" 1 "UNTIL" PLUS "DO"
283 ACI,J:=SUMPROD(DPDG,I-1,DPDG,J-1,N);
284 "END" J;
285 UNSYMDET(PLUS,2.0E-37,A,X,I,8,L);
286 UNSYMSOL(PLUS,1,A,B,C);
287 "FOR" J:=0 "STEP" 1 "UNTIL" MINUS "DO"
288 GCJ:=GCJ+CCJ+1,1;
289 "IF" SKEWED
290 "THEN"
291 K:=K+CCPLUS,1;
292 "GO TO" 07;
293 "END" COUNT;
294 L: "IF" STORE "THEN" "BEGIN" STORE:= "FALSE";
295 WRITE:="TRUE";
296 "GO TO" 06 "END"
297 "END";
298 "END" OF PROCEDURE BARKER;

```



```
290 "FOR" I:=0 "STEP" 1 "UNTIL" VEDIM-1 "DO"
300 "READ" V[I];
301 "READ" KVE;
302 "READ" T,P10,B11,V10,P20,B22,V20,B12,P12;
303 R1:=8.3143;
304 D12:=2*B12-B11-D22;
305 "FOR" I:=1 "STEP" 1 "UNTIL" N "DO"
306 "BEGIN"
307 "READ" U1[I],U2[I],P[I],V[I];
308 X1[I]:=U1[I]/(U1[I]+U2[I]);
309 V[I]:=V[I]-U1[I]*V10-U2[I]*V20;
310 "END" I;
311 "FOR" I:=1 "STEP" 1 "UNTIL" 10 "DO"
312 "BEGIN"
313 WRITE:="FALSE";
314 Q1: BARKER(X1,P,N,I,"FALSE",Y1,WRITE);
315 "IF" WRITE "THEN" "GO TO" Q2 "ELSE" WRITE:="TRUE";
316 "FOR" J:=1 "STEP" 1 "UNTIL" N "DO"
317 "BEGIN"
318 CFVP(U1[J],U2[J],Y1[J],P[J],V[J],X);
319 "IF" ((ABS(X-X1[J])>0.00001) "AND" WRITE) "THEN" WRITE:="FALSE";
320 X1[J]:=X;
321 "END" J;
322 "GO TO" Q1;
323 Q2:
324 "END" I;
325 "END"
326 "END" OF FREE ENERGY CALCULATIONS USING FULL EQUATIONS;
908 MC
3160 CODE
4068 TOTAL
```

&RUN;  
FREEENER  
DRO

## REFERENCES

1. R.L.Scott, J.Am. Chem.Sec. (1948) 70 4090
2. R.L.Scott, J.Phys.Chem. (1958) 62 136
3. C.R.Patrick and G.S.Prosser. Nature (1960) 187 1021
4. D.V.Fenby. Rev. Pure Appl.Chem. (1972) 22 55
5. F.L.Swinton Chpt.from Molecular Association. Ed.R.Foster, Acad. Press.
6. J.A.Godsell, M. Stacey, J.C.Tatlow Nature (1956) 178 199
7. W.A.Duncan, J.P.Sheriden, F.L.Swinton. Trans.Fara.Soc. (1966) 521, 62, 5 1090
8. W.A.Duncan, F.L.Swinton. Trans.Fara.Soc (1966) 521,62,5 1083
9. A. Andrews, K.W.Morcom, W.A.Duncan, F.L.Swinton, J.M.Pollock J.Chem.Thermo. (1970) 2 95
10. W.J.Gaw, F.L. Swinton Trans.Fara.Soc. (1968) 64 637
11. R.J.Powell, F.L.Swinton J Chem.Thermo (1970) 2 87
12. B.J.Skillerne de Bristowe, D.Stubley. J.Chem.Thermo (1973)5 865
13. P.J.Howell, B.J.Skillerne de Bristowe, D.Stubley. J.Chem. Thermo. (1972) 4 225
14. R.J.W. Le Févre, D.V.Redford, G.L.D. Ritchie,P.J.Stiles. J.Chem.Soc. B (1968) 148
15. C.Y.Leong, D.E.Jones, D.V.Fenby. J.Chem.Thermo (1974) 6 609
16. D.J.Hall, K.W.Morcom, J.M.Brindley. J.Chem.Thermo. (1974) 6 1133
17. D.A.Armitage, T.G.Beaumont, K.M.Davis, D.J.Hall, K.W. Morcom. Trans.Fara.Soc. (1971) 585 67 9 2548
18. W.J.Gaw, F.L.Swinton. Trans.Fara.Soc. (1968) 64 2023
19. T.Dahl. Acta. Chem. Scanda (1971) 25 1031
20. T.Dahl. Acta. Chem. Scanda. in press.
21. J.S.Brennan, N.M.D.Brown, F.L.Swinton. J.Chem.Soc.Fara.Trans. (1974) 70 1965
22. R.Foster, C.A.Fyfe. Chem.Comm. (1965) 642
23. D.Steele, P.N.Gates, W.Wheately. Paper presented at Chem.Soc. Anniversary meeting Exeter 1967

24. W.A.Duncan, F.L.Swinton. J.Phys.Chem. (1966) 70 2417
25. D.V.Fenby, I.A.McLure, R.L.Scott. J.Phys Chem.(1966) 70 602
26. Kelly, F.L.Swinton J.Chem.Thermo. (1974) 6 435
27. D.V.Fenby, R.L.Scott. J.Phys.Chem. (1967) 71 12 4103
28. M.W.Hanna. J.Am.Chem.Soc. (1968) 90 285
29. D.V.Fenby, S.Ruenkraitersga. J.Chem.Thermo. (1973) 5 227
30. D.V.Fenby, S.Ruenkraitersga. D.E.Jones. J.Chem.Thermo(1973)  
5 347
31. D.J.Hall, K.W.Morcom. J.Chem.Thermo (1975) 7
32. T.G.Beaumont, K.M.Davis J.Chem.Soc. (B) (1967) 1131
33. T.G.Beaumont, K.M.Davis, Nature (1968) 218 865
34. D.A.Armitage, J.M.Brindley, D.Hall, K.W.Morcom J.Chem.Thermo.  
(1975) 7 97
35. D.A.Armitage, K.W.Morcom. Trans.Fara.Soc. (1969)555 65 3 689
36. R.S.Mulliken. J.Am.Chem.Soc. (1952) 74 811
37. M.W.Hanna, J.L.Lippert. Molecular Complexes.Vol.1Chpt.1.Ed.R.  
Foster.
38. A.Andrews, D.Hall, K.W.Morcom. J.Chem.Thermo (1971) 3 527
39. M.L.Martin, R.S.Murray. J.Chem.Thermo (1972) 4 723
40. J.Bevan OH, J.R.Goates, J.Reeder, J.Chem.Thermo (1974) 6 281
41. J.Goates, J.OH, J.Reeder J.Chem.Thermo (1973) 5 135
42. S.Ruenkraitersga, N.F.Pasco, D.V.Fenby.Aust.J.Chem.(1973) 26  
2 431
43. A.Chand, D.V.Fenby J.Chem.Thermo. (1975) 7 403
44. B.I.Mattingley, Y.P.Handa, D.V.Fenby. J.Chem.Thermo (1975) 7 169
45. Y.P.Handa, D.V.Fenby. J.Chem.Thermo (1975) 7 405
46. N.F.Pasco, D.V.Fenby. Austr. J.Chem. (1974) 27 10 2159
47. L.Saroléa - Mathot Trans.Fara.Soc.(1953) 49 8
48. Miller Chem. Eng.News. (1942) 20 1528
49. A.I.Vogel. Practical Organic Chemistry. 3rd Ed.
50. J.D.Ray. Rev.Sci.Instr., (1957) 28 200
51. A.I.Vogel.Practical Organic Chemistry P.173

52. R.T.Fowler Ind.Chemist (1948) 24 717
53. R.T.Fowler Ind.Chemist (1948) 24 824
54. I.Brown.Austr. J.Sci.Res. (1952) 5A 530
55. J.H.Baxendale, B.V.Enüstün, J.Stern. Phil.Trans.(1951)  
A243 169.
56. D.H.Everett, P.W.Allen, M.F.Penney Proc.Roy.Soc.(1952) 212A 149
57. A.G.Williamson. Ph.D.Thesis, University of Reading (1957)
58. M.L.McGlashan, A.G.Williamson Trans.Fara.Soc. (1961) 57 588
59. N.F.Pasco, D.V.Fenby, T.G.Bissell. J.Chem.Thermo (1974) 6 1075
60. K.N.Marsh. Trans.Fara. Soc. (1968) 64 883
61. K.N.Marsh. J.Chem.Thermo. (1970) 2 359
62. M.M.Valle, G.C.Calero, C.G.Losa,Rev.Real.Acad.Genc Exactas,  
Fis.Natur. Madrid. (1969) 63 533
63. P.R.Garrett, Ph.D.Thesis,University of Leicester (1971)
64. P.R.Garrett, J.M.Pollack, K.W.Morcom. J.Chem.Thermo.(1973)5 569
65. D.A.Armitage, Ph.D.Thesis, University of Leicester (1969)
66. W.A.Andrews, Ph.D.Thesis, University of Leicester (1971)
67. G.W.C.Kaye, T.H.Laby; Tables of Physical and Chemical constants,  
Longmans (1959)
68. International Critical Tables, Volume 2 McGraw-Hill.
69. J.A.Barker Austr.J.Chem. (1953) 6 207
70. American Petroleum Institute Project 55 (1966)
71. C.R.Patrick, G.S.Prosser, Trans.Fara.Soc. (1964) 60 700
72. J.F.Counsell, J.H.Green, J.L.Hales, J.F.Martin. Trans.Fara.  
Soc. (1965) 61 212.
73. Kaulbaum Z. Physik.Chem (1898) 26 577
74. A.R.Martin, B.Collie J.Chem.Soc. (1932) 2 658
75. Nelson, Wales J.Am.Chem.Soc. (1925) 47 867
76. D.R.Stull Ind.Eng.Chem. (1947) 39 517
77. A.F.Forziati, W.R.Norris, F.D.Rossini J.Res.Natl.Bur.Std.,  
(1949) 43 555

78. Bristol Organics Ltd., unpublished data.
79. Douslin, Harrison, Moore. J.Chem.Thermo. (1969) 1 305
80. Hajjar, Kay, Leverett J.Chem.Eng.Data (1969) 14 377
81. J.A.Larkin, Ph.D.Thesis, University of Reading (1962)
82. J.A.Larkin, M.L.McGlashen, J.Chem.Soc. (1961) 3425
83. D.N.Travers, M.Sc.Thesis, University of Leicester (1967)
84. D.V.Fenby, G.J.Billing, D.B.Smythes J.Chem.Thermo.(1973)5 49
85. M.Lal, F.L.Swinton Physica. (1968) 40 446
86. P.R.Garrett, J.M.Pollock, K.W.Morcom, J.Chem.Thermo(1971)3 135
87. P.J.Howell, D.Stubley. J.Chem.Soc. A(1969) 2489
88. Adcock, M.L.McGlashan. Proc.Roy.Soc. A (1954) 226 266
89. W.Geffcken, A.Kruis, L.Solana. Z.Physik.Chem. (1937) 35B 317
90. H.D.Pflug, G.C.Benson. Can.J.Chem. (1968) 46 287
91. A.Desmyter, J.H.Vander Waals. Roc.Trav.Chim, (1958) 77 53.
92. H.E.Wirth, R.E.Lindström, J.N.Johnson, J.Phys.Chem.(1963) 672339
93. L.A.Beath, S.P.O'Neill, A.G.Williamson. J.Chem.Thermo (1969)1 293
94. R.H.Stokes, B.J.Levien, K.N.Marsh. J.Chem.Thermo. (1970) 2 43
95. D.B.Keyes, J.H.Hilderbrand. J.Am.Chem.Soc. (1917) 39 2126
96. A.Bellemans. Bull.Soc.Chim.Belges (1957) 66 636
97. I.Brown, F.Smith Aust.J.Chem. (1962) 15 1
98. R.P.Rastogi, J.Nath. Indian. J.Chem. (1967) 5 249
99. R.W.Smith. Ph.D.Thesis, University of Leicester (1970).
100. I.Prigogine, R.Defray. "Chemical Thermodynamics" Trans.D.M. Everett. 1st. Ed. (Longmans) p239
101. E.F.G.Herington, R.Handley. J.Chem.Soc. (1950) 199
102. K.W.Morcom, R.W.Smith J.Chem.Thermo (1971) 3 507
103. R.St.J.Preston, J.B.L.Worthington Chem. & Ind. (1947) 612
104. E.D.Hart, W.H.Elkin. J.Sci.Instr., (1946) 23 17
105. L.H.Adams, International Critical Tables Voll. p57
106. M.W.Hanna. J.Am.Chem.Soc.(1968) 90 285
107. Prigogine, Mathot, Desmyter Bull.Soc.Chim.Belg., (1949) 58 547



SUMMARY

An apparatus has been developed to measure the vapour pressures of mixtures by a static technique.

The apparatus has been tested by reproducing the vapour pressures and excess Gibbs functions for mixtures of hexafluorobenzene + cyclohexane.

Excess Gibbs functions have been determined for hexafluorobenzene + n,n-dimethylaniline, and isopropylcyclohexane. An equilibrium constant for complex formation  $K_x$ , has been calculated from these quantities and compares favourably with the spectroscopically determined  $K_x$ .

Excess Gibbs functions have also been determined for mixtures of pentafluorocyanobenzene + cyclohexane at two temperatures.

The solid-liquid phase diagram has been determined for hexafluorobenzene + n,n-dimethyl p-toluidine and shows the existence of a 1:1 complex in the solid.

The liquid-liquid phase diagram for pentafluorocyanobenzene + isopropylcyclohexane has also been determined, and the system shows an upper critical solution temperature.

Excess volumes of mixing have been obtained for hexafluorobenzene + n,n-dimethylaniline, n,n-dimethyl p-toluidine and isopropylcyclohexane and pentafluorocyanobenzene + n,n-dimethylaniline, n,n-dimethyl p-toluidine, benzene, toluene and p-xylene.

Excess enthalpies of mixing have been measured at two temperatures for pentafluorocyanobenzene + cyclohexane, benzene, toluene and p-xylene.

The experimental evidence suggests that strong complexing occurs in solution between aromatic fluorocarbons + aromatic hydrocarbons, and also aromatic amines.

In the former case the interaction appears to be mainly of an electrostatic nature, whereas in the latter case the major contribution to the interaction arises from charge transfer forces, the amine acting as an electron donor.

---